AD_____

CONTRACT NO: DAMD17-91-C-1100

TITLE: GENETIC AND PHYSIOLOGICAL STUDIES OF BACILLUS ANTHRACIS RELATED TO DEVELOPMENT OF AN IMPROVED VACCINE

PRINCIPAL INVESTIGATOR: Curtis B. Thorne, Ph.D.

CONTRACTING ORGANIZATION: University of Massachusetts
203 Morrill Science Center, Box 35720
Amherst, Massachusetts 01003-0081

REPORT DATE: July 29, 1994

TYPE OF REPORT: Final Report

PREPARED FOR: U.S. Army Medical Research and Materiel Command, Fort Detrick, Frederick, Maryland 21702-5012

DISTRIBUTION STATEMENT: Approved for public release; distribution unlimited

The views, opinions and/or findings contained in this report are those of the author(s) and should not be construed as an official Department of the Army position, policy or decision unless so designated by other documentation.

REPORT DOCUMENTATION PAGE

Form Approved
OMB No. 0704-0188

1. AGENCY USE ONLY *(Leave blank)*	2. REPORT DATE	3. REPORT TYPE AND DATES COVERED
	29 June 1994	Final 30 June 1991-29 June 1994

4. TITLE AND SUBTITLE
Genetic and Physiological Studies of Bacillus Anthracis Related to Development of an Improved Vaccine

5. FUNDING NUMBERS
Contract No.
DAMD17-91-C-1100

6. AUTHOR(S)
Curtis B. Thorne

7. PERFORMING ORGANIZATION NAME(S) AND ADDRESS(ES)
University of Massachusetts
203 Morrill Science Center, Box 35720
Amherst, Massachusetts 01003-0081

8. PERFORMING ORGANIZATION REPORT NUMBER

9. SPONSORING/MONITORING AGENCY NAME(S) AND ADDRESS(ES)
U.S. Army Medical Research and Materiel Command
Fort Detrick
Frederick, Maryland 21702-5012

10. SPONSORING/MONITORING AGENCY REPORT NUMBER

11. SUPPLEMENTARY NOTES

12a. DISTRIBUTION/AVAILABILITY STATEMENT
Approved for public release; distribution unlimited

12b. DISTRIBUTION CODE

13. ABSTRACT *(Maximum 200 words)*

Most of our effort was spent on studies concerning the biology of the two *B. anthracis* plasmids, pXO1 which encodes toxin synthesis and pXO2 which encodes capsule synthesis. Analysis of Tn*917* insertion mutants of pXO1 revealed several mutants that were altered in toxin production. In some instances, the altered phenotypes were the result of insertions within or deletions of one or more of the toxin structural genes. Analysis of another mutant, deficient in production of all three toxin components, led to the discovery and cloning of a gene, *atxA*, involved in *trans*-activation of toxin synthesis. Overproduction of toxin by another mutant suggested that Tn*917* had inserted in a negative regulatory gene. Restriction analysis and physical mapping of pXO1 from several *B. anthracis* strains revealed an inversion of the toxin-encoding region of pXO1 from the Sterne strain. The inverted segment was found to be flanked by imperfect 1336-bp inverted repeats, each containing a sequence resembling a full or truncated IS*150*-like transposase gene. Comparison of Sterne and Weybridge A, which carry the inverted segment in opposite orientations, revealed no differences in phenotypes that could be associated with the inversion. Studies of insertion mutants of pXO2 suggested that some of the mutations are located in genes regulating synthesis of capsules. Among such mutants are those that overproduce capsular material, some that no longer require bicarbonate and CO_2 for capsule synthesis, and some that have lost the ability to synthesize capsules.

14. SUBJECT TERMS			15. NUMBER OF PAGES
B. anthracis	Capsule	Protective antigen	77
Anthrax toxin	Plasmid pXO1	Transposon mutagenesis	16. PRICE CODE
	Plasmid pXO2	Regulatory genes	

17. SECURITY CLASSIFICATION OF REPORT	18. SECURITY CLASSIFICATION OF THIS PAGE	19. SECURITY CLASSIFICATION OF ABSTRACT	20. LIMITATION OF ABSTRACT
Unclassified	Unclassified	Unclassified	Unlimited

FOREWORD

Opinions, interpretations, conclusionS and recommendations are those of the author and are not necessarily endorsed by the US Army.

____ Where copyrighted material is quoted, permission has been obtained to use such material.

____ Where material from documents designated for limited distribution is quoted, permission has been obtained to use the material.

CBV Citations of commercial organizations and trade names in this report do not constitute an official Department of Army endorsement or approval of the products or services of these organizations.

____ In conducting research using animals, the investigator(s) adhered to the "Guide for the Care and Use of Laboratory Animals," prepared by the Committee on Care and Use of Laboratory Animals of the Institute of Laboratory Resources, National Research Council (NIH Publication No. 86-23, Revised 1985).

____ For the protection of human subjects, the investigator(s) adhered to policies of applicable Federal Law 45 CFR 46.

CBV In conducting research utilizing recombinant DNA technology, the investigator(s) adhered to current guidelines promulgated by the National Institutes of Health.

CBV In the conduct of research utilizing recombinant DNA, the investigator(s) adhered to the NIH Guidelines for Research Involving Recombinant DNA Molecules.

CBV In the conduct of research involving hazardous organisms, the investigator(s) adhered to the CDC-NIH Guide for Biosafety in Microbiological and Biomedical Laboratories.

Curtis C. Thorne July 28, 1994

PI - Signature Date

TABLE OF CONTENTS

FINAL REPORT

This is the final report submitted under contract DAMD17-91-C-1100. Research on the contract which began June 30, 1991 is a continuation of research previously carried out under contract DAMD17-85-C-5212.

During the three years represented by this report our research concentrated largely on (i) physical and genetic analysis of the *B. anthracis* toxin plasmid pXO1; and (ii) physical and genetic analysis of the *B. anthracis* capsule plasmid pXO2. A very small proportion of our effort was also directed toward development of the bacteriophage TP-21 as a vector for transposon mutagenesis.

In this report our main efforts are described and discussed following a general description of materials and methods. Specific procedures which themselves are results of the research are described as appropriate under individual sections.

MATERIALS AND METHODS

Organisms. Table 1 lists the bacterial strains and plasmids referred to in this report.

Media. For convenience to the reader, compositions of the various culture media referred to in this report are given below. All amounts are for one liter final volume. For preparation of solid medium, 15 grams of agar (Difco) were added per liter of the corresponding broth.

NBY broth: Nutrient broth (Difco), 8 g; Yeast extract (Difco), 3 g.

Phage assay (PA) broth: Nutrient broth (Difco), 8 g; NaCl, 5 g; $MgSO_4 \cdot 7H_2O$, 0.2 g; $MnSO_4 \cdot H_2O$, 0.05 g; $CaCl_2 \cdot 2H_2O$, 0.15 g. The pH was adjusted to 6.0 with HCl.

Phage assay agar: For bottom agar, 15 g of agar were added per liter of phage assay broth. For soft agar, 0.6 g of agar were added per liter.

L broth: Tryptone (Difco), 10 g; Yeast extract (Difco), 5 g; NaCl, 10 g. The pH was adjusted to 7.0 with NaOH.

LPA agar: L agar containing the salts of PA broth.

$LPACO_3$ agar: LPA agar with 5 g of $NaHCO_3$.

LG broth: L broth with 1 g of glucose.

BHI broth: Brain heart infusion broth (Difco), 37 g.

Peptone diluent: Peptone (Difco), 10 g. Used for diluting phage and bacterial cells.

Minimal I: $(NH_4)_2SO_4$, 2 g; KH_2PO_4, 6 g; K_2HPO_4, 14 g; trisodium citrate, I g; glucose, 5 g; L-glutamic acid, 2 g; $MgSO_4 \cdot 7H_20$, 200 mg; $FeCl_3 \cdot 6H_2O$, 40 mg; $MnSO_4 \cdot H_2O$, 0.25 mg. The pH was adjusted to 7.0 with NaOH. The glucose and $FeCl_3$ were sterilized separately.

Minimal IB: The basal medium is the same as Minimal I except that $FeSO_4$ (14 mg) is substituted for $FeCl_3$ and $MnSO_4 \cdot H_2O$ is increased to 12.5 mg. The following are added: thiamine hydrochloride, 10 μg; and 160 μg each of L-methionine, L-leucine, L-valine, L-alanine, L-serine, L-threonine, L-proline, and L-phenylalanine.

Minimal IC: Minimal I with 5 g of Vitamin-Free Casamino Acids (Difco) and 10 mg of thiamine hydrochloride.

Minimal IIIB: $(NH_4)_2SO_4$, 2.0; KH_2PO_4, 6.0; KH_2PO_4, 14.0; trisodium citrate, 1.0; $MgSO_4 \cdot 7H_2O$, 0.4; $MnSO_4 \cdot H_2O$, 0.05; $CaCl_2 \cdot 2H_2O$, 0.15; $FeSO_4$, 0.02; glucose, 5.0; thiamine·HCl, 0.01; nicotinamide, 0.01; glycine, 0.40; L-glutamic acid, 0.40; and 0.32 g each of L-leucine, L-valine, L-alanine, L-serine, L-threonine, L-proline, L-phenylalanine, L-glutamine, L-histidine, L-arginine, L-isoleucine, L-asparagine, and L-methionine.

Minimal XO: To Minimal 1 are added 10 mg of thiamine hydrochloride, 200 mg of glycine, and 40 mg of L-methionine, L-serine, L-threonine, and L-proline.

CA broth is the Casamino Acids medium as described by Thorne and Belton (24).

CA-agarose medium: CA-agarose medium for the detection of colonies producing protective antigen was prepared as follows: 0.75 g of agarose was added to 100 ml of CA broth, prepared as described by Thorne and Belton (24), and the mixture was steamed until the agarose was dissolved. When the medium cooled to about 50° C, 1 ml of 20% glucose, 8 ml of 9% $NaHCO_3$, 6 ml of goat antiserum to *B. anthracis* and 10 ml of horse serum were added. The medium was dispensed in petri plates (13 ml per plate) and the plates were left with their lids ajar while the agarose solidified. The plates were usable after 1 h.

Quantitative determination of PA, LF, and EF. In some instances, the culture filtrates were concentrated 2- to 40-fold by ultrafiltration in Centricon 30 microconcentrator units (Amicon, Beverly, MA). The amount of PA and LF in the sample filtrates were determined by a radial immunodiffusion assay. The radial immunodiffusion agarose medium consisted of 1% Seakem GTG agarose (FMC BioProducts, Rockland, ME), 2% polyethylene glycol 8000, 3% fetal bovine serum, 20 mM HEPES (pH 7.5), 0.15 M NaCl, 2 mM EDTA, 0.025% sodium azide, and either 0.5% goat antiserum to PA or 0.7% rabbit antiserum to LF. A well approx. 2.5 mm in diameter was cut into the agarose medium and 8 μl of the filtrate was added to each well. Each plate included a set of standards containing 5 to 50 μg of purified PA or LF per ml. The diameter of the precipitin ring was measured and the data were compared to a standard curve.

EF in the culture filtrates was determined by an adenylate cyclase assay according to a method described by Leppla (11). A set of standards containing 0.05 to 1 μg of purified EF per ml was included in each assay. Briefly, approx. 10 μl of sample filtrate or purified EF standard were mixed with 40 μl of a reaction mixture containing 50 mM HEPES (pH 7.5), 12.5 mM $MgCl_2$, 2.5 mM dithiothreitol, 1.25 mM $CaCl_2$, 1.25 mM EDTA, 1.25 mM ATP, 0.25 mM cyclic AMP, 2.5 mg of bovine serum albumin, fraction V per ml, 25

μg of calmodulin (Sigma Chemical Co., St. Louis, MO) per ml, and 1.25 μCi of α-^{32}P-ATP per ml. The reactions were incubated for 10 min at room temperature. The reactions were stopped by adding 100 μl of a stopping solution containing 1% SDS, 50 mM ATP, and 1.25 mM cyclic AMP. Approx. 1 ml of distilled water was added to each tube.

The radiolabelled cyclic AMP product was separated from the nonreacted radiolabelled ATP reactant by sequential chromatography on cation exchange and aluminum oxide (Alumina) columns. The reaction mixtures were poured over Dowex AG 50W-X4 (200-400 mesh) columns that had been washed previously with 2 X 8 ml of distilled water. When the mixtures had drained into the columns, the columns were washed twice with 1.5 ml of distilled water to elute the nonreacted radiolabelled ATP. Any radiolabelled material left on the column was eluted with 5 ml of distilled water directly onto neutral Alumina WN-3 columns which had been washed previously with 8 ml of 0.1 M Imidazole (pH 7.3). Once the effluent from the Dowex 50 columns had drained into the Alumina columns, the radiolabelled cyclic AMP was eluted with 6 ml of 0.1 M Imidazole (pH 7.3) directly into 7-ml scintillation vials. The sample effluents were then counted in a Beckman LS5000 TD scintillation counter. The Dowex 50 columns were recycled by washing them twice with 2 ml of 1 M HCl and the Alumina columns were recycled by washing them with 3 ml of 0.1 M Imidazole (pH 7.3). The data obtained for the culture filtrates was compared to a standard curve prepared for purified EF.

Transfer of DNA to nylon membranes. DNA electrophoresed on an agarose gel was transferred to a Magnagraph nylon membrane (Micron Separations Inc., Westboro, MA) using a modified method of that described by Boehringer Mannheim Corp. (Technical Update [Nov. 1990], Indianapolis, IN). The DNA in the gel was acid nicked by incubation in 0.25 N HCl for 10 to 15 min The gel was rinsed in distilled water and placed in 0.5 N NaOH-1.5 M NaCl for 30 min with gentle agitation to denature the DNA. The gel was then neutralized in 1.5 M NaCl-1.0 M Tris-HCl (pH 8.0) for 1 h with gentle agitation. The DNA was blotted from the neutralized gel onto a Magnagraph nylon membrane by capillary transfer using 10X SSC for 12 to 16 h. After the transfer, the membrane was gently washed in 6X SSC for 5 min, air dried for 1 h, and then baked at 80°C in a vacuum oven for 1 to 2 h. The membrane was either used immediately for hybridization or stored in a dry place for use later.

Labelling probe DNA with digoxigenin-11-dUTP. Digoxigenin-11-dUTP was incorporated into the probe DNA by random primer labelling according to a method described for nonradioactive labelling of DNA by Boehringer Mannheim Corp. (Indianapolis, IN). The hexanucleotide mixture, digoxigenin DNA labelling mixture, and the Klenow fragment were purchased from Boehringer Mannheim Corp. The reaction was carried out in a final volume of 50 μl in a 1.5-ml microcentrifuge tube. The probe DNA was denatured by placing the DNA solution in a boiling water bath for 10 min and then quickly chilling the solution for 3 min in an ice/ethanol bath. Each reaction mixture contained approx. 1 to 3 μg of denatured DNA, 5 μl of hexanucleotide mixture, 5 μl of digoxigenin DNA labelling mixture, and enough sterile distilled

water to bring the volume to 47.5 µl. DNA synthesis was started by adding 2.5 µl of Klenow fragment. The reactants were gently mixed and placed in a 37°C water bath for 16 to 20 h.

To terminate the reaction, 5 µl of 0.2 M disodium EDTA (pH 8.0) was added to the reaction mixture. The labeled DNA was precipitated with 1 µl of a glycogen solution (20 mg/ml), one-tenth volume of 4 M LiCl, and 3 volumes of 100% ethanol. The precipitation was carried out for 4 to 6 h at -20°C. The labeled DNA was collected by centrifugation and the DNA pellet was washed once with 70% ethanol. A dry DNA pellet was then resuspended in 50 µl of TE (10 mM Tris-HCl, 1 mM disodium EDTA, pH 7 to 8) containing 0.1% SDS for 10 min at 37°C. Prior to hybridization, the digoxigenin-labelled DNA probe was denatured in prehybridization solution by heating in a boiling water bath for 10 min and chilling the mixture quickly in an ice/ethanol bath for 3 min

DNA-DNA hybridization. DNA-DNA hybridizations were done according to a method described by Boehringer Mannheim Corp. for nonradioactive DNA labelling and detection. The Magnagraph nylon membrane containing the immobilized DNA was prehybridized in a sealed plastic bag at 68°C for 1 to 3 h in 20 ml of freshly prepared 5X SSC solution containing 0.1% (w/v) sodium N-lauroylsarcosine, 0.02% (w/v) SDS, and 1% (w/v) Genius blocking reagent (Boehringer Mannheim) per 100 cm^2 of membrane. After prehybridization, the solution covering the membrane was replaced with 2.5 ml of prehybridization solution containing 250 ng to 1 µg of denatured digoxigenin-labelled DNA probe per 100 cm^2 of membrane. The bag was sealed and the hybridization was continued at 68°C for 16 to 24 h.

The membrane was removed from the hybridization solution, washed twice in 2X SSC containing 0.1% SDS for 5 min at room temperature, and washed twice in 0.1X SSC containing 0.1% SDS for 15 min at 68°C with gentle shaking. The hybridized DNA probe was detected on the membrane by chemiluminescence.

Chemiluminescent detection of hybridized DNA. The method for detecting the hybridized DNA probe with Lumi-Phos 530 solution was described by Boehringer Mannheim Corp. After post-hybridization washes, the membrane was equilibrated for 1 min in Buffer A (100 mM Tris-HCl, 150 mM NaCl, pH 7.5). The membrane was transferred to Buffer B (Buffer A containing 2% (w/v) Genius blocking reagent) for 3 h with gentle shaking. The membrane was then transferred to 30 ml of a 1 to 5000 dilution of an anti-digoxigenin alkaline phosphatase antibody conjugate (diluted in Buffer B) per 100 cm^2 of membrane. The membrane was incubated in this solution for 30 min with gentle shaking. After the 30-min incubation, the membrane was washed two times for 15 min in Buffer A and then equilibrated for 2 min in Buffer C (100 mM Tris-HCl, 100 mM NaCl, 50 mM $MgCl_2$, pH 9.5). Finally, the membrane was placed on a clean sheet of acetate film with DNA side up and 2 to 3 ml of Lumi-Phos 530 (Boehringer Mannheim Corp.) was placed directly onto the membrane. A second sheet of acetate film was placed on top of the filter to spread the solution evenly over the membrane. The reaction was allowed to proceed for 15 to 30 min before the membrane (placed in a sealed bag) was exposed to X-ray film (Kodak XAR film). The membrane was

exposed to the X-ray film for 1 to 30 min and the X-ray film was developed according the instructions provided by the manufacturer.

Isolation of pBluescriptIIKS+. The pBluescriptIIKS+ was isolated from *E. coli* DH5α(pBluescriptIIKS+) by a modification of a boiling lysis method (14). Twelve ml of an overnight culture of *E. coli* DH5α(pBluescriptIIKS+) grown in L broth containing 100 μg of ampicillin per ml was centrifuged at 10,000 rpm for 10 min The pellet was resuspended in 0.7 ml of 8% sucrose/5% triton X-100/50 mM EDTA/50 mM Tris-HCl (pH 8) and the suspension was transferred to a 1.5-ml microcentrifuge tube. Fifty μl of a freshly prepared 10 mg/ml solution of lysozyme in 0.25 M Tris-HCl (pH 8) was added to the cell suspension and the mixture was placed in a boiling water bath for 1 min.The lysed mixture was centrifuged for 15 min at room temperature and the cell debris was removed with a sterile toothpick. Ten μl of a RNAse solution (10 mg/ml) was added to the supernatant and placed at 37°C for 15 min.An equal volume of a 1:1 mixture of phenol-chloroform was added to the tube and gently mixed. The mixture was centrifuged to separate the phases. The aqueous layer was transferred to a fresh tube and the phenol-chloroform extraction was repeated until no white interface was detected (usually 4 to 7 extractions). The final extraction was with an equal volume of 24:1 chloroform-isoamyl alcohol mixture.

The DNA was precipitated with 0.15 volume of 7.5 M ammonium acetate and an equal volume of cold isopropanol. The DNA was allowed to precipitate at -20°C for 20 min.The precipitated DNA was then recovered by centrifugation in a refrigerated microcentrifuge at 13,000 rpm for 30 min. The pellet was washed with 1 ml of cold 70% ethanol. The DNA was then allowed to air dry for 1 h and resuspended in 100 μl of TE (10 mM Tris-HCl, 1 mM EDTA, pH 8.0).

Preparation of vector for ligation. Approximately 20 μg of plasmid DNA was digested to completion with an excess amount of restriction endonuclease. The DNA was precipitated overnight at -20°C with one-tenth volume of 3 M sodium acetate (pH 5.2) and 2 volumes of 95% ethanol. The DNA was collected by centrifugation in a refrigerated microcentrifuge at 13,000 rpm for 30 min and washed with 1 ml of cold 70% ethanol. The pellet was allowed to air dry and then resuspended in 50 μl of TE (pH 8). Twenty μl was frozen at -20°C for use as a control in the ligation reactions.

The remaining DNA was treated with calf-intestine alkaline phosphatase (Promega Corp., Madison, WI) according to manufacturer's instructions. Briefly, the volume of the DNA suspension was brought to 40 μl with TE (pH 8). Five μl of a 10X reaction buffer containing 0.5 M Tris-HCl, pH 9, 10 mM $MgCl_2$, 1 mM $ZnCl_2$, and 10 mM spermidine and 2 μl of calf-intestine alkaline phosphatase (CIAP) were added to the DNA suspension. The mixture was placed at 37°C for 30 min. Another 2 μl of CIAP was added to the mixture and again placed at 37°C for 30 min. The reaction was stopped by the addition of 300 μl of solution containing 10 mM Tris-HCl, pH 7.5; 1 mM EDTA, pH 7.5; 200 mM NaCl; and 0.5% SDS. The mixture was placed at 60°C for 15 min. The DNA was then extracted with phenol-chloroform and the aqueous phase was precipitated with 0.5 volume of 7.5 M ammonium acetate and 2 volumes of 95%

ethanol. The precipitated DNA was collected by centrifugation, allowed to air dry, and finally resuspended in a total volume of 50 µl TE (pH 8).

Elution of DNA restriction fragments. Two methods were employed for isolating restriction fragments from agarose gels. In the first method elution of fragments was carried out using an Elutrap electroseparation chamber according to the manufacturer's instructions (Schleicher and Schuell, Inc., Keene, NH). The elution was run at 200 V for 2 to 3 h and the DNA was collected in 400 to 500 µl of 1X Tris-borate buffer. The DNA was then precipitated with one-tenth volume of 3 M sodium acetate (pH 5.2) and 2 volumes of 100% ethanol. The DNA was collected by centrifugation in a microcentrifuge at 4°C for 30 min. The DNA pellet was dried for 30 min at room temperature and resuspended in 50 ul of TE.

In the second method DNA fragments were transferred from agarose gels by electrophoresis onto DE-81 paper (Whatman, Inc., Clifton, NJ) and eluted from the paper according to a modification (A. Simon, personal communication) of a protocol described by Sambrook et al. (18) and Ausubel et al. (1). The agarose gels containing 0.5 µg of ethidium bromide per ml were prepared and run in 0.5X TBE. Following electrophoresis each restriction fragment to be eluted was cut from the gel under long wave UV light. A piece of DE-81 paper cut to the size of a gel slice and soaked in 0.5X TBE was placed on one side of each slice. Each slice was then placed in a slot of appropriate size in a second agarose gel which was free of DNA. The fragments were electrophoresed onto the paper for 15 to 20 min at 50 V.

The paper was then placed in the bottom of a 0.6-ml microcentrifuge tube containing a hole made with a 25 gauge needle. The 0.6-ml tube was placed into a 1.5-ml microcentrifuge tube and the paper was washed two times with 75 µl of a low salt wash buffer (10 mM Tris-HCl, pH 7.5; 1 mM EDTA, pH 7.5; and 0.1 M LiCl). The samples were centrifuged for 5 s at room temperature. The 0.6-ml tube containing the paper was placed inside a new 1.5-ml microcentrifuge tube. The DNA fragments were eluted from the paper by adding 75 µl of a high salt buffer (20% ethanol; 1 M LiCl; 10 mM Tris-HCl, pH 7.5; and 1 mM EDTA, pH 7.5) to the 0.6-ml tube and incubating the tubes at 65°C for 10 min. The elution mixture was collected in the 1.5-ml tube by centrifugation for 5 s at room temperature. The paper was washed with 75 µl of the high salt wash buffer and the wash was collected in the same 1.5-ml tube by centrifugation for 5 s at room temperature. The DNA fragments were precipitated by adding 300 µl of cold 100% ethanol to the 150-µl elution mixture and placing the mixture at -20°C for 20 min. The precipitated DNA was collected by centrifugation for 5 min at room temperature. The DNA pellet was washed twice with 0.5 ml of cold 70% ethanol and dried either at room temperature for 1 h or in a SpeedVac for 5 min. The pellet was resuspended in 5 µl of sterile distilled water by placing the tube at 65°C for 2 min and at 4°C overnight.

Ligation reactions. Ligation reactions were carried out according to methods described by Sambrook *et. al.* (18). Vector and insert DNA were mixed at a molar ratio of 1:3 in a total volume of 10 to 20 µl. Control ligations included digested vector alone to determine whether the ligation was successful and CIAP-treated digested vector alone to determine if the CIAP treatment had reduced vector religations. The concentration of DNA used in the control ligation was the same as that used for the vector in the

vector/insert ligation mixture. The mixtures were heated at 65°C for 5 min and chilled on ice for 5 min to melt any reannealed ends. A one-tenth volume of 10X reaction buffer containing 300 mM Tris-HCl at pH 7.8, 100 mM $MgCl_2$, 100 mM DTT, 10 mM ATP, and 3 weiss units of T4 DNA ligase (Promega Corp., Madison, WI) was added to each tube. The mixture was let stand overnight at room temperature. The following day an additional 1 Weiss unit of ligase was added to each tube and after 2 to 3 hours, the DNA was precipitated with one-tenth volume of 3 M sodium acetate (pH 5.2) and 2 volumes of 100% ethanol and dialyzed against TE (pH 8) for use in electroporation of electrocompetent *E. coli* DH5α cells.

Transformation of E. coli. *Two methods were used for transforming E. coli.* The first method involved transforming the ligation mixtures into electrocompetent cells of *E. coli* DH5α by electroporation using a GenePulser apparatus according to methods and instructions provided by the manufacturer (Bio-Rad Laboratories, Richmond, CA). Briefly, four 250-ml flasks of L broth were inoculated with 2.5 ml of an overnight culture of *E. coli* DH5α. The cultures were grown at 37°C until an OD_{600} of 0.5 to 0.7 was reached. The flasks were chilled for 15 min on ice and the cells were harvested by centrifugation. The pellets were washed one time in 1 liter and one time in 500 ml of cold sterile distilled water. Finally, the pooled pellet was washed one time in 20 ml of cold 10% glycerol. The final pellet was resuspended in 200 µl of cold 10% glycerol. The suspended electrocompetent cells were dispensed into 40-µl samples. To each sample 2 to 3 µl of the precipitated/dialyzed ligation mixture was added. The mixture was transferred to a chilled 0.2-cm electroporation cuvette and pulsed one time at 2.5 kV, 25µFD, and 200 ohm resistance. One ml of SOC medium was immediately added to the cuvette and the cell suspension was transferred to a cotton-plugged culture tube. The cultures were incubated at 37°C with shaking for 1 h. They were then plated onto L agar containing 100 µg of ampicillin per ml and which had been spread 1 h before with 100 µl of 100 mM isopropylthio-ß-D-galactoside (IPTG) and 40 µl of 2% 5-bromo-4-chloro-3-indolyl-ß-D-galactoside (Xgal). The plates were incubated at 37°C for 16 to 20 h. The blue color was allowed to develop further at room temperature. The plasmids from the white Lac$^-$ colonies were screened for possible inserts.

In the second method MAX efficiency or subcloning efficiency *E. coli* DH5α competent cell (Life Technologies, Inc., Gaithersburg, MD) were transformed with ligation mixtures according to a procedure described for each by the manufacturer. Transformants were plated and isolated as described above.

DNA sequencing and analysis. The sequences of cloned fragments of pXO1.1 (Weybridge A UM23) and pXO1 (Sterne) containing the junctions of the inverted segments were determined by the dideoxy chain termination method of Sanger et al. (19) using α-^{32}P dATP and the Sequenase ver. 1.0 sequencing kit (United States Biochemicals, Cleveland, OH). The sequencing reactions were performed according to the procedure described by the manufacturers. The fragments were cloned into pBluescriptIIKS+ and the resulting constructs were used to obtain double stranded templates that were denatured prior to sequencing. The sequences were determined for both DNA strands of the cloned inserts. Whenever possible, M13 forward and reverse universal primers were used for sequencing.

Additional oligonucleotide primers obtained from Integrated DNA Technology (Coralville, IA) were used to extend the sequences of the cloned inserts. The sequences were then analyzed extensively using the University of Wisconsin Genetics Computer Group (GCG) software package.

RESULTS AND DISCUSSION

I. Physical and genetic analysis of the *B. anthracis* toxin plasmid pXO1

Our general approach to studying the physical and genetic characteristics of the *B. anthracis* toxin plasmid, as well as the capsule plasmid, has been to employ transposon mutagenesis to obtain insertion mutations in the plasmid and then to examine the resulting mutants for acquisition of new phenotypes. In previous reports (7, 8, 20, 21) our methodology for transposon mutagenesis and characteristics of some of the pXO1::Tn*917* mutants have been described. In the Midterm Report (22) several of the insertion mutants were characterized further.

It should be recalled that Weybridge UM44 exhibited plasmid-derived phenotypic characteristics different from those observed in Weybridge A strains. Weybridge UM44 is a Trp$^-$ mutant which was isolated from the wild-type Weybridge strain, and Weybridge A was isolated from "wild-type" Weybridge as a mutant that grew much better than the parent strain on a minimal medium, minimal XO. The two strains, Weybridge UM44 and Weybridge A (and auxotrophs derived from the latter) differed in rate and extent of sporulation at 37°C, phage sensitivity, and growth characteristics on minimal medium. However, UM44-derived strains into which pXO1::Tn*917* derivatives from UM23 were introduced showed characteristics similar to those typical of UM23. Because of differences observed in the toxin plasmid from the two strains, we have suggested that the plasmid of the wild-type Weybridge strain (and that from Weybridge UM44) be designated pXO1 and the one from Weybridge A strain be designated pXO1.1 (20).

The Midterm Report (22) documents the characterization of several pXO1::Tn917 insertion mutants of Weybridge A UM23 and describes the construction of a restriction map of pXO1.1 Tn*917* inserted into a number of different sites on pXO1.1. Several insertion mutants exhibited charcteristics similar to those of the Weybridge A UM23 parent strain. Mutant tp28 exhibited alterations in its sensitivity to bacteriophage CP-51. Several insertion mutants, including some deletants, exhibited alterations in toxin production. Two insertion mutants, tp29 and tp32, appeared to have interrupted a gene involved in positive regulation of toxin synthesis. Further examination of these two mutants led to the identification of a gene involved in positive activation of toxin synthesis (26). Another very interesting mutant, tp62, produced toxin components in the absence of bicarbonate. In this mutant Tn*917* was determined to be located just upstream of the structural gene for lethal factor, suggesting that this region may be involved in negative regulation of toxin synthesis.

Quantitative analysis of toxin production by several insertions mutants. In the Midterm Report (22), results of two experiments examining toxin production by several insertion mutants grown in the absence of bicarbonate and horse serum were included. To provide more confidence in the values obtained for the amounts of toxin produced, a third experiment was performed with insertion mutants tp2A, tp21, tp29, tp32, tp39, tp62, and tp72 grown in the absence of bicarbonate and horse serum and the amounts of protective antigen (PA), lethal factor (LF), and edema factor (EF) in culture filtrates were determined as discussed previously (22). The averages of results from all three experiments are shown in Table 2 and standard error values are reported for those mutants producing toxin components in the absence of bicarbonate. The results confirmed that tp2A produced amounts of toxin components similar to those produced by the parent strain, Weybridge A UM23; tp21 did not produce detectable amounts of PA but, like UM23, it produced trace amounts of EF and LF; tp29, tp32, and tp39 were deficient in production of all three toxin components; tp62 overproduced the toxin components in the absence of bicarbonate; and tp72 was deficient in PA production (similar to tp21), but produced more LF than did UM23.

Analysis of altered *Bam*HI-*Sal*I fragments of pXO1.1::Tn*917* deletion derivatives from UM23 tp21 and tp39. Based on results from restriction analyses of the pXO1.1::Tn*917* deletion derivatives of UM23 tp21 and tp39, we determined that the origins of the 36- and 8.5-kb *Bam*HI-*Sal*I fragments of the plasmid from tp21 were the 34.8- and 13.9-kb *Bam*HI fragments, respectively, and the 33- and 5.5-kb *Bam*HI-*Sal*I fragments of the plasmid from tp39 were the 34.8- and 7.4-kb *Bam*HI fragments, respectively. To confirm these results, the altered *Bam*HI-*Sal*I fragments of the Tn*917*-tagged derivatives from tp21 and tp39 were isolated by electroelution and labelled with digoxigenin-labelled dUTP. Results of DNA-DNA hybridizations with *Bam*HI-, *Pst*I-, and *Eco*RI-digested pXO1 (Weybridge A UM23) using these isolated fragments as probes are shown in Table 3.

The 8.5-kb *Bam*HI-*Sal*I fragment of pXO1.1::Tn*917* (tp21) hybridized to the 13.9-kb *Bam*HI fragment, the 18.1-kb *Pst*I fragment, and the 8.0- and 3.1-kb *Eco*RI fragments of pXO1 (Weybridge A UM23). The 36-kb *Bam*HI-*Sal*I fragment of the plasmid from tp21 hybridized to the 34.8-kb *Bam*HI fragment, and the 9.3-, 6.6-, 6.3-, 5.2-, 2.8-, and 0.6-kb *Pst*I fragments of pXO1 (Weybridge A UM23). Interestingly, the altered fragment did not hybridize to the 6.0-kb *Pst*I fragment. Deletant tp21 had been shown previously to produce LF which suggested that at least a 1.4-kb portion of the 6.0-kb *Pst*I fragment (determined from the *lef* sequence [2]) must be present since it contains the 3' end of the LF structural gene. A reasonable explanation might be that the presence of Tn*917* sequences adjacent to this fragment interfered with the hybridization.

The 5.5-kb *Bam*HI-*Sal*I fragment of pXO1.1::Tn*917* (tp39) hybridized to the 7.4-kb *Bam*HI fragment, the 18.7- and 5.5-kb *Pst*I fragments, and the 3.1- and 1.05-kb *Eco*RI fragments of pXO1 (Weybridge A UM23). Results from previous restriction analysis and DNA-DNA hybridization analysis with the cloned toxin structural genes suggested that the 3.1-kb *Eco*RI fragment that hybridized to the 5.5-kb *Bam*HI-*Sal*I fragment of the plasmid from tp39 is different from the 3.1-kb *Eco*RI fragment that hybridized to the 8.5-kb

*Bam*HI-*Sal*I fragment of the plasmid from tp21. The 33-kb *Bam*HI-*Sal*I fragment of the plasmid from tp39 hybridized to the 34.8-kb *Bam*HI fragment, the 9.3-, 6.6-, 6.3-, 5.2-, 2.8-, and 0.6-kb *Pst*I fragments of pXO1 (Weybridge A UM23). Again, this large *Bam*HI-*Sal*I fragment did not hybridize to the 6.0-kb *Pst*I fragment. However, among the many *Eco*RI fragments that hybridized to the 33-kb fragment was an 0.8-kb fragment corresponding to the 0.8-kb *Eco*RI fragment in *lef*. Based on the sequence of *lef* (2), *Pst*I should cut the 0.8-kb *Eco*RI fragment into two fragments 0.5 and 0.3 kb in size and the 0.5-kb *Pst*I-*Eco*RI fragment should be homologous to the 6.0-kb *Pst*I fragment. These observations suggested that at least a portion of the 6.0-kb *Pst*I fragment must be present within the 33-kb *Bam*HI-*Sal*I fragment.

Attempts to Purify UM23 tp49 and tp71. Previously, we found discrepancies in the toxin phenotypes determined for deletants tp49 and tp71 from quantitative analysis of toxin production and DNA-DNA hybridizations of the digested pXO1.1::Tn*917* deletion derivatives with the cloned toxin components. Quantitative analysis showed that tp49 and tp71 were PA^{++}, LF^{+}, $EF^{+/-}$ and $PA^{+/-}$, LF^{++}, EF^{+}, respectively, while DNA-DNA hybridization analysis with the cloned toxin genes revealed that tp49 and tp71 should be PA^{+}, LF^{+}, EF^{-} and PA^{-}, LF^{+}, EF^{-}, respectively. Plasmid profiles of tp49 and tp71 and results from restriction analysis of the plasmids from these mutants double digested with *Bam*HI and *Sal*I showed that the mutants contained multiple plasmid derivatives. We attempted first to isolate colonies containing the 40- and 47.8-kb plasmids from tp49 and tp71 spore stocks, respectively, by single colony isolations on L agar with inhibitory concentrations of erythromycin and lincomycin. After four rounds of single colony isolations, all isolates of tp49 and tp71 contained mixed populations of plasmids. Since the 40- and 47.8-kb plasmids of tp49 and tp71, respectively, were the predominant plasmids observed from plasmid extractions of cells grown in BHI broth containing 10% horse serum, isolates of tp49 and tp71 were grown in this medium prior to single colony isolations. Again all of the colonies isolated contained a mixed population of plasmids.

Finally, CP-51-mediated transduction was used in an attempt to transfer the 40- and 47.8-kb plasmids from these insertion mutants to Weybridge A UM23C1-2, a rifampicin-resistant derivative of the pXO1.1-cured strain UM23C1. The propagations were repeated four times and the transductions were repeated seven times with lysates from cultures of tp49 or tp71. No MLS^{r}, Rif^{r} transductants were isolated that contained the small plasmid derivatives. These results suggested that the 40- and 47.8-kb plasmids from tp49 and tp71, respectively, may not be maintained stably within cells and that larger pXO1.1::Tn*917* derivatives may provide factors necessary to stabilize these smaller plasmids.

Genetic analysis of *atxA* gene. Insertion mutants tp29 and tp32 are deficient in production of PA, LF, and EF and the Tn*917* insertions within pXO1.1 from these two mutants were in the same fragment and outside of the toxin genes (8). These results suggested that Tn*917* inserted within a region involved in positive activation of toxin synthesis. While we were involved in cloning the region of pXO1.1 containing the putative positive regulatory gene, I. Uchida, working in S. Leppla's laboratory at NIDR in Bethesda, MD, and taking advantage of information presented by Hornung and Thorne (8), cloned a gene involved in

positve activation of toxin synthesis. We provided evidence that the two laboratories cloned the same region of the plasmid. DNA-DNA hybridization analysis of digested pXO1.1 with the 1.3-kb *Hpa*I-*Eco*RV fragment of Uchida's recombinant plasmid, pIU51, containing the ORF involved in positive regulation of toxin synthesis, showed that the putative gene hybridized to the 13.9-kb *Bam*HI fragment and the 18.1-kb *Pst*I fragment of pXO1.1, fragments altered by Tn*917* insertion in the plasmid derivatives from tp29 and tp32. To complete the project, the two laboratories collaborated and a gene, designated *atxA*, encoding a trans-acting positive regulatory factor was identified. The cloned gene complemented the insertion mutations within tp29 and tp32. A paper describing the cloning and characterization of *atxA* has been published (26).

The recombinant plasmid, pIU68, containing the subcloned *atxA* ORF was transferred to insertion mutants tp29 and tp32 to determine whether *atxA* restored production of all three toxin components in these mutants and to some other strains to determine the effect of *atxA* on toxin production.
We tested the constructed strains for toxin production in CA-HEPES broth with and without sodium bicarbonate and horse serum. The averages of the results from two experiments are shown Table 4. Although the absolute values differed from those obtained by Uchida when he grew the strains in R medium in the presence or absence of sodium bicarbonate (26), the results confirmed that *atxA* complements the insertion mutations in tp29 and tp32. These complemented mutants produced the three toxin components in the absence of sodium bicarbonate and horse serum. In the presence of sodium bicarbonate and horse serum, tp29(pIU68) and tp32(pIU68) produced amounts of toxin that were equivalent to or more than that produced by UM23-1, the streptomycin resistant isolate of UM23 used by Uchida for comparison of toxin synthesis. However, we observed that the parental strain of the insertion mutants, UM23, produced two to three times more PA and LF than did UM23-1. Thus, our results showed that the amounts of PA and LF produced by the complemented insertion mutants tp29 and tp32 were actually lower than those produced by the parental strain, a result that is usually expected in complementation studies.

Other results in Table 4 show that the *atxA* gene product activated *pag* on pIU71 in UM23C1-1. This provided supporting evidence that the *atxA* gene product is a positive trans-acting factor. UM23-1(pIU68) and UM23 tp62 (pIU68) grew poorly under the conditions used for toxin synthesis.

To provide more evidence that the product of *atxA* is a trans-acting positive regulator, the *ca.* 10-kb tetracycline-resistance recombinant plasmid, pIU51, containing cloned *atxA* was introduced by electroporation into deletant UM23 tp39, a mutant deficient in production of all three toxin components and whose plasmid contains deletions encompassing *pag*, *cya*, and *atxA*, but not *lef*. Two electrotransformants, UM23 tp39 etf3 and etf5, were isolated and the plasmids from these transformants were examined by agarose gel electrophoresis. These electrotransformants contained a plasmid comigrating with pXO1::Tn*917* from tp39 and a plasmid comigrating with pIU51.

UM23 tp39 etf3 and etf5 were analyzed for production of PA, LF, and EF by quantitative methods described previously and the results are shown in Table 5. Plasmid pIU51 was not maintained stably in the tp39 transformants unless they were grown under selection with tetracycline. When tp39 etf3 and etf5 were grown in CA-HEPES (pH 7.5) in the presence of added bicarbonate, horse serum, and inhibitory concentrations of tetracycline, LF was produced. However, the concentration of LF was about five- to ten-fold lower than that observed for UM23. No detectable amounts of PA or EF were present in the culture filtrates. Since *atxA* was deleted from pXO1::Tn*917* (tp39), then complementation of LF production by pIU51 provided evidence that *atxA* encodes a trans-acting positive activator. Although complementation of tp39 with cloned *atxA* did occur, the concentrations of LF in the culture filtrates of etf3 and etf5 was much lower than anticipated. Thus, the optimal conditions for LF production by the electrotransformants may not have been attained in broth cultures under the conditions tested. Also, other genes may have been deleted from the plasmid of tp39 that are involved in regulating toxin synthesis.

II. Analysis of an Inversion Encompassing the Toxin-Encoding Region of pXO1.1 (Weybridge A) and pXO1 (Sterne)

The Midterm Report (22) presented evidence that the order of the toxin genes on pXO1 from a Sterne strain obtained from USAMRIID is reversed from that of the same genes on pXO1.1 carried by the Weybridge A strain. The evidence available at that time suggested that an inversion had occurred in the toxin-encoding region of one of the plasmids. This evidence is summarized below and is then followed by results of further experiments which show conclusively that an inversion had occurred.

The main experimental points of evidence reported in the Midterm Report can be summarized as follows (refer to that report [22] for details and tabular and graphical data):

(1) The *Bam*HI and *Pst*I restriction profiles of pXO1.1 from *B. anthracis* Weybridge A UM23 as determined in our laboratory differed from those published by Robertson et al. (15) for pXO1 from a different pXO1$^+$, pXO2$^-$ strain (labeled Sterne). The difference was observed in the region surrounding the toxin structural genes (8). The 29-kb and 19-kb *Bam*HI fragments shown on the restriction map of pXO1 constructed by Robertson et al. differed from the 34.8-kb and 14.6-kb fragments generated by *Bam*HI digestion of pXO1.1.

Double digestion of pXO1.1 with *Bam*HI and *Sal*I showed a restriction profile which differed from that deduced from Robertson's map. Three *Sal*I restriction sites were observed in pXO1.1. They are located in the 38.7-kb 19.9-kb and 14.6-kb *Bam*HI fragments and corresponded to those in the 37-kb, 20-kb, and 29-kb *Bam*HI fragments on Robertson's map, respectively. These results suggested that the 14.6-kb fragment of pXO1.1 was homologous to the 29-kb fragment of pXO1 (Robertson).

(2) In addition to the differences observed for the *Bam*HI restriction profiles, *Pst*I digestion of pXO1.1 generated an 18.7-kb and a 9.3-kb fragment instead of a 20-kb and an 8.6-kb fragment depicted on

Robertson's map. Results from homologous DNA-DNA hybridizations showed that the 9.3-kb as well as the 6.6-kb, 6.3-kb, 6.0-kb, and 5.2-kb *Pst*I fragments from pXO1.1 were nested within the 34.8-kb *Bam*HI fragment. DNA-DNA hybridization studies using the cloned toxin structural genes as well as secondary digestion of the 34.8-kb fragment provided evidence that the *Pst*I fragments homologous with the *Bam*HI fragment are the five fragments listed above. DNA-DNA hybridizations of digested pXO1.1 with the cloned LF structural gene showed that it hybridized to the 34.8-kb *Bam*HI fragment and to the 6.6-kb and 6.0-kb *Pst*I fragments. According to Robertson's map *lef* is located on the 6.6-kb and 6.0-kb *Pst*I fragments which are nested within the 29-kb *Bam*HI fragment. Robertson's map also shows that the 19-kb *Bam*HI fragment contains *Pst*I fragments which may correspond to the 9.3-kb, 6.3-kb, and 5.2-kb *Pst*I fragments located within the 34.8-kb *Bam*HI fragment of pXO1.1. These results suggested that the 34.8-kb *Bam*HI of pXO1.1 shares homology with the 29-kb and 19-kb *Bam*HI fragments of pXO1 from Robertson's strain.

(3) The evidence presented above suggested that the region encompassing the toxin structural genes in pXO1.1 from Weybridge A UM23 may be inverted in comparison to the toxin-encoding region shown on the restriction map of pXO1 constructed by Robertson et al. (15). The orientation of the region encoding the toxin structural genes has been designated as α for pXO1 from Robertson's *B. anthracis* strain and as β for pXO1.1 from Weybridge A UM23 (23).

The restriction profiles for pXO1 isolated from other *B. anthracis* ($pXO1^+$, $pXO2^-$) strains, including Weybridge, Weybridge A, Weybridge B, Sterne (USAMRIID), Anvax, V770, PM36R-1, Ames ANR-1, and New Hampshire NNR-1, were examined (8). All except Sterne (USAMRIID) exhibited restriction profiles similar to the profiles exhibited by pXO1.1 from Weybridge A UM23 and therefore, all most likely carry the toxin-encoding region in the β orientation. The toxin plasmid from Sterne (USAMRIID) generated *Bam*HI, *Bam*HI-*Sal*I, and *Pst*I restriction patterns which corresponded to those shown for pXO1 by Robertson, suggesting that the toxin-encoding region of pXO1 from Sterne (USAMRIID) is most likely in the α orientation. The origin of the Sterne strain used by Robertson et al. (15) has not been determined; however, it seems likely that the strain he used is the same as the Sterne (USAMRIID) strain.

(4) By a series of restriction analyses and DNA-DNA hybridization tests the locations of the ends of the inverted segment were approximated (22). Then to provide evidence that an inversion had occurred within the toxin-encoding region, restriction fragments encompassing the ends of the inverted segment were used in DNA-DNA hybridizations to probe the *Bam*HI- and *Pst*I-digested plasmids from Sterne (USAMRIID) and from Weybridge A UM23. The results of these experiments confirmed that an inversion involving a segment of pXO1 as large as 40 kb had occurred.

Since the Midterm Report was prepared further experiments, reported below, have been carried out to confirm that an inversion had occurred. These experiments include cloning the junction fragments and determining their DNA sequences.

Restriction analyses of pXO1 from several *B. anthracis* strains. Previously, the *Bam*HI restriction patterns of pXO1 from Weybridge, Weybridge UM44-1, Weybridge B, Anvax, PM36-R1, and Vollum V770

were similar to that obtained for pXO1.1 from Weybridge A UM23 and different from that obtained for pXO1 from Sterne (6, 8, 22). All of the plasmids except pXO1 (Sterne) contain a 34.8- and 14.6-kb *Bam*HI fragment instead of a 29- and 19.5-kb *Bam*HI fragment found in pXO1 (Sterne). These results provided evidence that the toxin-encoding regions of pXO1 from the former strains existed in the same orientation as that observed for pXO1.1 from Weybridge A UM23, but lie in opposite orientation to that observed for pXO1 from Sterne. To provide more evidence supporting this hypothesis, we compared the *Pst*I and *Eco*RI restriction patterns of pXO1 from the various *B. anthracis* strains with those of pXO1.1 (Weybridge A UM23) and pXO1 (Sterne).

The results of the restriction analyses showed that pXO1 from Weybridge, Weybridge UM44-1, Weybridge B, Anvax, PM36-R1, and Vollum V770 contained the 18.7- and 9.3-kb *Pst*I fragments and the 5.4- and 2.4-kb *Eco*RI fragments, fragments comigrating with the *Pst*I and *Eco*RI fragments containing the junctions of the inverted toxin-encoding region of pXO1.1 (Weybridge A UM23). Only pXO1 (Sterne) contained the 19- and 8.6-kb *Pst*I junction fragments and the 4.8- and 3.1-kb *Eco*RI junction fragments. Thus, the orientation of the toxin-encoding region of pXO1 from the various *B. anthracis* kept in our laboratory appears to be the same as that for pXO1.1 from Weybridge A UM23 (referred to as β orientation).

Other differences were observed in the *Pst*I and *Eco*RI patterns of pXO1 from the various *B. anthracis* strains. The toxin plasmid from Weybridge was shown previously to contain an extra 10-kb *Bam*HI fragment. The *Pst*I restriction pattern of pXO1 (Weybridge) revealed an extra 6.3- and 2.9-kb fragment. The *Eco*RI restriction pattern was more difficult to interpret; however, pXO1 appears to contain extra fragments approx. 4.5 and 1.2 kb in size. Although no differences were observed for the *Bam*HI restriction profiles of pXO1 from Weybridge A UM23, Weybridge UM44-1, PM36-R1, and Vollum V770, we observed differences in the *Eco*RI and *Pst*I restriction patterns. The toxin plasmids from PM36-R1 and Vollum V770 were missing a *ca.* 7.2-kb *Eco*RI fragment observed in pXO1 from Weybridge derivatives, Anvax, and Sterne and there appeared to be an extra fragment approx. 7.4 kb in size. No differences were observed in the *Pst*I restriction profiles of the two former plasmids in comparison to that of pXO1.1 (Weybridge A UM23). These results suggested that pXO1 from PM36-R1 and Vollum V770 may contain approx. 0.2 kb of extra DNA. If the extra DNA is in the larger *Pst*I or *Bam*HI fragments, then the differences in migration of the fragments in an agarose gel may not be detected. The toxin plasmid from Weybridge UM44-1 contains an extra *Pst*I fragment approx. 4.1 kb in size and extra *Eco*RI fragments approx. 2.9 and 1.2 kb in size. The origins or locations of these extra pieces of DNA observed in pXO1 from Weybridge, Weybridge UM44-1, PM36-R1, and Vollum V770 have not been determined.

Analysis of the *Pst*I restriction map of the 34.8-kb *Bam*HI fragment of pXO1.1 (Weybridge A UM23). As reported in the Midterm Report (22), *Bam*HI, *Bam*HI-*Sal*I, and *Pst*I restriction maps had been constructed for a 77-kb region of pXO1.1 (Weybridge A UM23) encompassing the toxin structural genes. Results from DNA-DNA hybridization analysis with the altered 34.8-kb *Bam*HI-*Sal*I fragments of

pXO1.1::Tn*917* from tp21 and tp39 showed that the large *Bam*HI fragments hybridized to a 2.8- and 0.6-kb *Pst*I fragment not observed in previous restriction analyses.

Since the earlier analyses of the 34.8-kb *Bam*HI fragment were done, we have made improvements in electroelution methods that have increased the yield of large restriction fragments and in Southern transfer techniques that have increased the amount of smaller fragments adhering to the nylon membrane. Thus, restriction analysis and DNA-DNA hybridization analysis could be used with greater confidence to confirm whether the 0.6-kb and 2.8-kb *Pst*I fragments were contained within the 34.8-kb *Bam*HI fragment and to determine the location of these fragments within the large *Bam*HI fragment. The 34.8-kb *Bam*HI fragment was isolated from pXO1.1::Tn*917* (tp1A) by electroelution. The plasmid derivative from tp1A contains Tn*917* within the 38.7-kb *Bam*HI fragment which causes this altered fragment to migrate much slower than the 34.8-kb fragment in a 0.3% agarose gel, allowing better separation of the two large fragments. Because contamination of the 34.8-kb fragment with the 38.7-kb fragment has been a problem in the past, a much cleaner preparation of the 34.8-kb fragment could be isolated from pXO1.1::Tn*917* (tp1A). The 34.8-kb *Bam*HI fragment was digested with *Pst*I and the restriction pattern was determined by agarose gel electrophoresis. The 34.8-kb *Bam*HI fragment was shown to contain a 9.3-, 6.6-, 6.3-, 5.2-, 4.5-, 0.6-, and 0.3-kb *Pst*I fragment. As determined from the sequence of *pag* (30), the 6.0-kb *Pst*I fragment which contains *pag* should have a *Bam*HI site generating two fragments approx. 1.5 kb and 4.5 kb in size. Based on this information, the 4.5-kb fragment observed above should correspond to the 6.0-kb *Pst*I fragment. Thus, the 0.3-kb fragment should be part of the 2.8-kb *Pst*I fragment.

Restriction analysis of the small plasmid derivative of tp71 was used to determine whether the 0.3-kb fragment found in the 34.8-kb *Bam*HI fragment was part of the 2.8-kb *Pst*I fragment. Previous restriction analyses of the small plasmid derivative of tp71 showed that the plasmid had two *Bam*HI sites, generating an intact 34.8-kb fragment and a 13.9-kb fragment which contained Tn*917*. Restriction analysis also showed that the plasmid contained a 16-, 9.3-, 6.6-, 6.3-, 5.2-, 2.8-, and 0.6-kb *Pst*I fragment. The 2.8-kb *Pst*I fragment should be within one of the two *Bam*HI fragments of this plasmid. The 13.9-kb *Bam*HI fragment was isolated and digested with *Pst*I. Restriction analysis showed that an 11-kb and a 2.6-kb fragment were located within this *Bam*HI fragment. These results suggested that the 2.8-kb *Pst*I fragment contained a *Bam*HI restriction site generating a junction fragment approx. 0.2 to 0.3 kb in size corresponding to the end of the 34.8-kb *Bam*HI fragment.

To determine the location of the 0.6-kb *Pst*I fragment within the 34.8-kb *Bam*HI fragment, the 9.8-kb *Bam*HI-*Sal*I fragment of pXO1::Tn*917* (tp36) was digested with *Pst*I. The insertion of Tn*917* within the plasmid derivative from tp36 has been shown to be within the 6.3-kb *Pst*I fragment. *Sal*I digestion of the Tn*917*-containing *Bam*HI fragment generates two *Bam*HI-*Sal*I fragments approx. 33 and 9.8 kb in size. The *Pst*I restriction pattern of the 9.8-kb *Bam*HI-*Sal*I fragment showed that a *ca.* 9.0-kb fragment corresponding to the altered 6.3-kb *Pst*I fragment and a 0.6-kb fragment were observed. To confirm these results, the 9.8-kb fragment was labelled with digoxigenin-labelled dUTP and used in DNA-DNA hybridizations with *Bam*HI-

and *Pst*I-digested pXO1.1 (Weybridge A UM23). The 9.8-kb fragment hybridized to the 34.8-kb *Bam*HI fragment and the 6.3-, 2.8-, and 0.6-kb *Pst*I fragments. In addition, previous restriction analysis of the Tn*917*-tagged plasmids from tp2A and tp36 showed that the Tn*917* insertions were within the same 1.1-kb *Eco*RI fragment within the 34.8-kb *Bam*HI fragment and the locations of the insertions were approx. 0.1 kb apart (discussed below). Tn*917* was also shown to have inserted within the 5.2-kb *Pst*I fragment of the plasmid from tp2A and the 6.3-kb *Pst*I fragment of the plasmid from tp36. These results suggested that the 0.6-kb *Pst*I fragment was not located between the 5.2-kb and 6.3-kb *Pst*I fragments, but that it was located between the 6.3-kb and 2.8-kb *Pst*I fragments. The order of the *Pst*I fragments within the 34.8-kb *Bam*HI fragment is shown in Fig. 1.

EcoRI restriction mapping of pXO1.1 (Weybridge A). The *Eco*RI restriction map of pXO1.1 (Weybridge A UM23) was constructed to obtain a more precise location of the junction fragments of the inverted segment. The locations of many of the *Eco*RI fragments between the 5.6-kb fragment containing a portion of *lef* and the 3.1-kb fragment located upstream of *cya*, as shown in Fig. 1, were determined from DNA-DNA hybridization analyses with the cloned toxin structural genes. In addition the locations of the *Eco*RI restriction sites within the toxin structural genes were extrapolated from the sequences of each of these genes (2, 16, 30).

Based on restriction analysis of the Tn*917*-tagged deletion derivatives of tp21 and tp39, the deleted 5.6- and 3.1-kb *Eco*RI fragments were determined to be nested within the 13.9-kb *Bam*HI fragment. As shown in Table 3, the 8.5-kb *Bam*HI-*Sal*I fragment of pXO1.1::Tn*917* (tp21) hybridized to the 8.0- and 3.1-kb *Eco*RI fragments, suggesting that the 3.1-kb fragment lies adjacent to the 8.0-kb *Eco*RI fragment and the 5.6-kb fragment lies between the 3.1- and 6.2-kb *Eco*RI fragments (Fig. 1).

Restriction analysis was used to identify and localize the *Eco*RI restriction sites within the 14.6-kb *Bam*HI fragment. To obtain a preparation of the 14.6-kb fragment that was relatively free of the closely migrating 13.9-kb fragment, the 14.6-kb *Bam*HI fragment was isolated from pXO1.1::Tn*917* (tp29), a plasmid derivative containing Tn*917* within the 13.9-kb *Bam*HI fragment. The 14.6-kb fragment was digested with *Eco*RI or *Cla*I or double digested with both of these enzymes. The restriction digestion of the 14.6-kb fragment is shown in Table 6 and the probable location of the restriction sites are depicted in Fig. 2 (below Table 6). As will be discussed below, the 5.4-kb *Eco*RI fragment containing a junction of the inversion is cut by *Cla*I, generating two fragments approx. 4.0 and 1.5 kb in size. Based on the locations of the 8.0-, 3.1 -, and 1.05-kb *Eco*RI fragments within the 7.4-kb *Bam*HI fragment, the 3.1-kb *Eco*RI fragment (not to be confused with the 3.1-kb fragment lying downstream of *cya*, Fig.1) should contain a *Bam*HI site generating a 1.8- and 1.3-kb *Bam*HI-*Eco*RI fragment. The 1.3-kb *Bam*HI-*Eco*RI fragment should be the junction fragment of the 14.6-kb *Bam*HI fragment. As shown in Fig. 2, the results from the digestion of the 14.6-kb *Bam*HI fragment with *Eco*RI and *Cla*I suggested that the 5.4-kb fragment lies adjacent to the 3.1-kb *Eco*RI fragment (shown as the 1.3-kb *Bam*HI-*Eco*RI fragment). Since the 4.2-kb *Eco*RI fragment

does not contain a *Cla*I site, then it must be adjacent to the 5.4-kb *Eco*RI fragment. The origin of the 3.2-kb *Bam*HI-*Eco*RI junction fragment has not been determined.

With the exception of the 5.6-, 5.4-, and 0.8-kb *Eco*RI fragments which hybridized to *lef*, the locations of *Eco*RI restriction sites within the 34.8-kb *Bam*HI fragment of pXO1.1 (Weybridge A UM23) were determined by restriction analyses and DNA-DNA hybridization analyses. The *Eco*RI restriction pattern within the 9.3-kb *Pst*I fragment was determined for the cloned 9.3-kb fragment of pJMH28. Insertion mutants, UM23 tp2A, tp36, and tp62, have Tn*917* insertions in various locations within the 34.8-kb *Bam*HI fragment. *Sal*I which cleaves within Tn*917* but not within the 34.8-kb fragment has allowed the isolation of various regions of the large *Bam*HI fragment that can be used for further analysis. To determine the size of the *Eco*RI restriction fragment between the LF structural gene and the 9.3-kb *Pst*I fragment, the *lef*-containing 15-kb *Bam*HI-*Sal*I fragment of the plasmid derivative from tp62 was digested with *Eco*RI and the results are listed in Table 7. *Eco*RI digestion of the 15-kb *Bam*HI-*Sal*I fragment generated 5.6-, 4.0-, 3.3-, 0.8-, and 0.72-kb fragments. Based on the sequence of *pag* (30), we deduced that the 5.4-kb *Eco*RI fragment which contains the 3' end of the PA structural gene as well as the 3' end of the LF structural gene contains a *Bam*HI site, generating two fragments approx. 3.9 and 1.5 kb in size. Thus, the 4.0-kb fragment observed in the 15-kb *Bam*HI-*Sal*I fragment is most likely part of the 5.4-kb *Eco*RI fragment. The 5.6- and 0.8-kb *Eco*RI fragments corresponded to the other fragments that hybridized to the *lef* probe. As discussed previously, the location of the Tn*917* insertion within the plasmid derivative from tp62 was 0.7 kb within the 9.3-kb *Pst*I fragment (22). Restriction analysis of this fragment from pJMH28 showed that the *Eco*RI restriction site of the 1.2-kb *Eco*RI fragment is located near the *Pst*I restriction site of the 9.3-kb fragment near the site of Tn*917* insertion. Therefore, the 3.3-kb fragment should correspond to the 2.7-kb *Sal*I arm of Tn*917* plus a 0.7-kb region of the 1.2-kb *Eco*RI fragment. From these results, the location of the 0.72-kb fragment was determined to be between the 5.6-kb and 1.2-kb *Eco*RI fragments. The locations of these fragments are depicted in Fig. 1.

The locations of the *Eco*RI restriction sites to the right of the 2.4-kb *Eco*RI fragment within the 34.8-kb *Bam*HI fragment and the 9.3-kb *Pst*I fragment, shown in Fig. 1, were determined by restriction analysis of the 24-kb *Bam*HI-*Sal*I fragment of the plasmid from tp62 and the 9.8-kb *Bam*HI-*Sal*I fragments of the plasmids from UM23 tp2A and tp36. The results of these restriction analyses are summarized in Table 7. Digestion of all three of the *Bam*HI-*Sal*I fragments with *Eco*RI generated some fragments that do not correspond to *Eco*RI fragments of wild-type pXO1.1 (Weybridge A UM23). Fragments approx. 3.1 or 3.2 kb in size were observed in all three of the *Bam*HI-*Sal*I fragments that corresponded to *Sal*I digestion of a Tn*917*-containing *Eco*RI fragment. Digestion of the Tn*917*-containing 6.8-kb *Eco*RI fragment (1.2-kb *Eco*RI fragment plus Tn*917* [5.6 kb]) of the plasmid derivative from tp62 with *Sal*I generated an *Eco*RI-*Sal*I fragment in the 24-kb *Bam*HI-*Sal*I fragment that is approx. 3.1 kb in size. Similarly, digestion of the Tn*917*-containing 6.7-kb *Eco*RI fragments (1.1-kb *Eco*RI fragment plus Tn*917* [5.6 kb]) of the plasmid derivatives from tp2A and tp36 with *Sal*I generated *Eco*RI-*Sal*I fragments in each of the 9.8-kb *Bam*HI-*Sal*I fragments

that are approx. 3.2 and 3.1 kb in size, respectively. These results provided evidence that the Tn*917* insertions in the plasmids from tp2A and tp36 are approx. 0.1 kb apart.

A 2.1- to 2.2-kb fragment was observed when the *Bam*HI-*Sal*I fragments of the plasmid derivatives from UM23 tp2A, tp36, and tp62 were digested with *Eco*RI. Since these fragments do not correspond to any *Eco*RI fragments of wild-type pXO1 (Weybridge A UM23), they are most likely the *Eco*RI-*Bam*HI junction fragments. Thus, results from digestion of the 9.8-kb *Bam*HI-*Sal*I fragments of the plasmids from tp2A and tp36 suggested that the 4.3-kb *Eco*RI fragment is adjacent to the 2.2-kb junction fragment and the 1.1-kb *Eco*RI fragment is adjacent to the 4.3-kb *Eco*RI fragment. The origin of the 2.2-kb junction fragment has not been confirmed; however, results from DNA-DNA hybridization of *Eco*RI-digested pXO1 (Weybridge A UM23 or Sterne) with the digoxigenin-labelled 9.8-kb *Bam*HI-*Sal*I fragment of the plasmid derivative from tp36 suggested that the junction fragment may correspond to a 7.0-kb *Eco*RI fragment.

The *Eco*RI fragments generated by *Eco*RI digestion of the 24-kb *Bam*HI-*Sal*I fragment of pXO1::Tn*917* (UM23 tp62) were 7.3, 4.3, 3.1, 2.4, 2.1, 1.9, 1.1, 0.75, and 0.7 kb in size (Table 7). The locations of the 4.3-, 3.1-, 2.1-, and 1.1-kb fragments were discussed above. The locations of the 2.4-, 1.9-, 0.75- (rounded off to 0.8 in Fig. 1), and 0.7-kb *Eco*RI fragments were determined by restriction analysis of the 9.3-kb insert of pJMH28. By process of elimination, the 7.3-kb *Eco*RI fragment must be located between the 2.4- and 1.1-kb *Eco*RI fragments. The order of the *Eco*RI fragments within the 34.8-kb *Bam*HI fragment is shown in Fig. 1.

Cloning of the *Eco*RI fragments of pXO1.1 (Weybridge A) and pXO1 (Sterne) encompassing the junctions of the inverted segment. The restriction patterns of *Eco*RI-digested pXO1 (Sterne) and pXO1.1 (Weybridge A UM23) showed that pXO1 from Sterne contained 3.1- and 4.8-kb *Eco*RI fragments differing from the 2.4- and 5.4-kb *Eco*RI fragments found in pXO1.1 from Weybridge A UM23 (9). These observations suggested that these *Eco*RI fragments of pXO1.1 (Weybridge A UM23) and pXO1 (Sterne) contain the junctions of the inverted segment. Since most of the *Eco*RI fragments existed as doublets or triplets, we decided to shotgun clone the *Eco*RI restriction fragments and isolate the cloned fragments of interest. The regions of the agarose gel containing the 3.1- and 4.8-kb *Eco*RI fragments from pXO1 (Sterne) and the 2.4- and 5.4-kb *Eco*RI fragments from pXO1.1 (Weybridge A UM23) were gel purified and ligated into pBluescriptIIKS(+). The ligation mixture was introduced into MAX efficiency *E. coli* DH5α competent cells by transformation.

Recombinant plasmids containing the 3.1-kb *Eco*RI fragment from pXO1 (Sterne) and the 2.4-kb *Eco*RI fragment from pXO1.1 (Weybridge A UM23) were isolated based on similarities in the *Cla*I, *Sst*I, and *Hin*dIII restriction patterns. Two transformants containing recombinant plasmids carrying a 3.1-kb and a 2.4-kb *Eco*RI fragment were isolated and constructs were designated pJMH4 and pJMH5. Partial restriction maps of pJMH4 and pJMH5 with *Cla*I, *Hin*dIII, *Sst*I, and *Eco*RI are shown in Fig. 3. The 2.4-kb *Eco*RI insert contained a *Cla*I-*Eco*RI fragment approx. 0.8-kb in size which differed from the 1.5-kb *Cla*I-*Eco*RI fragment found in the 3.1-kb *Eco*RI insert. The difference of 0.7 kb in the sizes of the *Cla*I-*Eco*RI

fragments corresponded to the difference in the sizes of the two *Eco*RI fragments. The *Cla*I-*Eco*RI fragments of the two *Eco*RI inserts are depicted above the crosshatched boxes in Fig. 3.

Recombinant plasmids containing the 4.8-kb *Eco*RI fragment from pXO1 (Sterne) and the 5.4-kb *Eco*RI fragment from pXO1.1 (Weybridge A UM23) were isolated based on results from DNA-DNA hybridization analysis using digoxigenin-labelled 19-kb *Pst*I fragment from pXO1 (Sterne) as a probe. Restriction analysis of the cloned 9.3-kb *Pst*I fragment from pXO1.1 (Weybridge A UM23) showed that the 2.4-kb *Eco*RI fragment is nested within the 9.3-kb *Pst*I fragment. As discussed previously, the 9.3-kb *Pst*I fragment shares homology with the 8.6-kb *Pst*I fragment of pXO1 from Sterne (8 9 22). Since the 2.4-kb fragment showed similarities in restriction patterns to those of the 3.1-kb *Eco*RI fragment of pXO1 (Sterne), then the 3.1-kb fragment must be nested within the 8.6-kb *Pst*I fragment of pXO1 (Sterne). Thus, the 4.8-kb *Eco*RI fragment should be nested within the 19-kb *Pst*I fragment of pXO1 (Sterne) and should share homology with the 5.4-kb *Eco*RI fragment from pXO1.1 (Weybridge A UM23).

The 19-kb *Pst*I fragment of pXO1 (Sterne) hybridized to a recombinant plasmid containing a 4.8-kb *Eco*RI insert designated pJMH10 and to one recombinant plasmid containing a 5.4-kb insert designated pJMH9. As shown in Fig. 3, the locations of the *Ava*I, *Hin*dIII, *Eco*RV, and *Kpn*I restriction sites were similar for each insert. Similar to the 2.4- and 3.1-kb *Eco*RI inserts, the 5.4- and 4.8-kb *Eco*RI inserts contained a 1.5-kb and a 0.8-kb *Cla*I-*Eco*RI fragment, respectively, corresponding to the differences in the sizes of the two inserts (see region of pJMH9 and pJHM10 above crosshatched boxes in Fig. 3). Interestingly, these results suggested that the 1.5-kb *Cla*I-*Eco*RI fragment of the 3.1-kb *Eco*RI fragment of pXO1 (Sterne) may be homologous to that of the 5.4-kb *Eco*RI fragment of pXO1.1 (Weybridge A UM23) and the 0.8-kb *Cla*I-*Eco*RI fragment of the 4.8-kb *Eco*RI fragment of pXO1 (Sterne) may be homologous to that of the 2.4-kb *Eco*RI fragment of pXO1.1 (Weybridge A UM23).

Subcloning of the cloned *Eco*RI fragments of pXO1.1 (Weybridge A) and pXO1 (Sterne) containing the junctions of the inverted segment. Although pXO1 (Sterne) and pXO1.1 (Weybridge A UM23) exhibited differences in *Pst*I, *Bam*HI, and *Eco*RI restriction patterns, no differences were observed in the *Cla*I restriction patterns of these plasmids (data not shown). The difference in the *Cla*I-*Eco*RI fragments of the 2.4-kb and 3.1-kb inserts and of the 5.4-kb and 4.8-kb inserts suggested that the inversion occurred at or near the *Cla*I restriction site. To isolate smaller fragments containing the junctions of the inverted toxin-encoded region of pXO1, the 1.0-kb *Hin*dIII fragment of pJMH4, the 1.7-kb *Hin*dIII fragment of pJMH5, the 2.7-kb *Kpn*I fragment of pJMH9, and the 1.9-kb *Kpn*I fragment of pJMH10 (depicted by the crosshatched boxes in Fig. 3) were subcloned into pBluescriptIIKS(+). The orientation of the inserts was determined by restriction analysis with *Cla*I. Transformants were isolated containing recombinant plasmids carrying each of the subcloned fragments in either orientation and the recombinant plasmids were designated pJMH12 to pJMH26. Partial restriction maps of pJMH12, pJMH16, pJMH20, and pJMH24 are shown in Fig. 4.

DNA-DNA hybridization analysis of pXO1.1 (Weybridge A) and pXO1 (Sterne) with the cloned junction fragments of the inverted toxin-encoding region. To confirm that the junctions of the inverted segment in each plasmid had been cloned, the 2.7-kb *Kpn*I fragment of pJMH12 and the 1.0-kb *Hin*dIII fragment of pJMH24 that originated from the 5.4-kb and 2.4-kb *Eco*RI fragments of pXO1.1 (Weybridge A UM23), respectively, as well as the 1.9-kb *Kpn*I fragment of pJMH16 and the 1.7-kb *Hin*dIII fragment of pJMH20 that originated from the 4.8-kb and 3.1-kb *Eco*RI fragments of pXO1 (Sterne), respectively, were used in DNA-DNA hybridizations of *Bam*HI-, *Pst*I-, and *Eco*RI-digested pXO1.1 from Weybridge A UM23 and pXO1 from Sterne under high stringency conditions. The results of these hybridization experiments are shown in Table 8. As depicted in Fig. 5, the junctions of the inverted segment in pXO1.1 (Weybridge A UM23) are contained within the 34.8- and 14.6-kb *Bam*HI fragments, the 18.7- and 9.3-kb *Pst*I fragments, and the 5.4- and 2.4-kb *Eco*RI fragments. Likewise, the junctions of the inverted segment in pXO1 (Sterne) are contained within the 29- and 19.5-kb *Bam*HI fragments, the 19- and 8.6-kb *Pst*I fragments, and the 4.8- and 3.1-kb *Eco*RI fragments.

As expected, each subcloned fragment originating from one pXO1 plasmid hybridized to the two restriction fragments of the other pXO1 plasmid containing the junctions of the inverted segment. For example, the 2.7-kb *Kpn*I fragment of the 5.4-kb *Eco*RI fragment of pXO1.1 (Weybridge A UM23) hybridized to the 4.8- and the 3.1-kb *Eco*RI fragments of pXO1 (Sterne) because the 2.7-kb fragment contains regions that are homologous to both *Eco*RI fragments of pXO1 (Sterne). In addition, each subcloned fragment not only hybridized to the *Eco*RI fragment from which it originated, but it also hybridized to the *Eco*RI fragment of the same plasmid containing the other junction of the inverted toxin-encoding region. In the example above, the 2.7-kb *Kpn*I fragment hybridized not only to the 5.4-kb *Eco*RI fragment of pXO1.1 (Weybridge A UM23), but it also hybridized to the 2.4-kb *Eco*RI fragment of the same plasmid. These results suggested that the ends of the inverted segment encompassing the toxin genes may be inverted repeats. Because of the high stringency conditions used in the hybridizations, these results also suggested that the sequences of the inverted repeats may be a perfect or near perfect match.

Determination and analysis of the sequences of the cloned junctions fragments of the inverted segments of pXO1.1 (Weybridge A) and pXO1 (Sterne). The sequencing strategies for determining the sequences of the cloned junction fragments of the inverted segments of pXO1.1 (Weybridge A UM23) and pXO1 (Sterne) are shown in Fig. 6. The cloned inserts of pJMH28 (9.3-kb *Pst*I insert containing WeyAR), pJMH4 (2.4-kb *Eco*RI insert, WeyAR), and pJMH5 (3.1-kb *Eco*RI insert, SterneR) and the subcloned inserts of pJMH12 (WeyAL), pJMH24 (WeyAR), pJMH16 (SterneL), and pJMH20 (SterneR) were sequenced using the dideoxy chain termination method of Sanger et al. (19). Synthetic oligonucleotide primers were used to extend the sequence of each of the cloned inserts. The letter "L" or "R" is attached to the cloned fragment designation, i.e. WeyAL, to represent the left or right inverted repeat flanking the toxin-encoding region of pXO1 as depicted in Fig. 5. WeyAL and WeyAR originated from the 5.4- and 2.4-kb *Eco*RI

fragments of pXO1 (Weybridge A), respectively, and SterneL and SterneR originated from the 4.8- and 3.1-kb *Eco*RI fragments of pXO1 (Sterne), respectively.

The sequences obtained for the junction fragments are shown in Figs. 7 to 10. In all instances, the sequence begins at or near the *Eco*RI restriction site and proceed past the *Cla*I restriction site. The sequences were determined for both strands and analyzed by the Pileup and Bestfit programs of the GCG package software. We found that the ends of the inverted segments of pXO1.1 (Weybridge A UM23) and pXO1 (Sterne) are flanked by imperfect 1336-bp inverted repeats. As shown in Fig. 11, the results of the Bestfit of the sequences of WeyAL and WeyAR revealed several basepair mismatches and deletions. A 68-bp gap was discovered in the sequence of WeyAL inverted repeats. Analysis of the sequence of WeyAR inverted repeat (nt1168 to nt1236, Fig. 11) revealed a direct repeat sequence. Recombination of these direct repeats may have resulted in the 68-bp deletion in the WeyAL inverted repeat. A 13-bp gap was observed in the WeyAR inverted repeat corresponding to nt1930 to nt1942 in WeyAL inverted repeat. Analysis of the sequences at the ends of each of WeyAL and WeyAR revealed an imperfect 19-bp inverted repeat in WeyAR and an imperfect 28-bp inverted repeat in WeyAL (shown in Figs. 3, 4, and 7). The 19-bp inverted repeats of WeyAR are deletion derivatives of the 28-bp inverted repeats of WeyAL. These results suggest that WeyAL and WeyAR may be IS elements; however no target duplications were observed in the sequence.

As shown in Fig. 12, a Bestfit analysis of the sequences of SterneL and SterneR inverted repeats revealed similarities in the basepair mismatches and deletions observed for WeyAL and WeyAR shown in Fig. 11. The analysis of the patterns of the mismatches and deletions within the sequences of WeyAL, WeyAR, SterneL, and SterneR provided evidence that the inversion occurred within the inverted repeats at or near the *Cla*I restriction sites. A probable site of the inversion is illustrated in Fig. 13. The imperfect 19-bp inverted repeat shown for WeyAR was found at the ends of SterneR (Fig. 8, 10). Similar to WeyAL, SterneL may have the imperfect 28-bp inverted repeats at both ends (depicted in Fig. 9); however, the complete sequence for the right 28-bp inverted repeat (see Fig. 6 and beginning of Fig. 9) was not determined because no fragment within this region of pXO1 (Sterne) had been cloned.

The sequences of the four cloned junction fragments were analyzed with the Frames program of the GCG package to determine the location of any ORFs. The locations of the ORFs as well as the directions of transcription are shown in Fig. 14. Two major ORFs (ORF1 and ORF2) exist in WeyAR, ORF1 exists in SterneL, a shorter ORF1 exists in WeyAL, and ORF2 and a shorter ORF1 exist in SterneR. The beginnings and ends of the ORFs are also shown in Figs. 7 to 10. ORF1 appears to code for the same protein in all instances except that ORF1 terminated earlier in WeyAL and SterneR because of a frameshift mutation caused by the deletion of a T (nt535 WeyAR and nt286 SterneR, Fig. 11 and 12). Thus, ORF1 in WeyAR and SterneL is approx. 822 bp in size and may encode a protein approx. 274 aa in size. The truncated ORF1 in WeyAL and SterneR is comprised of 642 bp and may encode a protein approx. 214 aa in size.

The nucleotide sequence of the 822-bp ORF was used to search the GenBank and EMBL databases. The results revealed that the sequence shared a 56% identity with those of *Mycoplasma hyopneumoniae* ORF1 and ORF2 of a genetic element that Ferrell et al. (4) reported resembles a procaryotic insertion sequence, and *Mycoplasma hyorhinis* GDL-1 repeat region. The deduced amino acid sequence of the 822-bp ORF was then used to search the PIR-Protein and Swiss-Prot databases. The results showed that the deduced peptide shares homology with peptide sequences of probable transposases of *E. coli* IS*150* (an IS*3*-related element) and IS*150*-related elements, e.g. *Streptococcus agalactiae* IS*861*. In addition, the translated product of the 822-bp ORF also exhibited homology to IS*3* and other IS3-related transposases. The translated product of the 642-bp ORF also exhibited homology to IS*150* and IS*3*; however, the product exhibited some differences at the carboxy terminus suggesting that the truncated ORF1 may encode a truncated transposase. Preliminary results from a Bestfit analysis of the 274-aa translated product showed that it exhibited a 42% identity and 60% similarity with IS*150* ORFB translated product (thought to be a transposase) and a 31% identity and 52% similarity with the IS*3* probable transposase.

A GenBank search of the nucleotide sequence of ORF2 (234 bp) and a SwissProt search of the putative amino acid sequence of ORF2 (78 aa) did not reveal any sequences or proteins of significance. Since ORF2 is immediately upstream of ORF1 and shifted by one base, then the two ORFs may encode a transframe protein composed of the product of ORF2 fused to that of ORF1. This phenomenon, known as translational frameshifting, is used by bacterial insertion sequences, e.g. IS*1*, IS*150*, and IS*911*, as a method of controlling transposition (3). Since the putative transposase encoded by ORF1 in WeyAR shares homology with IS*150*, then transposition of the putative IS element (WeyAR) of pXO1 may also be controlled by translational frameshifting. Further analysis would be necessary to determine whether ORF1 and ORF2 encode functional genes or encode a transframe protein.

Distribution of inverted repeats. DNA-DNA hybridization of genomic DNA from *B. anthracis* with the 1.0-kb *Eco*RI-*Hin*dIII subcloned fragment of pJMH24 (WeyAR inverted repeat, subcloned from the 2.4-kb *Eco*RI fragment of pXO1 from Weybridge A UM23) was used to determine whether the inverted repeats can be detected in the chromosome and pXO2. Total genomic DNA was isolated from *B. anthracis* Weybridge A UM23 ($pXO1^+$, $pXO2^-$), Weybridge A UM23-2 ($pXO1^-$, $pXO2^-$), and Pasteur 4229 UM12 ($pXO1^-$, $pXO2^+$). The 1.0-kb *Eco*RI-*Hin*dIII insert of pJMH24 was chosen as the DNA probe because it contains only DNA of the WeyAR inverted repeat with no extraneous DNA of pXO1. The results of the DNA-DNA hybridizations showed that the inverted repeat of WeyAR hybridized only to pXO1 and not to the chromosome or pXO2 (data not shown). Thus, these inverted repeats appear to be located only on pXO1. Although a putative transposase gene is present within the inverted repeats, the elements do not appear to transpose to other regions of the genome.

Lack of correlation of observed phenotypes with orientation of the inverted segment. As discussed in the Midterm Report (22), differences between Sterne and Weybridge A UM23 in the pXO1-

associated phenotypes, i.e., extent and rate of sporulation, ability to grow on minimal medium, and sensitivity to bacteriophage CP-51, did not correlate with the orientation (α or β) of the toxin-encoding region of pXO1. The amounts of PA, LF, and EF produced by *B. anthracis* Weybridge UM44-1, Weybridge A UM23, and Sterne in the presence or absence of bicarbonate were determined. The results, as shown in Table 9, varied between experiments; however, no significant differences in the amounts of PA, LF, or EF produced by these strains were apparent. Thus, we have been unable to demonstrate any phenotypic effects of the two orientations of the inverted segment.

III. Physical and genetic analysis of the *B. anthracis* capsule plasmid pXO2

Until recently *B. anthracis* strains harboring pXO2 could be divided into three groups with respect to capsule phenotype; (i) strains that produce capsule only when grown on media containing bicarbonate and incubated in a CO_2-rich atmosphere (Cap^{c+}, wild-type phenotype); (ii) mutants that produce capsule when grown in air in the absence of bicarbonate (Cap^{a+} phenotype); and (iii) mutants that are noncapsulated under all growth conditions yet retain pXO2 (Cap^- phenotype). Utilization of the temperature-sensitive transposition selection vector pTV1 has allowed the isolation of a collection of pXO2::Tn*917* derivatives. In addition to the mutant phenotypes described above, insertion mutants exhibit the following phenotypes: (i) Mutants that produce greater amounts of capsular material than does wild type in the presence of bicarbonate and CO_2; (ii) Mutants that are CO_2-independent for capsule synthesis and whose growth is inhibited by bicarbonate; (iii) Mutants that are Cap^+ when grown in air, and whose growth is inhibited by CO_2; (iv) Mutants that require CO_2 for growth and are Cap^+ in the presence of CO_2 and bicarbonate.

Although pXO2 has been demonstrated to be involved in capsule synthesis by *B. anthracis* (5, 28) and although some, if not all, of the structural genes have been cloned (12), little is known regarding possible regulatory genes which may be present on the plasmid. However, Vietri, et al. (29) recently reported the identification of a regulatory gene involved in capsule synthesis. The phenotypes of some of our insertion mutants suggest that Tn*917* may be inserted in sequences involved in bicarbonate regulation of capsule synthesis.

Efforts in my laboratory have been concentrated on characterization of insertion mutants of pXO2. Restriction analysis with different enzymes has been conducted to narrow the location of the putative regulatory regions and they have revealed four regions that may contain sequences responsible for regulation of capsule synthesis. The work reported in the Midterm Report (22) is summarized below and followed by details of more recent results. For reference, a map of pXO2 is shown in Fig. 15.

Restriction analyses of the Tn*917*-tagged pXO2 derivatives from *B. anthracis* 4229 UM12. To locate the insertions in the pXO2::Tn*917* derivatives restriction analyses with several restriction endonucleases were performed. The results showed that Tn*917* inserted into a number of different sites in

pXO2. The locations of Tn*917* were confirmed in all cases by DNA-DNA hybridizations using digoxigenin-labelled Tn*917* as a probe. Results obtained from *Eco*R1 digestions, *Hin*dIII digestions, and *Cla*I digestions, which are detailed in tabular form in the Midterm Report (22), made it possible to locate more precisely the Tn*917* insertions on the pXO2 restriction map reported by Robertson et al. (15). Based on this map as a reference, in nine of eleven mutants in which the capsule phenotype was altered, Tn*917* appeared to have inserted into regions of pXO2 which are external to the *cap* structural genes. Specifically, in tp21, tp24, tp49, tp58, and tp60 a 6.3-kb *Eco*RI fragment and in tp18 and tp20 a 2.8-kb *Hin*dIII appeared to have regions involved in regulation of capsule synthesis. In the remaining two insertion mutants that had an altered capsule phenotype, i.e., tp22 and tp59, the transpososn was located in a 1.5-kb and a 1.3-kb *Hin*dIII fragment, respectively. These two fragments are widely separated on the pXO2 map. The 6.3-kb *Eco*R1 fragment has been shown to be nested within the 13-kb *Hin*dIII fragment and to be part of the 10.5-kb *Cla*I fragment, narrowing the location of the putative regulatory region.

Analysis of insertion mutants that appear to be polypeptide overproducers. Insertion mutants tp49, tp50, and tp60 appeared to be polypeptide overproducers. The stringy properties of their colonies, the confluent growth they form on agar plates, and the loss of capsular material in a short period of time resemble polypeptide production by *B. licheniformis*. Tn*917* has been shown by DNA-DNA hybridization experiments to be located in the chromosome of tp50 and in the capsule plasmid of tp49 and tp60. The phenotype of tp60 is different from that of tp49 and tp50 in that tp60 is CO_2-independent for synthesis of capsular material. However, it overproduces capsular material only when it is grown in the presence of CO_2. Restriction analysis of plasmid DNA from strains tp49 and tp60 show the same restriction pattern with insertion of Tn*917* within the same fragment. To determine whether the orientation of Tn*917* might account for the difference in these phenotypes, the orientation of Tn*917* was determined by probing the *Hin*dIII-digested plasmids with the *Ava*I arms of Tn*917*. The results showed that Tn*917* is in the same orientation in pXO2 from both of these mutants.

Colonies of the mutants that are overproducers of glutamyl polypeptide are extremely mucoid and they spread over the agar surface much more than do colonies of the encapsulated wild-type. As noted above, the capsular material produced by the mutants appears to "dry up" after a rather short time of incubation. It appeared to us that the material was probably being degraded. This is characteristic of *B. licheniformis* strains which produce glutamyl polypeptide and which also produce a peptidase that hydrolyzes the peptide to free glutamic acid. An analogous enzyme has not been shown to be produced by *B. anthracis*. It should be pointed out, however, that recently Uchida, et al. (27) reported the occurrence of an enzyme produced by *B. anthracis* which degrades capsular poly-D-glutamic acid to smaller fragments. Unlike the enzyme from *B. licheniformis* the *B. anthracis* enzyme apparently did not degrade the peptide to free glutamic acid.

Results of our further experiments on the phenomenon reported above, which appeared to be complete degradation of capsular material by the over-producing mutants, have suggested another

possibility. We observed that when cells were grown on top of a dialysis membrane spread over the agar surface, the capsular material was still produced in large quantities but it did not "dry up" or disappear in the way that it appeared to when cells were grown directly on the agar surface. It now seems to us that in the overproducing mutants the capsular material is not "contained" in the same way that it is in wild-type cells, and it is therefore free to diffuse into the agar medium. However, when a dialysis membrane separates the cells from the agar surface, the material can not go through the membrane and thus persists on the surface. These observations and interpretations suggest that the capsule of wild-type *B. anthracis* contains more than glutamyl polypeptide.

Quantitative determination of glutamyl polypeptide produced by overproducing mutants. To conduct quantitative determinations on the composition and amount of capsular material produced by the over-producing mutants described above, it was desirable to have a synthetic medium that would support capsule formation and polypeptide synthesis to the extent that many natural media do. Strain 4229 does not grow on minimal XO medium and it grows poorly on minimal IB, which is a suitable medium for growth of some strains. However, this strains grows well and produces capsular material on minimal IIIB (see Materials and Methods).

Dialysis membranes were placed on minimal IIIB-$NaHCO_3$ agar plates and three loopfuls of cells grown on $LPACO_3$ medium (for wild-type strain) and $LPACO_3$ containing erythromycin and lincomycin (for mutants) were spread on each of three plates. One set of three plates was incubated at 37°C in 20% CO_2 for 24 hours and another set was incubated under the same conditions for 48 hours. After incubation the membranes from three plates were removed from the agar surface with forceps, placed in a beaker containing 35 ml of distilled water, and autoclaved for 30 minutes at 121°C to extract the peptide. After autoclaving, the membranes were discarded and cells were removed by centrifugation. The supernatant samples were analyzed for glutamyl polypeptide by determining free glutamic acid (by paper chromatography) before and after acid hydrolysis (25, 10). Results from these experiments showed that the overproducing mutants, tp49, tp50, and tp60, produced approximately 1.7 times as much glutamyl polypeptide as did the parental wild-type strain (22).

Determination of the configuration of glutamic acid in glutamyl polypeptide produced by *B. anthracis* 4229 UM12 and insertion mutants tp49, tp50, and tp60. As pointed out above the appearance of colonies of the insertion mutants growing on media conducive to polypeptide production resembles that of *B. licheniformis* more than that of *B. anthracis*. Therefore, it was of interest to test whether the configuration of the glutamic acid in the capsular material of these mutants resembled that of glutamyl polypeptide produced by *B. licheniformis*. The latter organism produces an L-glutamyl polypeptide and a D-glutamyl polypeptide and the proportions of the two will vary depending on the Mn^{++} concentration in the growth medium (10). Peptide was extracted from 4229 UM12 and the three insertion mutants by autoclaving encapsulated cells in aqueous suspension and isolated by precipitation with four volumes of ethanol. The precipitated peptide was dissolved in water and dialyzed against distilled water at 4°C. The

dialyzed samples were stirred for 30 min with Norit A (10 mg/ml), then centrifuged twice at 12,000 rpm for 20 min and filtered through Millipore DA filters to remove the Norit. The peptide was precipitated by adding saturated $CuSO_4$ solution until a precipitate no longer formed. Samples were centrifuged at 12,000 rpm for 20 min and the supernatant solutions were discarded. Pellets were dissolved in 1 N citric acid and the solutions were dialyzed against water at 4°C for 24 h. These solutions were centrifuged at 12,000 rpm for 20 min to remove any insoluble material and then lyophilized. The lyophilized samples were dried in vacuo overnight at 50°C. The peptide was suspended in sterile distilled water to a concentration of 1 mg/ml. Following acid hydrolysis samples were analyzed by paper chromatography for total glutamic acid. Paper chromatography showed that no amino acids other than glutamic acid were present after acid hydrolysis. L-Glutamic acid was determined by a method employing L-glutamic acid oxidase (United States Biochemical L-glutamic acid assay kit). D-glutamic acid was estimated by subtracting the amount of L-isomer from the total glutamic acid. Results (Table 10) from three different experiments show that the polypeptide from wild-type and mutant strains contained more than 98% D-glutamic acid. Thus, our conclusion is that the polypeptide produced by the insertion mutants does not differ from that produced by the parent strain with respect to the configuration of the glutamic acid.

Transduction of the chromosomal insertion mutation from *B. anthracis* 4229 UM12 tp50 to wild-type strains. Insertion mutant tp50, which is a polypeptide overproducer, has been shown to contain Tn*917* within the chromosome. The mutation was transferred to *B. anthracis* 4229 UM12 and *B. anthracis* 6602 by CP-51-mediated transduction. Bacteriophage CP-51 was propagated on tp50 (Cap^{c++}, MLS^r) and tp50C1 (Cap^-, MLS^r, cured of pXO2). Recipient strains were streptomycin resistant and contained the capsule plasmid pXO2. Transductants were screened on LPA agar containing inhibitory concentrations of erythromycin, lincomycin and streptomycin. In all cases transductants showed overproduction of capsular material, providing more evidence that polypeptide overproduction by mutant tp50 is related to the chromosomal insertion of Tn*917*. DNA-DNA hybridization tests showed that transductants did not have Tn*917* in pXO2.

More evidence that overproduction of the capsular material by mutant tp50 is related to the chromosomal insertion of Tn*917* comes from experiments in which pXO2 from tp50 was transferred to strains cured of pXO2 by CP-51-mediated transduction. Bacteriophage CP-51 propagated on tp50 (Cap^{c++}, MLS^r) was used to transduce pXO2 into *B. anthracis* 4229 UM12C1 (cured of pXO2). Transductants were screened on $LPACO_3$ agar without any antibiotic selection. Bacteriophage CP-54, which lyses noncapsulated cells but does not adsorb to capsulated cells, was used to select Cap^{c+} transductants. All $pXO2^+$ transductants were MLS sensitive and they all exhibited the capsule phenotype of wild-type pXO2-containing strains, i.e., they were not polypeptide overproducers. This is further evidence that the chromosomal insertion in tp50 is responsible for polypeptide overproduction in that transposant.

Analysis of pXO2::Tn917 from mutant tp24-17, a deletion derivative. Mutant tp24-17 has a deleted version of pXO2 which is approximately only 10.5 kb in size including the transposon. Tp24-17 makes smooth, but not mucoid, colonies when grown in the presence of bicarbonate and CO_2. However, the amount of capsular material produced (if the smooth phenotype is indeed a reflection of synthesis of capsular material) is much less than that observed for wild-type pXO2-containing strains. Evidence that this mutant synthesizes some component of the capsule comes from experiments with bacteriophage CP-54 which can not adsorb to encapsulated cells, allowing selection of encapsulated cells. Smooth colonies of tp24-17 appear after two days of incubation on plates spread with CP-54. Results from DNA-DNA hybridization experiments show that the mutant plasmid in tp24 does not contain any of the *cap* structural genes identified by Makino, et al. (12, 13). However, colonies of tp24-17 are more smooth than colonies of strain TE704 which is the strain containing the cloned *cap* structural genes in plasmid pUBCAP1. These results, along with results shown below, suggest that this plasmid may contain a structural gene encoding an additional component of the capsule. The glutamyl polypeptide produced by *B. anthracis* is contained around the cell as a capsule but in *B. licheniformis* the glutamyl polypeptide is liberated into the growth medium. This difference suggests that there is more to the capsule of *B. anthracis* than just glutamyl polypeptide.

Plasmid DNA from tp24-17 gives two new fragments upon digestion with *Eco*RI, a 7.8 kb fragment and a 2.7 kb fragment. These fragments were isolated by electroelution, labeled with digoxigenin-labeled dUTP, and used as probes in DNA-DNA hybridization experiments to (i) locate their origin on pXO2 from *B. anthracis* 4229 UM12, and (ii) detect any homology with pXO2 from *B. anthracis* 6602, plasmid DNA from strain TE702, and the cloned *cap* structural genes in pUBCAP1.

In summary, the 7.8-kb *Eco*RI fragment hybridized to the following fragments of pXO2 and pTE702 from wild-type strains; (i) 6.3-kb and 4.2-kb *Eco*RI fragments, (ii) 13-kb *Hin*dIII fragment, (iii) 8.2-kb *Xba*I fragment. Similarly the 2.7-kb *Eco*RI fragment hybridized to the following fragments in pXO2 and pTE702 from wild-type strains; (i) 2.7-kb *Eco*RI fragment, (ii) 13-kb *Hin*dIII fragment, (iii) 8.5-kb *Xba*I fragment. No homology was found with the *cap* structural genes identified by Makino, et al. (12, 13).

Bacteriophage CP-51 was propagated on the insertion mutant tp24-17 and the lysate was used to transduce the deleted version of pXO2 into *B. anthracis* 4229 UM12C1 (cured of pXO2) and *B. anthracis* Davis TE704 which contains pUBCAP1 (carries the cloned *cap* genes, but produces rough colonies that are not resistant to CP-54). Transductants were selected on $LPACO_3$ agar containing inhibitory concentrations of erythromycin and lincomycin (for 4229 UM12C1) or these two antibiotics plus kanamycin (for TE704), and transduction plates were spread with phage CP-54 to select for Cap^{c+} and/or smooth cells. No Cap^{c+} transductants were found but several smooth (not mucoid) colonies were isolated and analyzed for their plasmid content. All of them were shown to harbor a plasmid which migrated at the same rate as the plasmid from the donor strain. In addition smooth transductants of TE704 carried a second plasmid, as expected, which migrated at the same rate as pUBCAP1. The smooth (not mucoid)

phenotype of the transductants derived from 4229 UM12C1 suggests strongly that the smooth phenotype is conferred by the small deletion derivative of pXO2. (No spontaneous smooth cells were found in control experiments in which 4229 UM12C1 or TE704 were plated with CP-54 in the absence of transducing phage). The smooth (not mucoid) transductants of TE704 suggest that pUBCAP1 and the pXO2 deletion derivative carried by tp24-17, and which confers the smooth phenotype, do not complement each other to produce fully encapsulated cells.

Transduction of pUBCAP1 from *B. anthracis* Davis TE704 to *B. anthracis* 4229 UM12C1 and insertion mutants 4229 UM12 tp6 and tp38. Insertion mutants tp6 and tp38 carry large deletions of about 20 kb and 50 kb, respectively. Each of the deletions includes the *cap* region, rendering the strains Cap$^-$. However, each of the plasmids retains three of the four regions that are believed to be involved in regulation of capsule synthesis. Therefore, it was of interest to see whether pUBCAP1, which carries the cloned *cap* genes (12), and either of the deleted derivatives could complement each other to produce encapsulated cells.

Phage CP-51 was propagated on strain TE704 and the lysate was used to transfer pUBCAP1 to *B. anthracis* 4229 UM12C1 (cured of pXO2) and insertion mutants tp6, tp38, and tp24-17. Since pUBCAP1 carries the gene for kanamycin resistance, transductants of 4229 UM12C1 were selected on $LPACO_3$ agar containing inhibitory concentrations of kanamycin and transductants of the three transposants were selected on $LPACO_3$ agar containing inhibitory concentrations of erythromycin, lincomycin and kanamycin.

Several kanamycin-resistant transductants of 4229 UM12C1 were isolated. Plasmid profiles showed that they contained one plasmid that migrated to the same position as pUBCAP1 from the donor strain. Their phenotype was Cap$^-$. Thus, the cloned *cap* genes carried by pUBCAP1 did not function in strain 4229 UM12C1 to produce encapsulated cells. (It should be recalled that strain TE704 which was obtained from I. Uchida and which carries pUBCAP1 is not encapsulated, presumably because regulatory genes are missing).

Several Kan^r MLS^r transductants of tp6 and tp38 were isolated and cells were analyzed for plasmid content. All transductants were shown to harbor two plasmids, one which migrated to the same position as pUBCAP1 and another which migrated the same as the plasmid from the respective recipient strain. Colonies of all such transductants showed a rough phenotype and could not be selected with bacteriophage CP-54. Thus, apparently complementation to produce encapsulated cells did not occur.

Attempts to clone the 2.8-kb *Hin*dIII and the 10.5-kb *Cla*I fragments into an *E. coli* host. Based on phenotypes of insertion mutants it seems that at least two to four regions of pXO2 may be involved in regulation of capsule synthesis. These include the 2.8-kb *Hin*dIII fragment and the 10.5-kb *Cla*I fragment. We made a few attempts to clone the putative regulatory genes into *E. coli* without any success. However, Ana Guaracao-Ayala, who was doing the work on characterization of pXO2 finished the requirements for the Ph.D. degree and returned to Colombia. Since I was approaching retirement from the university it was not feasible for me to accept another graduate student. Although I had hoped that Jan Hornung might be

able to continue the cloning experiments, her work on characterizing the inversion in pXO1 consumed all of her time. Therefore, this part of the project was not completed.

IV. Investigation of phage TP-21 whose prophage is a plasmid

We have shown previously that the 46-kb plasmid of *Bacillus thuringiensis* subsp. *kurstaki* strain HD-1 is the prophage of a phage which we have named TP-21 (17, 21). This appears to be the first phage with a plasmid prophage described for the genus *Bacillus*. We have shown that TP-21 is a generalized transducing phage. It is likely that some of the transfer of genetic material attributed by other workers to conjugation-like processes in this strain is the result of TP-21-mediated transduction. TP-21 plaque-forming particles contain greater than 48 kilobase pairs of DNA which appears to be circularly permuted and terminally redundant. We isolated TP-21 lysogens which have the 5.2-kb MLS resistance transposon Tn*917* inserted in the prophage. Although insertion of Tn*917* rendered some isolates defective, several isolates carrying this element produced viable phage which conferred erythromycin resistance upon lysogenized hosts. Results of tests with TP-21::Tn*917* demonstrated a broad host range among *B. anthracis*, *B. cereus* and *B. thuringiensis* strains.

TP-21 lysogens were very stable during growth at high temperatures. A mutant of TP-21, TP-21*c7*, was isolated following nitrosoguanidine mutagenesis of a *B.anthracis* lysogen; this derivative appeared to be temperature sensitive for replication. *B. cereus* lysogens of TP-21*c7* grown at 30°C stably maintained the plasmid prophage. At 42°C strains apparently cured of TP-21*c7* could be isolated from broth cultures grown from lysogens. A derivative of TP-21*c7* was isolated which has Tn*917* inserted. Lysogens of the transposon-tagged derivative, like those of the parental mutant phage, were stable at 30°C but apparently could be cured of the prophage at 42°C.

For many reasons TP-21c7::Tn*917* seemed as if it should serve as an ideal transposition selection vector for *B. anthracis*, *B. cereus*, and *B. thuringiensis*. However, several experiments in which it was tested as a mutagenic vehicle for *B. cereus* and *B. anthracis* were unsuccessful. The reasons for this were not clear at first. However, results of experiments carried out under this contract have shown that the temperature-sensitive mutant of TP-21 which is tagged with Tn*917* mutates to defective forms during the curing procedure at 42°C in the presence of erythromycin and lincomycin. Thus, colonies of *B. cereus* or *B. anthracis* that appeared to be transposants, i.e., ones that retained MLS resistance and seemed to be cured of TP-21 because they produced no lysis when planted in indicator lawns, were not transposants. Instead they harbored defective mutants of TP-21 which retained Tn*917*. Electrophoretic gels of plasmid extracts of presumed transposants revealed defective prophage plasmids of various sizes. Because the presence of erythromycin and lincomycin during the curing procedure apparently selected for defective phage mutants that were not temperature sensitive for replication, we carried out some experiments in which the curing procedure was done without selection for antibiotic resistance. However, these

experiments were unsuccessful. The frequency of MLS^r colonies that were cured of TP-21 was too low for this procedure to be useful for transposon mutagenesis. Because of these findings we discontinued work on this problem early in the contract period, electing to put our full effort into studying the biology of the *B. anthracis* plasmids pXO1 and pXO2.

CONCLUSIONS

The significance of the inversion of the toxin encoding region of pXO1 carried by the Sterne (USAMRIID) strain is not clear. Thus far, no phenotypic changes can be associated with the inversion. If the segment is actively invertible, it seems likely that the frequency of inversion is quite low. However, because there is no known phenotype attributable to either orientation of the segment, there is no obvious way to select cells in which the inversion has occurred.

The discovery of the positive regulatory gene for toxin synthesis, *atxA*, made possible by the utilization of transposon mutagenesis, is probably the single most important accomplishment resulting from our work on pXO1 during this contract period. Another potentially important accomplishment is the demonstration of what appears to be insertional inactivation of a negative regulatory gene involved in toxin synthesis. However, our preliminary attempts to clone the putative negative regulatory gene were unsuccessful. Unfortunately time did not permit further investigation of this intriguing problem. If I were to continue working on *B. anthracis*, this problem would have high priority.

With respect to the capsule plasmid, pXO2, several interesting problems remain. Although the group at USAMRIID has recently reported the discovery of a regulatory gene involved in capsule synthesis, out studies strongly suggest that additional regulatory genes for capsule synthesis are located on pXO2. One of our most interesting findings is that insertion of transposon Tn*917* into the chromosome at an undetermined site resulted in overproduction of capsular material. The nature of this enhancement of capsule synthesis is unknown and should be investigated further. Another problem that I would enjoy investigating further is the possibility that other gene(s) in addition to those responsible for synthesis of polyglutamic acid may be involved in capsule synthesis. This supposes that polyglutamic acid is not the only constituent of the *B. anthracis* capsule and that one or more additional components function to "contain" the polyglutamic acid around the cells as a capsule. This final report includes some evidence for this.

Table 1. Bacterial strains and plasmids used in this report

Strain or plasmid[a]	Relevant Characteristics[b]	Plasmids	Source
B. anthracis			
Anvax	Tox$^+$	pXO1	Jensen-Salsiberg Laboratories
PM36-R1	Tox$^+$	pXO1	C. B. Thorne
Sterne	Tox$^+$	pXO1	USAMRIID
Vollum V770	Tox$^+$	pXO1	C. B. Thorne
Weybridge	Tox$^+$	pXO1	Microbiological Research Establishment, Porton, England
UM44-1	Ind$^-$, Tox$^+$	pXO1	C. B. Thorne
Weybridge A	Tox$^+$	pXO1.1	C. B. Thorne
A UM23	Ura$^-$, Tox$^+$	pXO1.1	C. B. Thorne
A UM23 tp1A	Ura$^-$, PA$^+$, LF$^+$, EF$^+$, MLS^r	pXO1.1::Tn*917*	This study
A UM23 tp2A	Ura$^-$, PA$^+$, LF$^+$, EF$^+$, MLS^r	pXO1.1::Tn*917*	This study
A UM23 tp21	Ura$^-$, MLS^r, PA$^-$, LF$^+$, EF$^+$, Δ*pag*	pXO1.1::Tn*917* deletion derivative (Δ15 kb)	This study
A UM23 tp29	Ura$^-$, MLS^r, PA$^-$, LF$^-$, EF$^-$, *atxA*::Tn*917*	pXO1.1::Tn*917*	This study
A UM23 tp29 (pHY300PLK)	Ura$^-$, MLS^r, Tc^r, PA$^-$, LF$^-$, EF$^-$, *atxA*::Tn*917*	pXO1.1::Tn*917*, pHY300PLK	Uchida et al. (26)
A UM23 tp29 (pIU68)	Ura$^-$, MLS^r, Tc^r, PA$^-$, LF$^-$, EF$^-$, *atxA*::Tn*917*	pXO1.1::Tn*917*, pIU68	Uchida et al. (26)
A UM23 tp32	Ura$^-$, MLS^r, PA$^-$, LF$^-$, EF$^-$, *atxA*::Tn*917*	pXO1.1::Tn*917*	This study

Continued next page

Table 1. Continued

Strain or plasmid[a]	Relevant Characteristics[b]	Plasmids	Source
A UM23 tp32 (pHY300PLK)	Ura$^-$, MLS^r, Tc^r, PA$^-$, LF$^-$, EF$^-$, *atxA*::Tn*917*	pXO1.1::Tn*917*, pHY300PLK	Uchida et al. (26)
A UM23 tp32 (pIU68)	Ura$^-$, MLS^r, Tc^r, PA$^-$, LF$^-$, EF$^-$, *atxA*::Tn*917*	pXO1.1::Tn*917*, pIU68	Uchida et al. (26)
A UM23 tp36	Ura$^-$, PA$^+$, LF$^+$, EF$^+$, MLS^r	pXO1.1::Tn*917*	This study
A UM23 tp39	Ura$^-$, MLS^r, PA$^-$, LF$^-$, EF$^-$, *lef*$^+$, Δ*pag*, Δ*cya*, Δ*atxA*	pXO1.1::Tn*917* deletion derivative (Δ27 kb)	This study
A UM23 tp39 etf3 and etf5	Ura$^-$, MLS^r, Tc^r, PA$^-$, LF$^+$, EF$^-$, *lef*$^+$, Δ*pag*, Δ*cya*, Δ*atxA*	pXO1.1::Tn*917* deletion derivative (Δ27 kb), pIU51	This study
A UM23 tp49	Ura$^-$, MLS^r	pXO1.1::Tn*917* deletion derivative (Δ150 kb)	This study
A UM23 tp62	Ura$^-$, MLS^r, PA^{a++}, LF^{a++}, EF^{a+}	pXO1.1::Tn*917*	This study
A UM23 tp62 (pHY300PLK)	Ura$^-$, MLS^r, Tc^r, PA^{a++}, LF^{a++}, EF^{a+}	pXO1.1::Tn*917*, pHY300PLK	Uchida et al. (26)
A UM23 tp62 (pIU68)	Ura$^-$, MLS^r, Tc^r, PA^{a++}, LF^{a++}, EF^{a+}	pXO1.1::Tn*917*, pIU68	Uchida et al. (26)
A UM23 tp71	Ura$^-$, MLS^r	pXO1.1::Tn*917* deletion derivative (Δ142 kb)	This study
A UM23 tp72	Ura$^-$, MLS^r, PA$^{+/-}$, LF^{++}, EF$^+$, *pag*::Tn*917*	pXO1.1::Tn*917*	This study
A UM23-1	Ura$^-$, Str^r, Tox$^+$	pXO1.1	C. B. Thorne
A UM23-1 (pHY300PLK)	Ura$^-$, Str^r, Tc^r, Tox$^+$	pXO1.1, pHY300PLK	Uchida et al. (26)
A UM23-1 (pIU68)	Ura$^-$, Str^r, Tc^r, Tox$^+$	pXO1.1, pIU68	Uchida et al. (26)
A UM23C1	Ura$^-$, Tox$^-$	(pXO1.1)$^-$	C. B. Thorne
A UM23C1-1	Ura$^-$, Str^r, Tox$^-$	(pXO1.1)$^-$	C. B. Thorne

Continued next page

Table 1. Continued

Strain or plasmid[a]	Relevant Characteristics[b]	Plasmids	Source
A UM23C1-1 (pIU71)	Ura$^-$, Str^r, Km^r, Tox$^-$	(pXO1.1)$^-$, pIU71	Uchida et al. (26)
A UM23C1-1 (pIU71, pHY300PLK)	Ura$^-$, Str^r, Km^r, Tc^r, Tox$^-$	(pXO1.1)$^-$, pIU71, pHY300PLK	Uchida et al. (26)
A UM23C1-1 (pIU71, pIU68)	Ura$^-$, Str^r, Km^r, Tc^r, Tox$^-$	(pXO1.1)$^-$, pIU71, pIU68	Uchida et al. (26)
A UM23C1-2	Ura$^-$, Rif^r, Tox$^-$	(pXO1.1)$^-$	C. B. Thorne
B	Tox$^+$	pXO1	C. B. Thorne
Davis			
TE702	Cap^{c+}	pTE702	I. Uchida
TE704	Cap^{c+}	pUBCAP1	I. Uchida
Pasteur			
6602	Cap^{c+}	pXO2	USAMRIID
4229	*Cap*$^{c+}$	pXO2	USAMRIID
4229UM12	Cap^{c+}, Nal^r	pXO2	C.B. Thorne
4229UM12 tp1	Cap^{c+}, Nalr, MLS^r, Cm^s	pXO2::Tn*917*	This study
4229UM12 tp3	Cap^{c+}, Nal^r, MLS^r, Cm^s	pXO2::Tn*917*	This study
4229UM12 tp4	Cap^{c+}, Nal^r, MLS^r, Cm^s	pXO2::Tn*917*	This study
4229UM12 tp6	Cap$^-$, Nal^r, MLS^r, Cm^s	pXO2::Tn*917*	This study
4229UM12 tp7	Cap$^-$, Nal^r, MLS^r, Cm^s	pXO2::Tn*917*	This study
4229UM12 tp10	Cap^{c+}, Nal^r, MLS^r, Cm^s	pXO2::Tn*917*	This study
4229UM12 tp11	Cap^{c+}, Nal^r, MLS^r, Cm^s	pXO2::Tn*917*	This study
4229UM12 tp17	Cap^{c+}, Nal^r, MLS^r, Cm^s	pXO2::Tn*917*	This study
4229UM12 tp18	Cap$^-$, Nal^r, MLS^r, Cm^s	pXO2::Tn*917*	This study

Continued next page

Table 1. Continued

Strain or plasmid[a]	Relevant Characteristics[b]	Plasmids	Source
4229UM12 tp20	Cap$^-$, Nal^r, MLS^r, Cm^s	pXO2::Tn*917*	This study
4229UM12 tp21	Cap$^-$, Nal^r, MLS^r, Cm^s	pXO2::Tn*917*	This study
4229UM12 tp22	Cap$^-$, Nal^r, MLS^r, Cm^s	pXO2::Tn*917*	This study
4229UM12 tp24	Cap^{a+}, Nal^r, MLS^r, Cm^s	pXO2::Tn*917*	This study
4229UM12 tp24-17	Cap^{c+}, Nal^r, MLS^r, Cm^s	pXO2::Tn*917*	This study
4229UM12 tp30	Cap^{c+}, Nal^r, MLS^r, Cm^s	pXO2::Tn*917*	This study
4229UM12 tp38	Cap$^-$, Nal^r, MLS^r, Cm^s	pXO2::Tn*917*	This study
4229UM12 tp40	Cap$^-$, Nal^r, MLS^r, Cm^s	pXO2::Tn*917*	This study
4229UM12 tp49	Cap^{c++}, Nal^r, MLS^r, Cm^s	pXO2::Tn*917*	This study
4229UM12 tp58	Cap^{a+}, Nal^r, MLS^r, Cm^s	pXO2::Tn*917*	This study
4229UM12 tp59	Capa$^+$, Nal^r, MLS^r, Cm^s	pXO2::Tn*917*	This study
4229UM12 tp60	Cap^{a++}, Nal^r, MLS^r, Cm^s	pXO2::Tn*917*	This study
Plasmids			
pBluescriptIIKS+	2.9-kb, LacZα, Ap^r		Stratagene Cloning Systems
pHY300PLK	*E. coli-B. subtilis* shuttle vector, Ap^r, Tc^r		See Uchida et al. (26)
pIU51	5.0-kb insert containing *atxA*, cloned into pHY300PLK		Uchida et al. (26)
pIU68	2.0-kb insert containing only *atxA* ORF, cloned into pHY300PLK		Uchida et al. (26)

Continued next page

Table 1. Continued

Strain or plasmid[a]	Relevant Characteristics[b]	Plasmids	Source
pIU71	6.0-kb *Bam*HI fragment of pXO1 containing *pag* in pAT187, Ap^r, Km^r		Uchida et al. (26)
pJMH4	WeyAR, 2.4-kb *Eco*RI fragment of pXO1.1 (Weybridge A UM23), cloned into pBluescriptIIKS+		This study
pJMH5	SterneR, 3.1-kb *Eco*RI fragment of pXO1 (Sterne), cloned into pBluescriptIIKS+		This study
pJMH9	WeyAL, 5.4-kb *Eco*RI fragment of pXO1.1 (Weybridge A UM23), cloned into pBluescriptIIKS+		This study
pJMH10	SterneL, 4.8-kb *Eco*RI fragment of pXO1 (Sterne), cloned into pBluescriptIIKS+		This study
pJMH12	WeyAL, 2.7-kb *Kpn*I fragment from 5.4-kb *Eco*RI fragment of pXO1.1 (Weybridge A UM23), subcloned into pBluescriptIIKS+		This study
pJMH16	SterneL, 1.9-kb *Kpn*I fragment from 4.8-kb *Eco*RI fragment of pXO1 (Sterne), subcloned into pBluescriptIIKS+		This study
pJMH20	SterneR, 1.7-kb *Hin*dIII fragment from 3.1-kb *Eco*RI fragment of pXO1 (Sterne), subcloned into pBluescriptIIKS+		This study

Continued next page

Table 1. Continued

Strain or plasmid[a]	Relevant Characteristics[b]	Plasmids	Source
pJMH24	WeyAR, 1.0-kb *Hin*dIII fragment from 2.4-kb *Eco*RI fragment of pXO1.1 (Weybridge A UM23), subcloned into pBluescriptIIKS+		This study
pJMH28	9.3-kb *Pst*I fragment of pXO1 (Weybridge A UM23), cloned into pBluescriptIIKS+ (contains WeyAR)		This study

[a] tp, insertion mutant; etf, transformant by electroporation.

[b] Abbreviations: Ap^r, plasmid-encoded ampicillin resistance; Cap^{c+}, capsule synthesis in presence of CO_2 and bicarbonate; Cap^{a+}, capsule synthesis in air; Cap^-, inability to synthesize capsule; Cap^{c++}, overproduction of capsular material in the presence of CO_2 and bicarbonate; EF^+, production of edema factor; EF^{a+}, production of edema factor in the presence or absence of added sodium bicarbonate; EF^-, no edema factor detected; Ind, indole; Km^r, plasmid-encoded kanamycin resistance; Lac, lactose utilization; LF^+, production of lethal factor; LF^{a++}, overproduction of lethal factor in the presence or absence of added sodium bicarbonate; LF^-, no lethal factor detected; MLS^r, *Tn917*-encoded macrolide, lincosamide, and streptogramin B resistance; Nal, nalidixic acid; PA^+, production of protective antigen; PA^{a++}, overproduction of protective antigen in the presence or absence of added sodium bicarbonate; $PA^{+/-}$, negligible quantities of protective antigen produced; PA^-, no protective antigen detected; Rif^r, rifampicin resistance; Str^r, streptomycin resistance; Tc^r, plasmid-encoded tetracycline resistance; Tox^+, production of anthrax toxin; Tox^-, no anthrax toxin detected; Ura, uracil; *pag*, PA structural gene; *lef*, LF structural gene; *cya*, EF structural gene; *atxA*, trans-activator of *pag*, *lef*, and *cya*.

Table 2. Yields of toxin components produced by *B. anthracis* Weybridge A UM23 and UM23 insertion mutants grown in the absence of added bicarbonate and horse serum[a]

	CA-HEPES without bicarbonate and horse serum[b]		
Filtrate	PA, μg/mg dry wt.	LF, μg/mg dry wt.	EF, μg/mg dry wt.
UM23 (pXO1.1$^+$)	2 ± 0.5	<0.4	<0.2
UM23C1 (pXO1.1$^-$)	0	0	0
UM23 tp2A	1 ± 0.6	<0.4	<0.2
UM23 tp21[c]	0	<0.4	<0.2
UM23 tp29	0	0	<0.1
UM23 tp32	0	0	<0.1
UM23 tp39[c]	0	0	0
UM23 tp62	40 ± 10	3 ± 0.3	1 ± 0.4
UM23 tp72	<0.3	2 ± 1	≤0.4

[a] Cultures were grown in 100 ml of CA-HEPES (pH 7.5) broth in the absence of added sodium bicarbonate and horse serum in 250-ml screw-capped flasks at 37°C with slow shaking (100 rpm). Uracil was added to a final concentration of 40 μg/ml to satisfy the auxotrophic requirement. Filtrates were collected from cultures grown for 14 h.

[b] PA and LF concentrations were determined by radial immunodiffusion assays using goat antiserum to PA or rabbit antiserum to LF (provided by S. Leppla, NIDR, Bethesda, MD). EF concentrations were determined by adenylate cyclase assays. The values shown for the concentrations of PA, LF, and EF in the cultures filtrates are the averages of three experiments.

[c] These insertion mutants contain deletions within pXO1.1::Tn*917* derivatives.

Table 3. Origins of the altered *Bam*HI-*Sal*I fragments of pXO1.1::Tn*917* deletion derivativesfrom UM23 tp21 and tp39

Probe[a]	Hybridizations to restriction fragments (kb) of pXO1.1 (Weybridge A UM23) generated by:		
	*Bam*HI	*Pst*I	*Eco*RI
36-kb *Bam*HI-*Sal*I fragment of pXO1.1::Tn*917* (tp21)	34.8	9.3, 6.6, 6.3, 5.2, 2.8, 0.6	ND[b]
8.5-kb *Bam*HI-*Sal*I fragment of pXO1.1::Tn*917* (tp21)	13.9	18.1	8.0, 3.1
33-kb *Bam*HI-*Sal*I fragment of pXO1.1::Tn*917* (tp39)	34.8	9.3, 6.6, 6.3, 5.2, 2.8, 0.6	7.3, 5.6, 4.3, 2.4, 1.9, 1.2, 1.1, 0.8, 0.75, 0.72, 0.7
5.5-kb *Bam*HI-*Sal*I fragment of pXO1.1::Tn*917* (tp39)	7.4	18.7, 5.5	3.1, 1.05

[a] The *Bam*HI-*Sal*I fragments were isolated from agarose gels by electroelution and labelled with digoxigenin-labelled dUTP.

[b] ND, not done.

Table 4. Production of anthrax toxin components by *B. anthracis* strains complemented with the cloned *atxA* gene

Strain	Plasmids	Toxin Components in Filtrates[a] (μg/ml)					
		PA		LF		EF	
		-	+	-	+	-	+
UM23	pXO1.1	0.5	18	<0.1	6.9	<0.05	3.1
UM23-1	pXO1.1	≤0.2	5.9	<0.1	3.7	<0.05	2.8
UM23-1	pXO1.1, pHY300PLK	<0.1	5.1	<0.1	2.6	<0.05	1.3
UM23-1	pXO1.1, pIU68	0.2[b]	NG[b]	<0.1	NG	<0.05	NG
UM23 tp29	pXO1.1::Tn*917*	<0.1	<0.1	<0.1	≤0.1	<0.05	≤0.2
UM23 tp29	pXO1.1::Tn*917*, pHY300PLK	<0.1	<0.1	<0.1	≤0.1	<0.05	≤0.1
UM23 tp29	pXO1.1::Tn*917*, pIU68	7.0	6.5	0.7	5.9	0.4	7.8
UM23 tp32	pXO1.1::Tn*917*	<0.1	<0.1	<0.1	<0.1	<0.05	≤0.2
UM23 tp32	pXO1.1::Tn*917*, pHY300PLK	<0.1	<0.1	<0.1	<0.1	<0.05	≤0.2
UM23 tp32	pXO1.1::Tn*917*, pIU68	1.6	3.0	0.3	5.2	<0.05	3.6
UM23 tp62	pXO1.1::Tn*917*	16	30	1.0	14	0.4	6.0
UM23 tp62	pXO1.1::Tn*917*, pHY300PLK	4.6	22	<0.1	8.7	≤0.05	2.6
UM23 tp62	pXO1.1::Tn*917*, pIU68	1.8[b]	4.0[b]	≤0.5	3.3	≤0.05	0.9
UM23C1-1		<0.2	<0.2	<0.2	<0.2	<0.05	<0.05
UM23C1-1	pIU71	<0.1	<0.1	<0.1	<0.1	<0.05	<0.05
UM23C1-1	pIU71, pHY300PLK	<0.1	<0.1	<0.1	<0.1	<0.05	<0.05
UM23C1-1	pIU71, pIU68	≤0.4	2.2	<0.1	<0.1	<0.05	<0.05

[a] The concentrations of the toxin components in the filtrates obtained from cultures growth in CA-HEPES (pH 7.5) in the absence (-) or presence (+) of 0.72% sodium bicarbonate and 3% horse serum were determined by radial immunodiffusion (PA and LF) or adenylate cyclase (EF) assays. All strains carrying pHY300PLK or recombinant plasmids, pIU68 or pIU71, were grown in the presence of tetracycline, kanamycin, or both antibiotics.

[b] The cultures did not grow (NG) or they grew slowly.

Table 5. Yields of toxin components produced by *B. anthracis* Weybridge A UM23 tp39 and tp39 electrotransformants[a]

Filtrate	CA-HEPES with bicarbonate and horse serum[b]			CA-HEPES without bicarbonate and horse serum[b]		
	PA, μg/mg dry wt.	LF, μg/mg dry wt.	EF, μg/mg dry wt.	PA, μg/mg dry wt.	LF, μg/mg dry wt.	EF, μg/mg dry wt.
UM23	36	11	9	1	<0.4	<0.2
UM23C1	0	0	0	0	0	0
UM23 tp39	0	0	0	0	0	0
UM23 tp39 etf3	0	1	0	0	0	0
UM23 tp39 etf5	0	2	0	0	0	0

[a] Cultures were grown in 100 ml of CA-HEPES (pH 7.5) broth in the presence or absence of 0.72% sodium bicarbonate and 3% horse serum in 250-ml screw-capped flasks at 37°C with slow shaking (100 rpm). Filtrates were collected from cultures grown for 13 h in broth supplemented with sodium bicarbonate and horse serum or for 14 h in broth without added bicarbonate and horse serum.

[b] Same as Table 2 footnote b. The values obtained for the concentrations of PA, LF, and EF in the filtrates from cultures grown in the presence or absence of added bicarbonate and horse serum are the averages of two experiments.

Table 6. Restriction analysis of the 14.6-kb *Bam*HI fragment of pXO1.1 (Weybridge A UM23)

Sizes of restriction fragments (kb) of the 14.6-kb *Bam*HI fragment generated by:		
*Eco*RI	*Eco*RI and *Cla*I	*Cla*I
		ca. 10.5
5.4		
4.2	4.2	
	4.0	
3.2		
		2.8
	2.2	
	1.5	
1.3	1.3	
	0.9	0.9

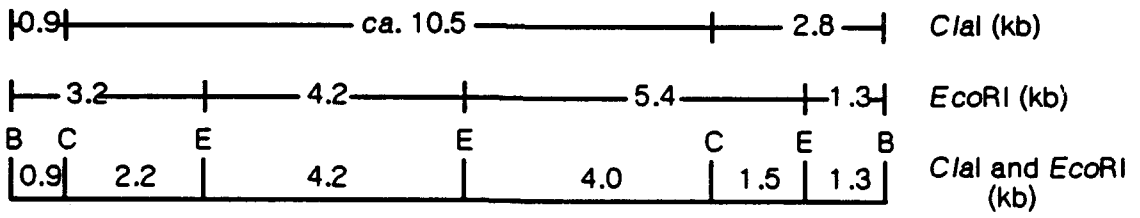

Figure 2. Construction of *Eco*RI and *Cla*I restriction maps of the 14.6-kb *Bam*HI fragment of pXO1.1 (Weybridge A UM23). The *Bam*HI fragment was digested with *Cla*I, *Eco*RI, or double digested with both enzymes. The sizes of the fragments (kb) from each digestion are shown.

Table 7. *Eco*RI digestion of *Bam*HI-*Sal*I fragments of pXO1.1::Tn*917* derivatives from *B. anthracis* Weybridge A UM23 tp2A, tp36, and tp62

Sizes of *Eco*RI restriction fragments (kb) generated from:			
15-kb *Bam*HI-*Sal*I fragment of pXO1.1::Tn*917* (tp62)[a]	24-kb *Bam*HI-*Sal*I fragment of pXO1.1::Tn*917* (tp62)[a]	9.8-kb *Bam*HI-*Sal*I fragment of pXO1.1::Tn*917* (tp2A)[a]	9.8-kb *Bam*HI-*Sal*I fragment of pXO1.1::Tn*917* (tp36)[a]
5.6	7.3	4.3	4.3
4.0[b]	4.3	3.2[d]	3.1[e]
3.3[c]	3.1[c]	2.2[f]	2.2[f]
0.8	2.4		
0.72	2.1[f]		
	1.9		
	1.1		
	0.75		
	0.7		

[a] The *Bam*HI-*Sal*I restriction fragments were isolated from an agarose gel by electroelution and digested with *Eco*RI.

[b] Fragment corresponds to the *Eco*RI-*Bam*HI fragment of the 5.4-kb *Eco*RI fragment.

[c] Fragments correspond to the *Sal*I digestion of the Tn*917*-containing 1.2-kb *Eco*RI fragment of the plasmid derivative from UM23 tp62.

[d] Fragment corresponds to the *Sal*I digestion of the Tn*917*-containing 1.1-kb *Eco*RI fragment or the 5.2-kb *Pst*I fragment of the plasmid derivative from UM23 tp2A.

[e] Fragment corresponds to the *Sal*I digestion of the Tn*917*-containing 1.1-kb *Eco*RI fragment or the 6.3-kb *Pst*I fragment of the plasmid derivative from UM23 tp36.

[f] Fragment most likely corresponds to the *Eco*RI-*Bam*HI junction fragment of a 7.0-kb *Eco*RI fragment.

Table 8. DNA-DNA hybridization analysis of pXO1.1 (Weybridge A UM23) and pXO1 (Sterne) with the subcloned fragments of each plasmid containing the junctions of the inverted segment

Probe[a]	Hybridization to fragments (kb) of pXO1.1 (Weybridge A UM23) generated by:			Hybridization to fragments (kb) of pXO1 (Sterne) generated by:		
	*Bam*HI	*Pst*I	*Eco*RI	*Bam*HI	*Pst*I	*Eco*RI
2.7-kb *Kpn*I insert from pJMH12 (part of 5.4-kb *Eco*RI fragment of pXO1.1 [Weybridge A UM23])	34.8, 14.6	18.7, 9.3	5.4, 2.4	29, 19.5	19, 8.6	4.8, 3.1
1.0-kb *Hin*dIII insert from pJMH24 (part of 2.4-kb *Eco*RI fragment of pXO1.1 [Weybridge A UM23])	34.8, 14.6	18.7, 9.3	5.4, 2.4	29, 19.5	19, 8.6	4.8, 3.1
1.9-kb *Kpn*I insert from pJMH16 (part of 4.8-kb *Eco*RI fragment of pXO1 [Sterne])	34.8, 14.6	18.7, 9.3	5.4, 2.4	29, 19.5	19, 8.6	4.8, 3.1
1.7-kb *Hin*dIII insert from pJMH20 (part of 3.1-kb *Eco*RI fragment of pXO1 [Sterne])	34.8, 14.6	18.7, 9.3	5.4, 2.4	29, 19.5	19, 8.6	4.8, 3.1

[a] The probes were isolated from the recombinant plasmids digested with *Kpn*I or *Hin*dIII and labelled with digoxigenin-labelled dUTP.

Table 9. Yields of toxin components produced by *B. anthracis* Sterne and Weybridge derivatives

Filtrate	CA-HEPES with bicarbonate and horse serum[b]						CA-HEPES without bicarbonate and horse serum[b]					
	PA, µg/mg dry wt.		LF, µg/mg dry wt.		EF, µg/mg dry wt.		PA, µg/mg dry wt.		LF, µg/mg dry wt.		EF, µg/mg dry wt.	
	Expt. 1	Expt. 2	Expt. 1	Expt. 2	Expt. 1	Expt. 2	Expt. 1	Expt. 2	Expt. 1	Expt. 2	Expt. 1	Expt. 2
Sterne	18	32	7	6	4	11	2	2	<0.4	<0.5	0.2	0.2
Weybridge UM44-1	48	23	9	8	4	3	0.3	<0.6	<0.2	0	<0.1	<0.2
Weybridge A UM23	34	39	13	10	9	10	1	1	<0.4	<0.4	<0.2	<0.1

[a] Cultures were grown as described in Table 5. Filtrates were collected from cultures grown for 13 h in broth supplemented with bicarbonate and horse serum or for 14 h in broth without bicarbonate and horse serum.

[b] See Table 2 footnote b.

Table 10. Configuration of glutamic acid in glutamyl polypeptide from *B. anthracis* 4229 UM12 and insertion mutants tp49, tp50 and tp60

Polypeptide from strain[a]	Peptide as glutamic acid[b]		
	Total %	L-isomer % of total	D-isomer % of total
4229 UM12	102.3	1.4	98.6
tp49	115.6	1.3	98.7
tp50	105.0	1.4	98.6
tp60	117.6	1.3	98.7

[a] Strains were grown on minimal IIIB-CO_3 medium.

[b] Results presented are the averages of values from three determinations. The theoretical value for percent glutamic acid in the free acid form of glutamyl polypeptide is 113.9%.

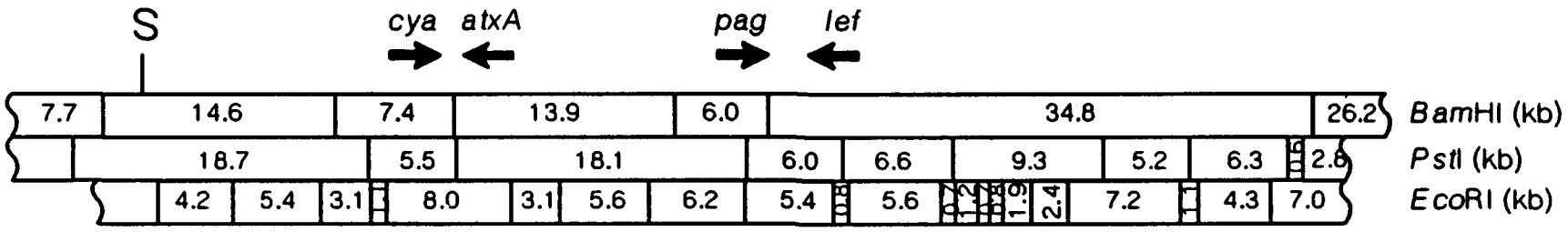

Figure 1. *Bam*HI, *Pst*I, *Eco*RI restriction maps of the toxin-encoding region of pXO1.1 (Weybridge A UM23). The *Bam*HI, *Pst*I, and *Eco*RI restriction maps for a 77-kb region of pXO1.1 from *B. anthracis* Weybridge A UM23 encompassing the toxin structural genes are shown. The map was constructed based on data obtained from single, double, and triple digestions of pXO1.1, pXO1.1::Tn*917* derivatives, and deletion derivatives. Results from DNA-DNA hybridization analysis with the cloned toxin structural genes (*pag*, *lef*, and *cya*) were also used in the construction of these restriction maps. The locations and directions of transcription of the toxin structural genes and positive activating factor are shown by the arrows. S, *Sal*I.

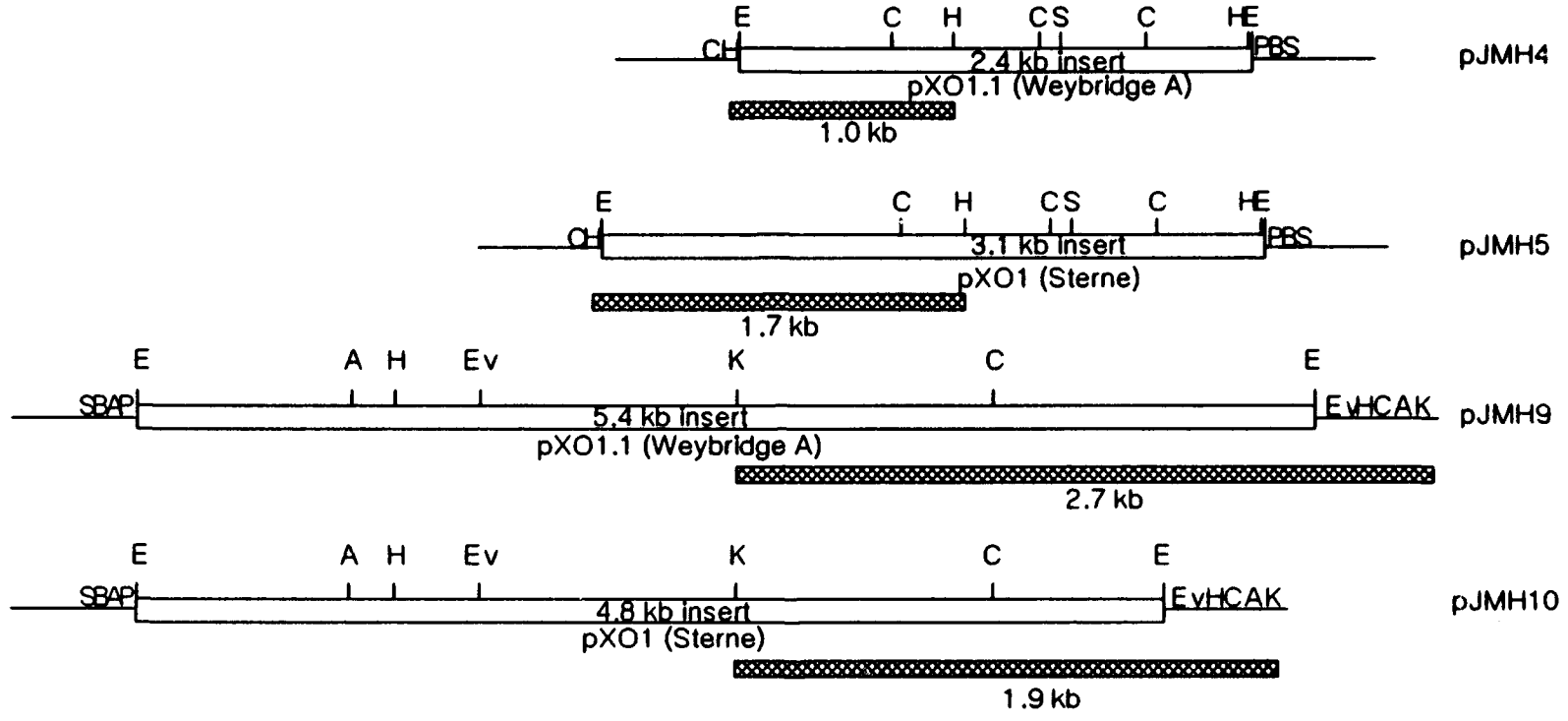

Figure 3. Cloning of the 2.4- and 5.4-kb *Eco*RI fragments of pXO1.1 (Weybridge A UM23) and the 3.1- and 4.8-kb *Eco*RI fragments of pXO1 (Sterne). The fragments were cloned into pBluescriptIIKS+ and the cloned inserts are shown. The crosshatched boxes below each insert represent the *Hin*dIII and *Kpn*I fragments that were subcloned into pBluescriptIIKS+. A, *Ava*I; B, *Bam*HI; C, *Cla*I; E, *Eco*RI; Ev, *Eco*RV; H, *Hin*dIII; K, *Kpn*I; P, *Pst*I; S, *Sst*I.

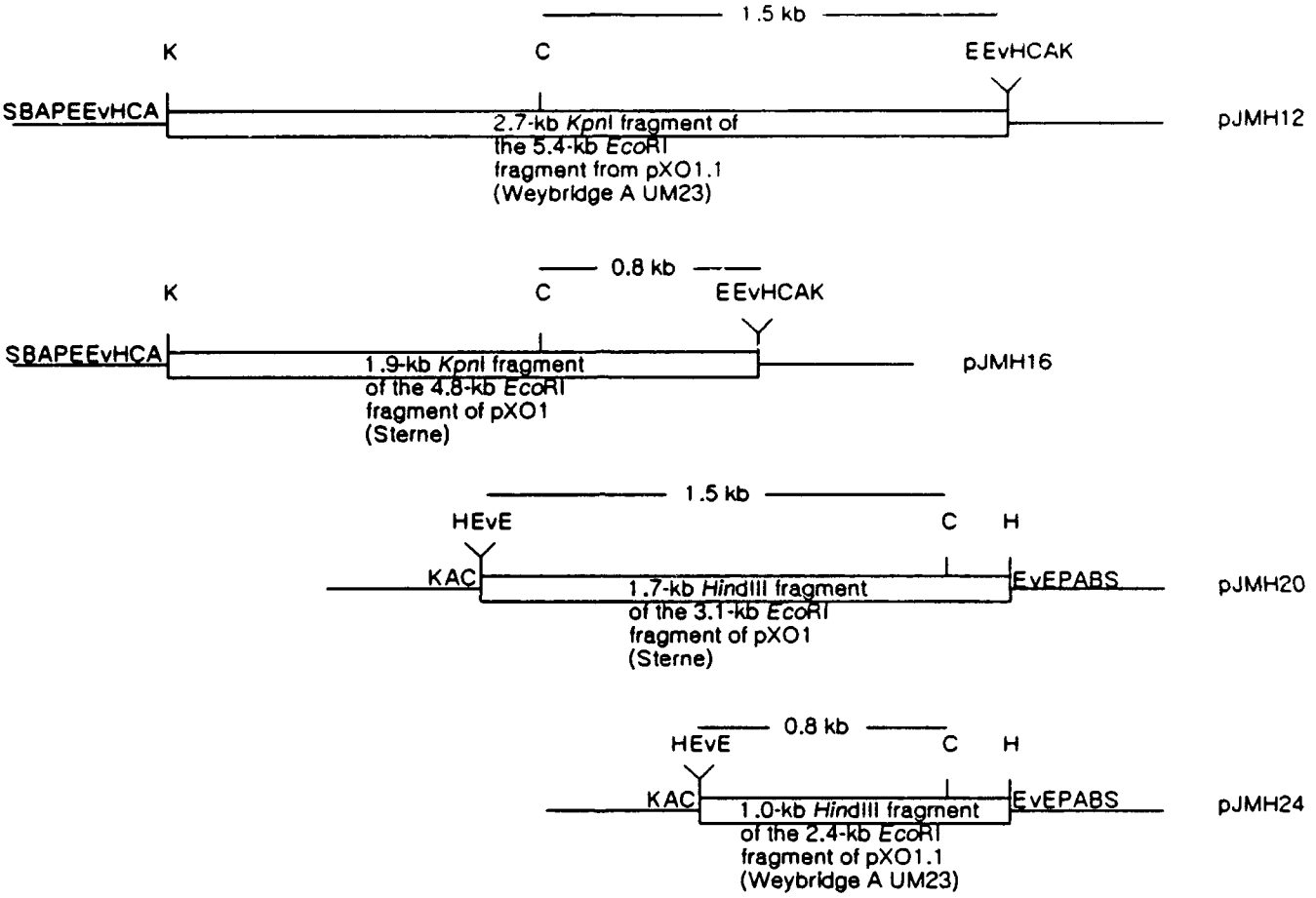

Figure 4. Subcloned inserts originating from the 2.4-kb and 5.4-kb *Eco*RI fragments from pXO1.1 (Weybridge A UM23) and the 3.1-kb and 4.8-kb *Eco*RI fragments from pXO1 (Sterne). The size of the *Eco*RI-*Cla*I fragments in each insert is shown with the line above the insert. With the exception of the *Eco*RI site, the restriction sites shown above the Y-shaped line represent the restriction sites found in the MCS of pBluescriptIIKS(+). E, *Eco*RI; S, *Sst*I; C, *Cla*I; H, *Hin*dIII; P, *Pst*I; B, *Bam*HI; A, *Ava*I; Ev, *Eco*RV; K, *Kpn*I.

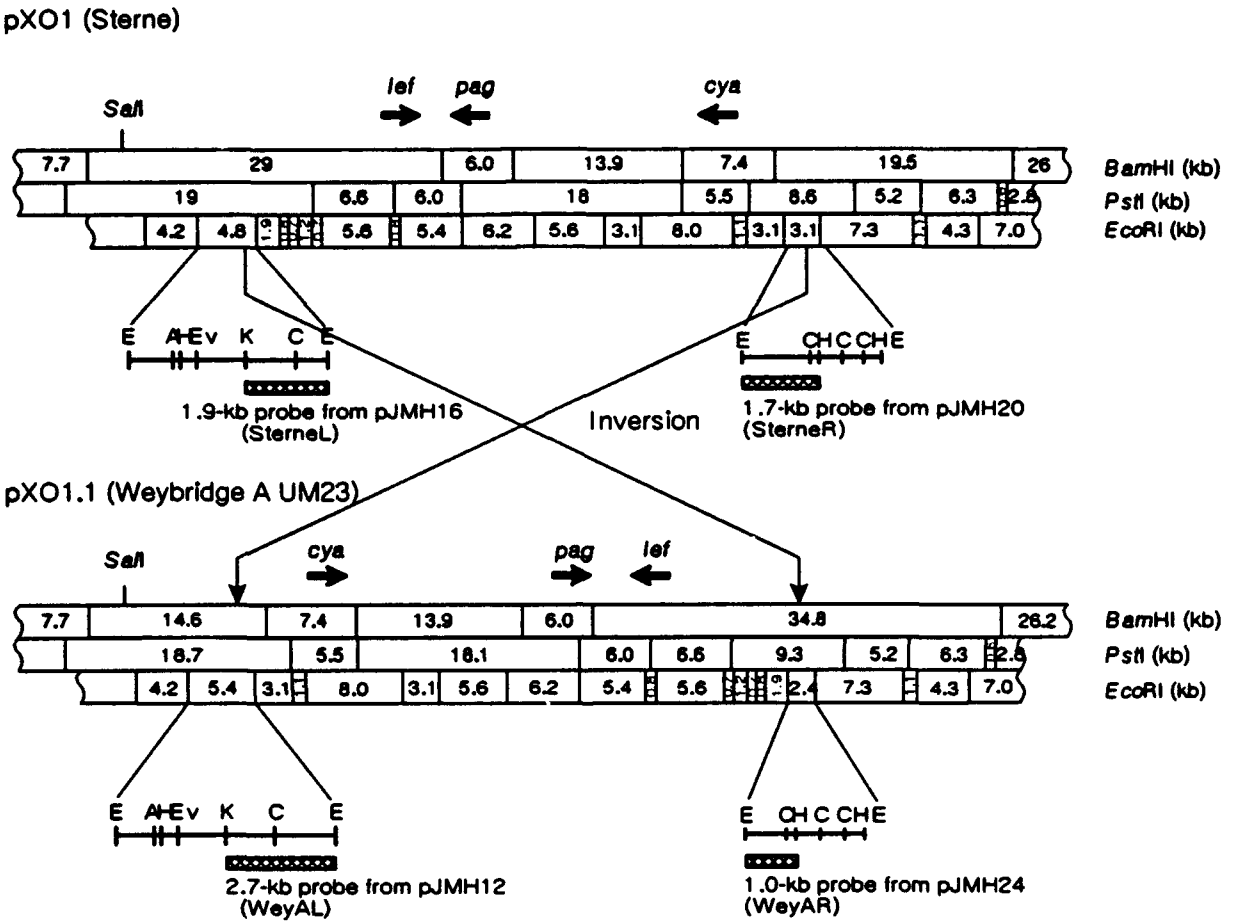

Figure 5. Comparison of restriction maps of the toxin-encoding regions of pXO1.1 (Weybridge A UM23) and pXO1 (Sterne). A 77-kb region of pXO1 encompassing the toxin structural genes is shown. The ends of the inversion are shown by the vertical arrows. The crosshatched boxes below the enlarged *Eco*RI fragments represent the junctions fragments of the inverted segments that have been subcloned into pBluescriptIIKS+. The letter "L" or "R" is attached to the cloned fragment designation, i.e. WeyAL, to represent the left and right junction fragments. The subcloned fragments were isolated from the recombinant plasmids and used in DNA-DNA hybridization analysis of the inverted regions of pXO1.1 (Weybridge A UM23) and pXO1 (Sterne). E, *Eco*RI; C, *Cla*I; K, *Kpn*I; H, *Hind*III; A, *Ava*I; and Ev, *Eco*RV.

WeyAL (pJMH12): 2.7-kb *Kpn*I fragment of the 5.4-kb *Eco*RI fragment from pXO1.1 (Weybridge A UM23)

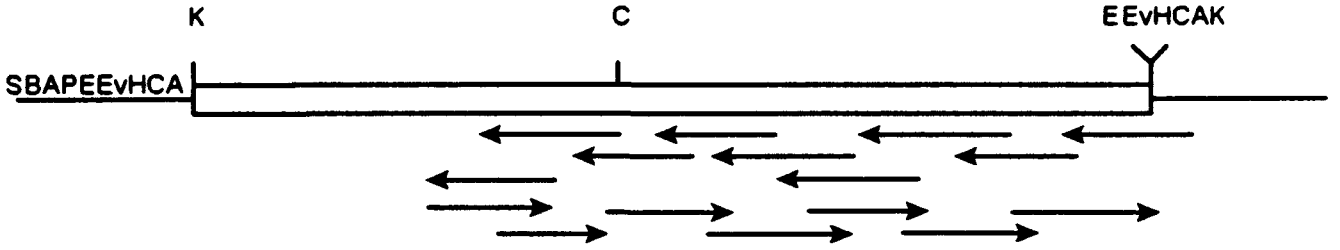

WeyAR group

WeyAR (pJMH24): 1.0-kb *Hind*III fragment of the 2.4-kb *Eco*RI fragment of pXO1.1 (Weybridge A UM23)

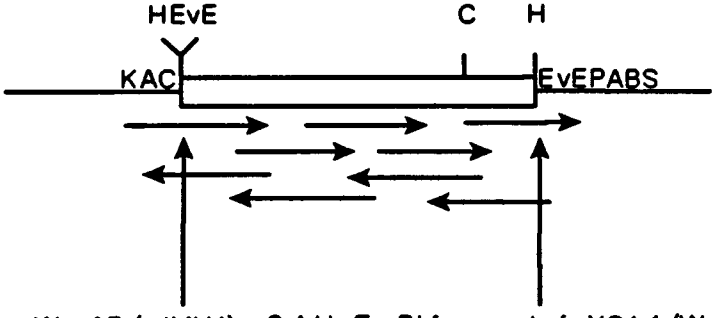

WeyAR (pJMH4): 2.4-kb *Eco*RI fragment of pXO1.1 (Weybridge A UM23)

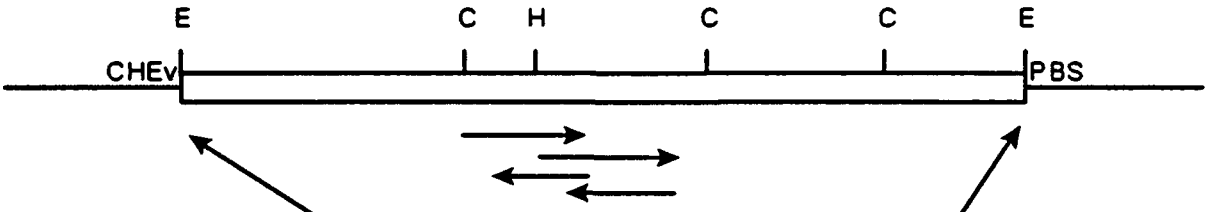

pJMH28: 9.3-kb *Pst*I fragment of pXO1.1 (Weybridge A UM23)

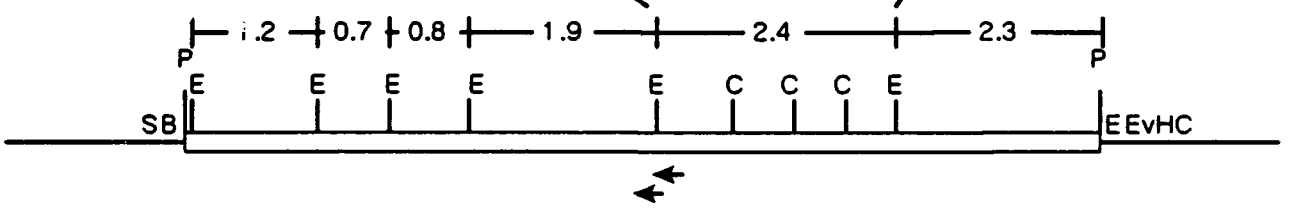

Continued next page

SterneR group

SterneR (pJMH20): 1.7-kb *Hin*dIII fragment of the 3.1-kb *Eco*RI fragment of pXO1 (Sterne)

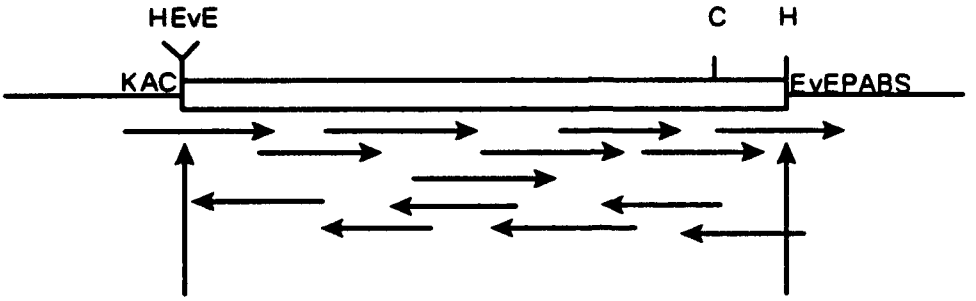

SterneR (pJMH5): 3.1-kb *Eco*RI fragment

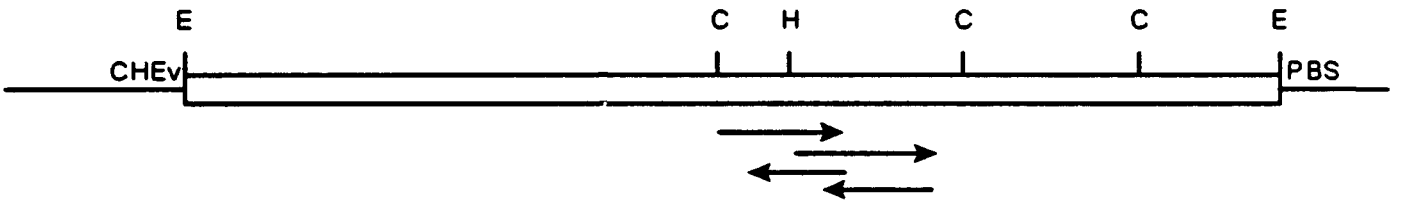

SterneL (pJMH16): 1.9-kb *Kpn*I fragment of the 4.8-kb *Eco*RI fragment of pXO1 (Sterne)

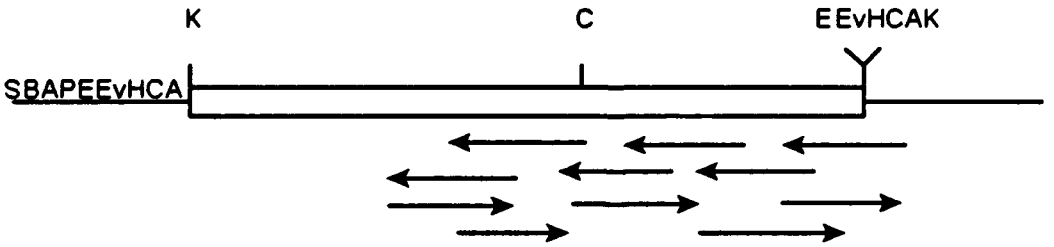

Figure 6. Sequencing strategies for the cloned junction fragments of the inverted segments of pXO1.1 (Weybridge A UM23) and pXO1 (Sterne). A partial restiction map of each cloned fragment is shown. The horizontal arrows indicate the direction and extent of sequencing using different synthetic oligonucleotide primers. The vertical arrows represent the direction of subcloning within a particular junction fragment. With the exception of the *Eco*RI site, the restriction sites shown above the Y-shaped line represent the restriction sites found in the MCS of pBluescriptIIKS(+). E, *Eco*RI; S, *Sst*I; C, *Cla*I; H, *Hin*dIII; P, *Pst*I; B, *Bam*HI; A, *Ava*I; Ev, *Eco*RV; K, *Kpn*I.

EcoRI

```
   1  GAATTCCTTC GCAATATAAA ATACTTCCTT AATCTGAGTG ACGGATGACA
  51  TTTTCTACTT TTCGGCCTCT TCCTGCTCGT TTTAACTTCC TCAAATCTAA
 101  TGTCAAAGTT TGTAATTCAC TGATGATATA ACTAATGATT TCACGATTAG
 151  AAGCATCTAT AATCGTTGAT AAATACAACG TAAGCTCTCC AAATAATAGA
 201  TACGTGACAT CTGTAACTCC CTTTTCGGTT GGGATTGCCA CTTCAAATTG
 251  GCATTCTAAT TGATGCGAAA CTAGAACAGG TTCCATATCT TAATTTATAT
 301  CTAAAACAGA CCTTCTCTTC TGTATCGTCT TTAGGACGTT CTGTTGTCTG
 351  TAACCAACGA TAAAATGTGG AACGTGGTAA TTCTAATATT TTACTCAGTT
 401  CTTGTATGGT TAATTTTGTT ATTTAGCGCT TATTTTCTAA TCATAACTGT
 451  TCCAATTCAC TTAGCTCTTT TGGCTTTTCC CATAAAAGTA TTGTTTTCCT
 501  ACAGTTTGTT GAAGACGGTA CGTTTAATCT ATTCAGCACC ATTTCATTCA
 551  TGGTTTAATT TGGGGAACAT TTTTAATTCT GTTTTTTCTA AAATAAGGAA
 601  ATTATAATGA CCATCCTGTT TCATTTTCAT CGCTTTTCAC TTTATTTCTT
 651  CTAGATAATG CACCCTTGTC TTCAAACGAA AAACACCTCC ATTAAATCCA
 701  CATACTAAGT GAACTGACCC ACGAATTTGG TACATAAAAA AAACACCTAT
 751  GCTACCTGTT TCTTGTATTC TATAGGAGAC AGGTAGTTTA ACTTTTCTTG
 801  AATACGTTCC GTATTATAAT ACTCAATGTA ATCGTGAATG AGTTGTTTGA
 851  GAGTAGAAGT TGAATGTATT TGTTTTTCTT GGGAATAAAA CAATTCAGAT
                              AAT
 901  TTCAATGAGG AATGAAAAGA TTCTATTACG GCATTATCAT GACAATTTCC
 951  TTTACGGGAC ATACTTGTGG TAATGCCATT TTTTTAGATA ACGTTTGGAA
1001  AGCGTAGGAG GTATACACGG CCCCTTGATC ACTATGTAGT ATAATTTGAG
1051  TCTTTTGTTG CAGTTTTATC GCCTTCTCAA CTGTTCTTAA GACGAGTGTT
1101  ACGTCTTGTC TGTTACTTAT TTCATATGCA ATGATTTCAT TGTTATATAA
1151  ATCCATAATA CTTAATAAAT ACAACATCTC TGTACCAAAT GGCAAATATG
1201  TAATGTCTGT AACCCATTTT TCATTTGGCT TGTTAGCTTG AAAGTTTCTA
1251  TTTAAGAGAT TCTCTACAAC AATTCTACTT TCTCCATTGA TCCAGGTTCT
1301  TCTCTTTCTT TTAACCCTAC ATTGTAAATT TTTCTTTTGC ATTATTTTTT
1351  GTACAGTTTT TCGATTTGGG TGATAATTAT ATTTTCGTTT CAATAAAGCA
1401  GTAACTTTTC GATGGCCATA TCGAAAGTGA TTTGTCATAC AAATTGTCAA
1451  AATAGCCTGT TCTAATTTTG CTTCCTTTAC ATCTTTTTCT TTATTTTTCC
```

Continued next page

```
      ClaI
1501  ATCGATAATA AGTAGAACGA GGTATACCAA TTAATATACA TATCTCTTTA
            ORF1  GTA
1551  ATGGAGTACT CATCTTTCAT CAACTCCACT ACTTCTACAA CTACTTCTTT

1601  AACCAACTCC TCTCGATTTC AGTTATGCCT TCTTCACTAG TCTTTTGTAG

1651  CGTACTTTGT TTTCCTACAG GGCGATTAAA ACGATACGTT TCACCTTCAC

1701  GATGCCACTT CATCCAAGTT TTAATCTGTG CTTTATTTTT AATTCCTAAT

1751  TGTTCCATAA TTTCTTTGTT TGTGTATCCT TGTTTTTTTC AGTTCGATTG

1801  TTTTCCATTT AATTTCTTCT GAATAAGATT TTCTCGTTCC CATAAAAGAA

1851  ACACCTCCGT ATATTCGTAT TTAAATTAAA TACGGTATAA GAGGTGTTTT

1901  TTCCTTGTCT TATTTCATTG GATCAGTTCA CAAAGTATGT GAATTTAATG

1951  GAGGTGTTTT TTTCATGCTC ACTATTCGGA TTCACTTCAG ATAGACCATG

2001  AGGTTTTTAA TTACTTAATA CCTTATCTTT TATTTTCAAC TTTCTATAAT

2051  ATAAGTTGGA TAGGGAAAAG TTGA
```

Figure 7. Nucleotide sequence of the cloned insert (WeyAL) from pJMH12 (2.7-kb *Kpn*I fragment of the 5.4-kb *Eco*RI fragment of pXO1.1 from Weybridge A UM23). The sequence starts at the *Eco*RI restriction site (shown above sequence) and proceeds past the *Cla*I restriction site (shown above sequence). The start and stop codons of ORF1 (truncated putative transposase gene) and direction of transcription are indicated. The 28-bp inverted repeats of the element are shown with a line above the sequence. The gaps in the line represent deletions or mismatches.

```
   1  CCCTTTGGTA AGGATTCATT TGGTTTTCAT CTGTGCTTTG ACTAACCGTA

  51  GCAATCCTGA ATCACCGACA GTAGTATTTT GGGATCATGA GGAAGAAAAC

 101  ACAGAGGAAG CAATACATCC TGTATGCTCA ACATTTACAG AATTACTTGC

 151  TAGTCTACGT GATTTTGAAG AAGAAGATTG AGGTAACAAA AAAACGGCCT

 201  AGGATTCTGA AGTGAACCCG AATAGTGGTA CATGAAAAAA ACACCTCCTG
      EcoRI
 251  AATTCGCATA CTAAGTGAAC TGACCCACGA ATTTGGTACA TGAAAAAAAC
        GAT
 301  ACCTATGCTA CCTGTTTCTT GTATTCTATA GGAGACAGGT AGTTTAACTT

 351  TTCTTGAATA CGTTCCGTAT TATAATACTC AATGTAATCG TGAATGAGTT

 401  GTTTGAGAGT AGAAGTTGAA TGTATTTGTT TTTCTTGGGA ATAAAACAAT

 451  TCAGATTTCA ATGAGGAATG AAAAGATTCT ATTACGGCAT TATCATGACA

 501  ATTTCCTTTA CGGGACATAC TTGTGGTAAT GCCATTTTTT TTAGATAACG

 551  TTTGGAAAGC GTAGGAGGTA TACACGGCCC CTTGATCACT ATGTAGTATA

 601  ATTTGAGTCT TTTGTTGCAG TTTTATCGCC TTCTCAACTG TTCTTAAGAC

 651  GAGTGTTACG TCTTGTCTGT TACTTATTTC ATATGCAATG ATTTCATTGT

 701  TATATAAATC CATAATACTT AATAAATACA ACATCTCTGT ACCAAATGGC

 751  AAATATGTAA TGTCTGTAAC CCATTTTTCA TTTGGCTTGT TAGCTTGAAA

 801  GTTTCTATTT AAGAGATTCT CTACAACAAT TCTACTTTCT CCATTGATCC

 851  AGGTTCTTCT CTTTCTTTTA ACCCTACATT GTAAATTTTT CTTTTGCATT

 901  ATTTTTTGTA CAGTTTTTCG ATTTGGGTGA TAATTATATT TTCGTTTCAA

 951  TAAAGCAGTA ACTTTTCGAT GGCCATATCG AAAGTGATTT GTCATACAAA

1001  TTGTCAAAAT AGCCTGTTCT AATTTTGCTT CCTTTACATC TTTTTCTTTA
           ClaI
1051  TTTTTCCATC GATAATAAGT AGAACGAGGT ATACCAATTA ATATACATAT
                    ORF1    GTA                        GAT
1101  CTCTTTAATG GAGTACTCAT CTTTCATTAA CTCCACTACT TCTACAACTA

1151  CTTCTTTAAC CAACTCCTCT CGATTTCTTG GTACTTTTTT AAAATATCTA
                                       HindIII
1201  GTTGCATTTT TAATTTCCGA TTCTCTATCT GAAGCTTCTC GATTTCAGTT

1251  ATACCTTCTT CACTAGCCTT TTGTAGCGTA CTTTGTTTTC CTACAGGGCG

1301  ACTAAAACGA TACGTTTCAC CTTCACGATG CCACTTCATC CAAGTTTTAA
                              ORF2    GTA
1351  TCTGTGCTTT ATTTTTAATT CCTAATTGTT CCATAATTTC TTTATTTGTG

1401  TATCCTTGTT TTTTCAGCTC GATTGCTTTC CATTTAATTT CTTCTGAATA

1451  AGATTTTCTC GTTCCCATAA AAGAAACACC TCCGTATATT CGTATTTAAA

1501  TTAAATACGG TATAAGAGGT GTTTTTCCTT GTCTTATTTC ATTGGGTCAC
```

Continued next page

```
1551  TTCATTCAAT GGAGGTGTTT TTCGTTTGAA GACAAGAGTT CATTACCCAG

1601  AAGAAACAAA GTGGAAAGTC ATTGAAATGA AGAAAGAAAG TTATTCAAAC

1651  CGTACAATTA TGGAGAAACT CGGAATTAAA AATGTTTCCA AATTAAGACA

1701  TGGATGAAAT GGTATCG
```

Figure 8. Nucleotide sequence of the cloned inserts (WeyAR) from pJMH24 (1.0-*Hin*dIII fragment of the 2.4-kb *Eco*RI fragment of pXO1.1 from Weybridge A UM23), pJMH4 (2.4-kb *Eco*RI fragment), and pJMH28 (9.3-kb *Pst*I fragment of pXO1.1 from Weybridge A UM23). The sequence starts before the *Eco*RI restriction site (shown above sequence) and proceeds past the *Hin*dIII restriction site (shown above sequence). The *Cla*I restriction site is also shown. The start and stop codons of ORF1 and ORF2 and the direction of transcriptions are indicated. The 19-bp inverted repeats of the element are shown with a line above the sequence. The gaps in the line represent deletions or mismatches.

EcoRI

```
   1  GAATTCGCAT ACTAAGTGAA CTGACCCACG AATTTGGTAC ATGAAAAAAA
        GAT ==
  51  CACCTATGCT ACCTGTTTCT TGTATTCTAT AGGAGACAGG TAGTTTAACT
 101  TTTCTTGAAT ACGTTCCGTA TTATAATACT CAATGTAATC GTGAATGAGT
 151  TGTTTGAGAG TAGAAGTTGA ATGTATTTGT TTTTCTTGGG AATAAAACAA
 201  TTCAGATTTC AATGAGGAAT GAAAAGATTC TATTACGGCA TTATCATGAC
 251  AATTTCCTTT ACGGGACATA CTTGTGGTAA TGCCATTTTT TTTAGATAAC
 301  GTTTGGAAAG CGTAGGAGGT ATACACGGCC CCTTGATCAC TATGTAGTAT
 351  AATTTGAGTC TTTTGTTGCA GTTTTATCGC CTTCTCAACT GTTCTTAAGA
 401  CGAGTGTTAC GTCTTGTCTG TTACTTATTT CATATGCAAT GATTTCATTG
 451  TTATATAAAT CCATAATACT TAATAAATAC AACATCTCTG TACCAAATGG
 501  CAAATATGTA ATGTCTGTAA CCCATTTTTC ATTTGGCTTG TTAGCTTGAA
 551  AGTTTCTATT TAAGAGATTC TCTACAACAA TTCTACTTTC TCCATTGATC
 601  CAGGTTCTTC TCTTTCTTTT AACCCTACAT TGTAAATTTT TCTTTTGCAT
 651  TATTTTTTGT ACAGTTTTTC GATTTGGGTG ATAATTATAT TTTCGTTTCA
 701  ATAAAGCAGT AACTTTTCGA TGGCCATATC GAAAGTGATT TGTCATACAA
 751  ATTGTCAAAA TAGCCTGTTC TAATTTTGCT TCCTTTACAT CTTTTTCTTT
                ClaI
 801  ATTTTTCCAT CGATAATAAG TAGAACGAGG TATACCAATT AATA ACATA
                    == ORF1 == GTA
 851  TCTCTTTAAT GGAGTACTCA TCTTTCATCA ACTCCACTAC TTCTACAACT
 901  ACTTCTTTAA CCAACTCCTC TCGATTTCAG TTATGCCTTC TTCACTAGTC
 951  TTTTGTAGCG TACTTTGTTT TCCTACAGGG CGATTAAAAC GATACGTTTC
1001  ACCTTCACGA TGCCACTTCA TCCAAGTTTT AATCTGTGCT TTATTTTTAA
1051  TTCCTAATTG TTCCATAATT TCTTTGTTTG TGTATCCTTG TTTTTTTCAG
1101  TTCGATTGTT TTCCATTTAA TTTCTTCTGA ATAAGATTTT CTCGTTCCCA
1151  TAAAAGAAAC ACCTCCGTAT ATTCGTATTT AAATTAAATA CGGTATAAGA
1201  GGTGTTTTTT CCTTGTCTTA TTTCATTGGA TCAGTTCACA AAGTATGTGA
1251  ATTTAATGGA GGTGTTTTTT TCATGCTCAC TATTCGGATT CACTTCAGAT
```

Continued next page

```
1301  AGACCATGAG GTTTTTAATT ACTTAATACC TTATCTTTTA TTTTCAACTT

1351  TCTATAATAT AAGTTGGATA GGGAAAAGTT GA
```

Figure 9. Nucleotide sequence of the cloned insert (SterneL) from pJMH16 (1.9-kb *Kpn*I fragment of the 4.8-kb *Eco*RI fragment of pXO1 from Sterne). The sequence starts at the *Eco*RI restriction site (shown above sequence) and proceeds past the *Cla*I restriction site (shown above sequence). The start and stop codons of ORF1 and the direction of transcription are indicated. The putative 28-bp inverted repeats of the element are shown with a line above the sequence. The gaps in the line represent deletions or mismatches. The complete sequence of the right inverted repeat (shown at the beginning of this sequence) is not shown because no sequence was obtained before the *Eco*RI restriction site.

EcoRI

```
   1  GAATTCCTTC GCAATATAAA ATACTTCCTT AATCTGAGTG ACGGATGACA
  51  TTTTCTACTT TTCGGCCTCT TCCTGCTCGT TTTAACTTCC TCAAATCTAA
 101  TGTCAAAGTT TGTAATTCAC TGATGATATA ACTAATGATT TCACGATTAG
 151  AAGCATCTAT AATCGTTGAT AAATACAACG TAAGCTCTCC AAATAATAGA
 201  TACGTGACAT CTGTAACTCC CTTTTCGGTT GGGATTGCCA CTTCAAATTG
 251  GCATTCTAAT TGATGCGAAA CTAGAACAGG TTCCATATCT TAATTTATAT
 301  CTAAAACAGA CCTTCTCTTC TGTATCGTCT TTAGGACGTT CTGTTGTCTG
 351  TAACCAACGA TAAAATGTGG AACGTGGTAA TTCTAATATT TTACTCAGTT
 401  CTTGTATGGT TAATTTTGTT ATTTAGCGCT TATTTTCTAA TCATAACTGT
 451  TCCAATTCAC TTAGCTCTTT TGGCTTTTCC CATAAAAGTA TTGTTTTCCT
 501  ACAGTTTGTT GAAGACGGTA CGTTTAATCT ATTCAGCACC ATTTCATTCA
 551  TGGTTTAATT TGGGGAACAT TTTTAATTCT GTTTTTTCTA AAATAAGGAA
 601  ATTATAATGA CCATCCTGTT TCATTTTCAT CGCTTTTCAC TTTATTTCTT
 651  CTAGATAATG CACCCTTGTC TTCAAACGAA AAACACCTCC ATTAAATCCA
 701  CATACTAAGT GAACTGACCC ACGAATTTGG TACATAAAAA AAACACCTAT
 751  GCTACCTGTT TCTTGTATTC TATAGGAGAC AGGTAGTTTA ACTTTTCTTG
 801  AATACGTTCC GTATTATAAT ACTCAATGTA ATCGTGAATG AGTTGTTTGA
 851  GAGTAGAAGT TGAATGTATT TGTTTTTCTT GGGAATAAAA CAATTCAGAT
                              AAT ==
 901  TTCAATGAGG AATGAAAAGA TTCTATTACG GCATTATCAT GACAATTTCC
 951  TTTACGGGAC ATACTTGTGG TAATGCCATT TTTTTAGATA ACGTTTGGAA
1001  AGCGTAGGAG GTATACACGG CCCCTTGATC ACTATGTAGT ATAATTTGAG
1051  TCTTTTGTTG CAGTTTTATC GCCTTCTCAA CTGTTCTTAA GACGAGTGTT
1101  ACGTCTTGTC TGTTACTTAT TTCATATGCA ATGATTTCAT TGTTATATAA
1151  ATCCATAATA CTTAATAAAT ACAACATCTC TGTACCAAAT GGCAAATATG
1201  TAATGTCTGT AACCCATTTT TCATTTGGCT TGTTAGCTTG AAAGTTTCTA
1251  TTTAAGAGAT TCTCTACAAC AATTCTACTT TCTCCATTGA TCCAGGTTCT
1301  TCTCTTTCTT TTAACCCTAC ATTGTAAATT TTTCTTTTGC ATTATTTTTT
1351  GTACAGTTTT TCGATTTGGG TGATAATTAT ATTTTCGTTT CAATAAAGCA
1401  GTAACTTTTC GATGGCCATA TCGAAAGTGA TTTGTCATAC AAATTGTCAA
1451  AATAGCCTGT TCTAATTTTG CTTCCTTTAC ATCTTTTTCT TTATTTTTCC
       ClaI
1501  ATCGATAATA AGTAGAACGA GGTATACCAA TTAATATACA TATCTCTTTA
```

Continued next page

```
          ORF1 ——— GTA
1551  ATGGAGTACT CATCTTTCAT TAACTCCACT ACTTCTACAA CTACTTCTTT

1601  AACCAACTCC TCTCGATTTC TTGGTACTTT TTTAAAATAT CTAGTTGCAT
                                HindIII
1651  TTTTAATTTC CGATTCTCTA TCTGAAGCTT CTCGATTTCA GTTATACCTT

1701  CTTCACTAGC CTTTTGTAGC GTACTTTGTT TTCCTACAGG GCGACTAAAA

1751  CGATACGTTT CACCTTCACG ATGCCACTTC ATCCAAGTTT TAATCTGTGC

1801  TTTATTTTTA ATTCCTAATT GTTCCATAAT TTCTTTATTT GTGTATCCTT

1851  GTTTTTTCAG CTCGATTGCT TTCCATTTAA TTTCTTCTGA ATAAGATTTT

1901  CTCGTTCCCA TAAAAGAAAC ACCTCCGTAT ATTCGTATTT AAATTAAATA

1951  CGGTATAAGA GGTGTTTTTC CTTGTCTTAT TTCATTGGGT CACTTCATTC

2001  AATGGAGGTG TTTTTCGTTT GAAGACAAGA GTTCATTACC CAGAAGAAAC

2051  AAAGTGGAAA GTCATTGAAA TGAAGAAAGA AAGTTATTCA AACCGTACAA

2101  TTATGGAGAA ACTCGGAATT AAAAATGTTT CCAAATTAAG ACATGGATGA

2151  AATGGTATCG
```

Figure 10. Nucleotice sequence of the cloned inserts (SterneR) from pJMH20 (1.7-kb *Hin*dIII fragment of the 3.1-kb *Eco*RI fragment of pXO1 from Sterne) and pJMH5 (3.1-kb *Eco*RI fragment). The sequence starts at the *Eco*RI restriction site (shown above sequence) and proceeds past the *Hin*dIII restriction site (shown above sequence). The *Cla*I restriction site is also shown. The start and stop codons of ORF1(truncated putative transposase gene) and direction of transcription are indicated. The 19-bp inverted repeats of the element are shown with a line above the sequence. The gaps in the line represent deletions or mismatches.

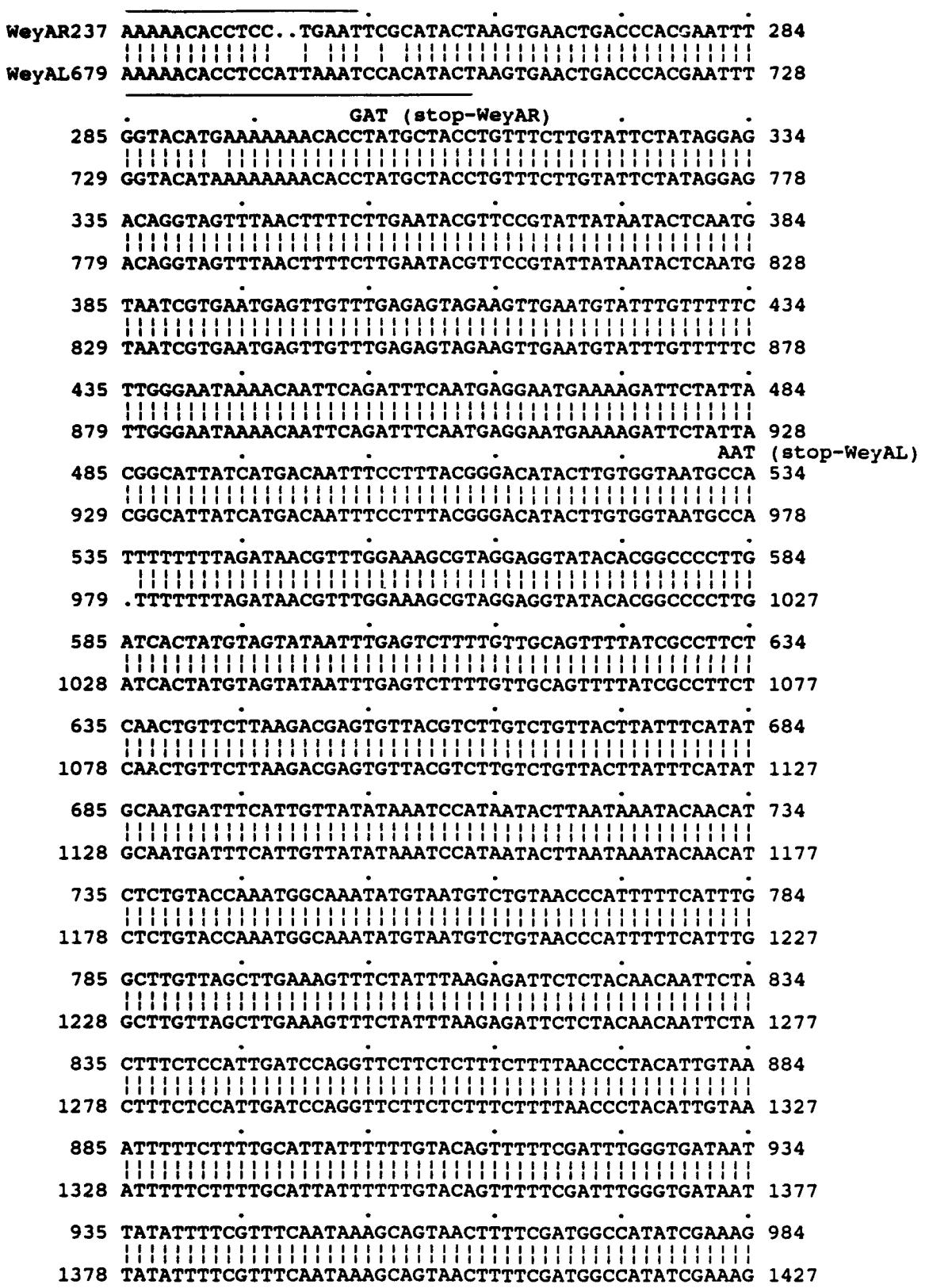

Continued next page

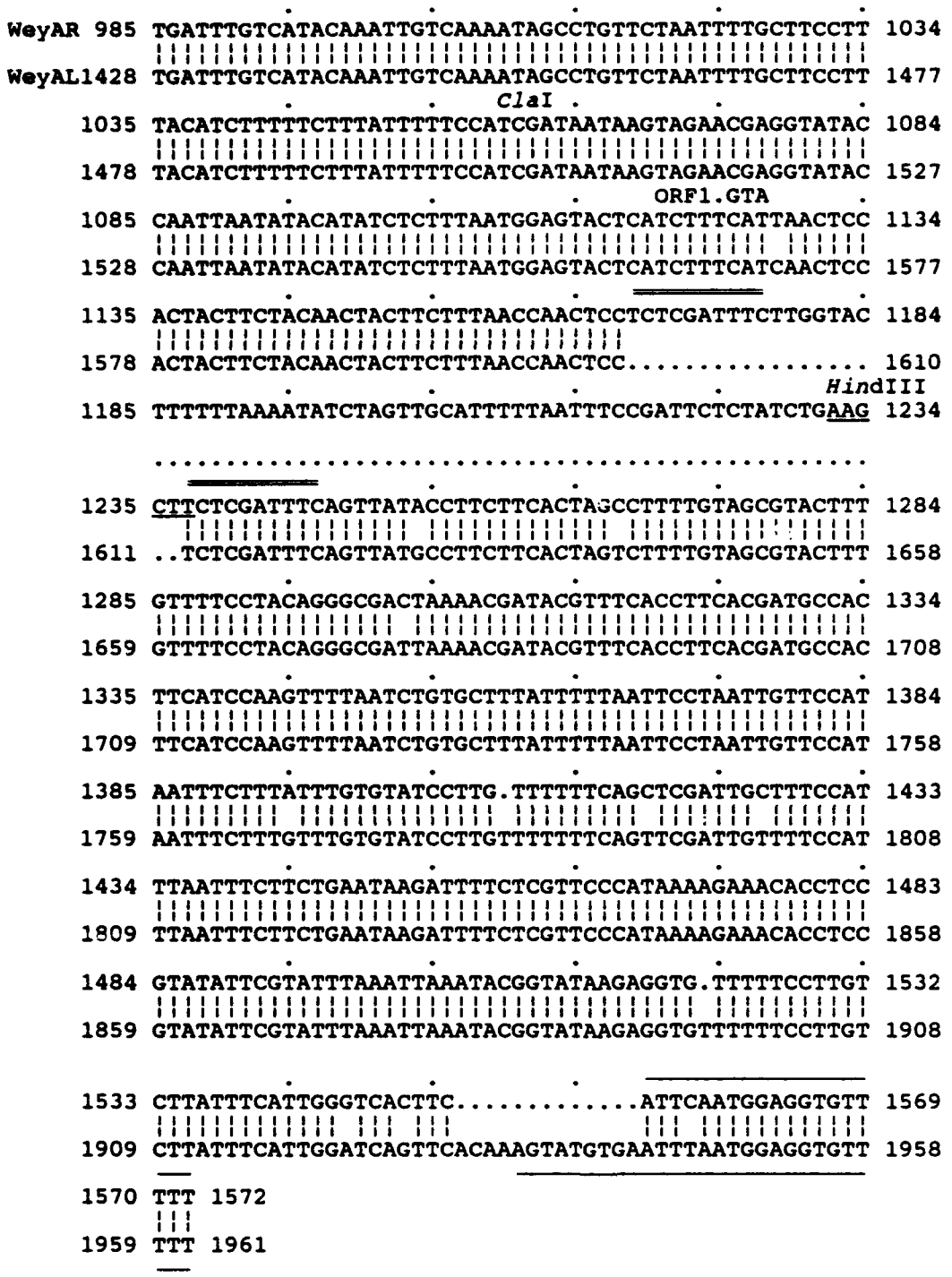

Figure 11. Bestfit of sequences of WeyAR and WeyAL. The *Cla*I and *Hin*dIII restriction sites are shown with the *Hin*dIII site underlined. The start and stop codons of ORF1 for WeyAR and WeyAL are shown above or below the sequences. The 19-bp and 28-bp inverted repeats of WeyAR and WeyAL, respectively, are shown with the lines above or below the sequences. Deletions or gaps within the sequences are shown by a period. A direct repeat in WeyAR is shown by double lines above the sequence and may have been involved in the formation of the deletion of this region in WeyAL. The sizes of the inverted repeats/IS elements are approx. 1336 bp in size.

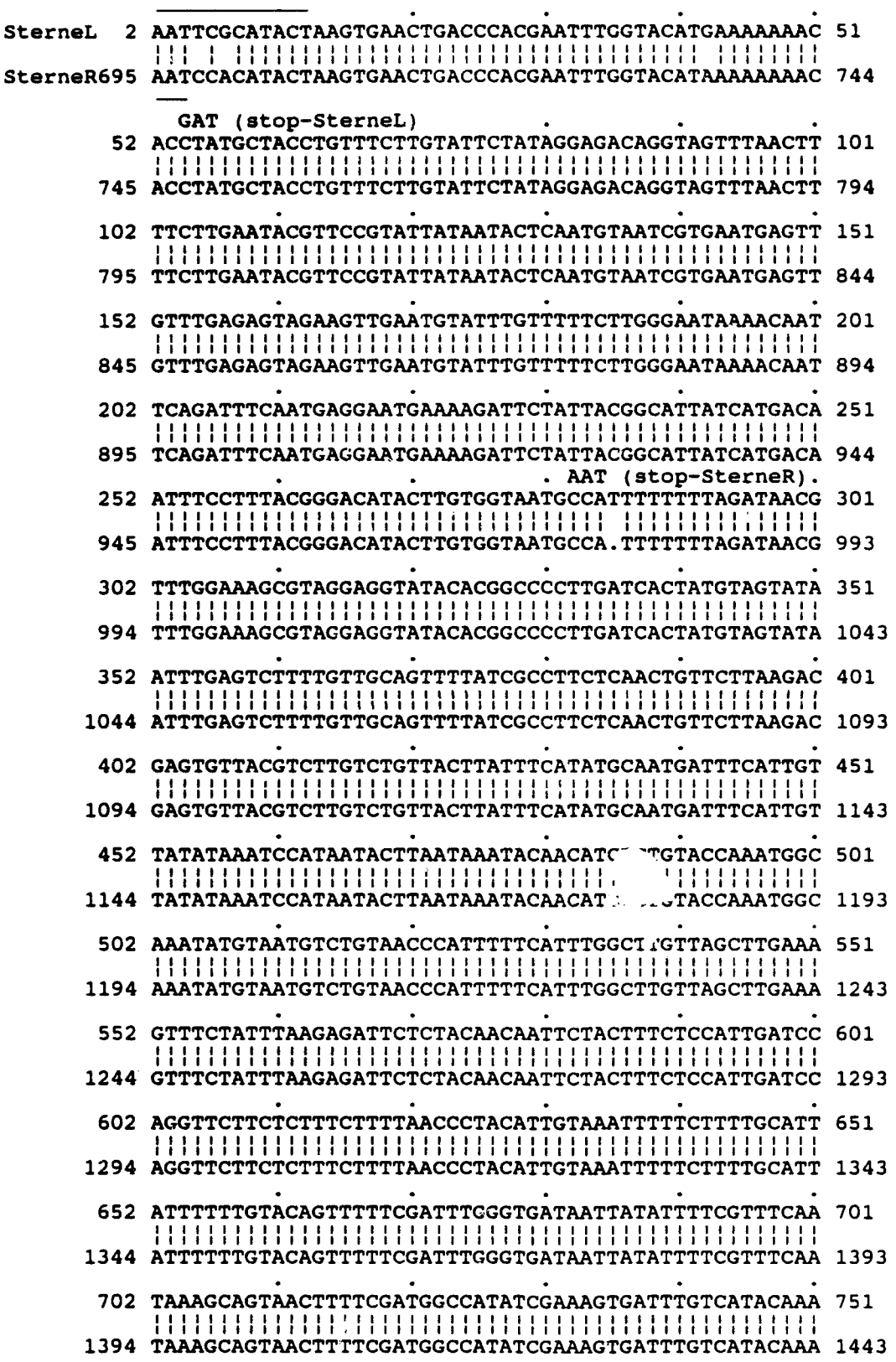

Continued next page

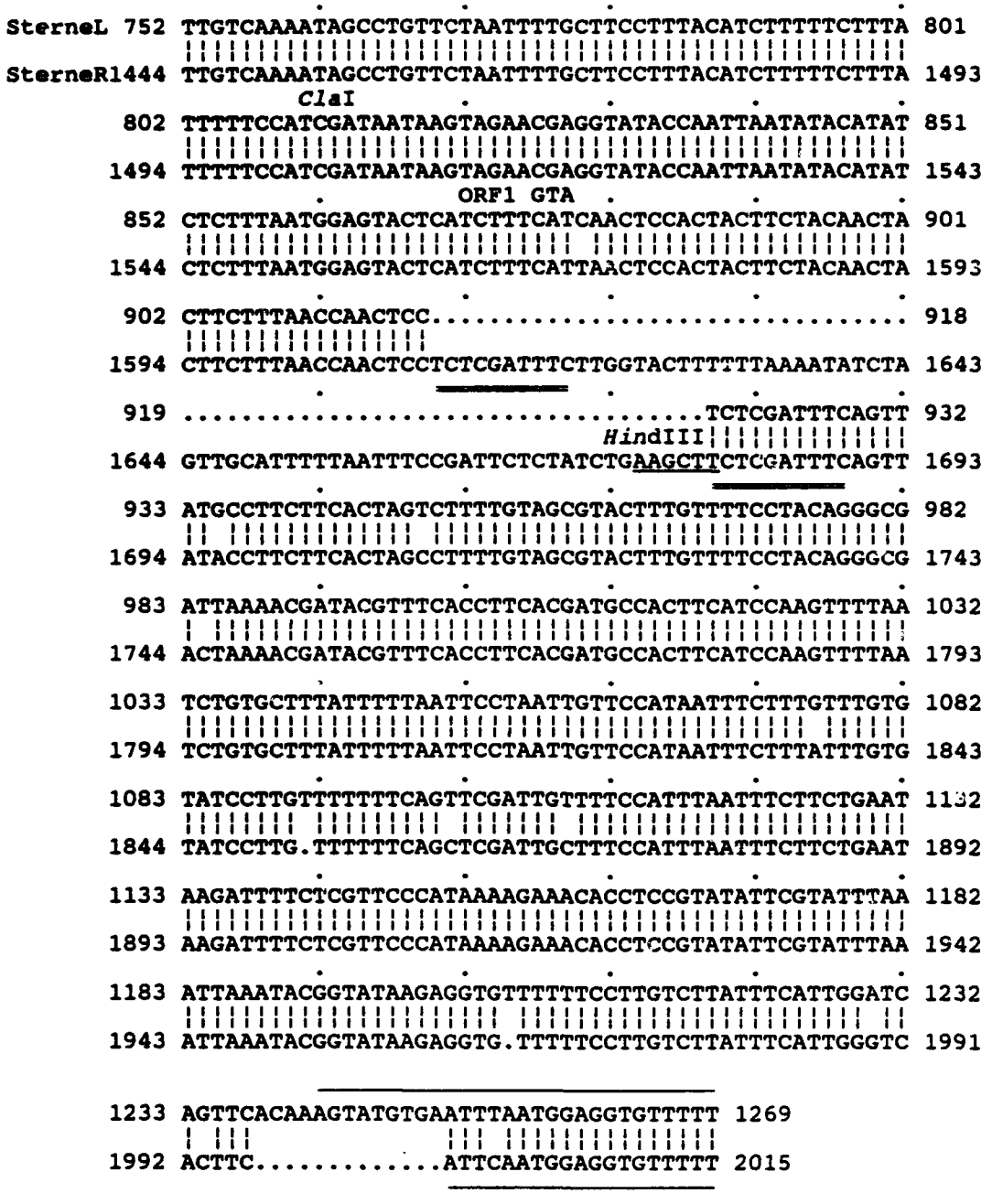

Figure 12. Bestfit of sequences of SterneL and SterneR. The *Cla*I and *Hin*dIII restriction sites are shown with the *Hin*dIII site underlined. The start and stop codons of ORF1 for SterneL and SterneR are shown above or below the sequences. The 28-bp and 19-bp inverted repeats of SterneL and SterneR, respectively, are shown with the lines above or below the sequences. Only 3 nt of the left 19-bp inverted repeat of SterneR are shown (nt695 to nt697). Only 12 nt of the right 28-bp inverted repeat of SterneL are shown (nt2 to nt13) because a fragment of pXO1 (Sterne) containing the remaining sequence of the inverted repeat has not been cloned or sequenced. Deletions or gaps within the sequences are shown by a period. A direct repeat in SterneR is shown by double lines below the sequence and may have been involved in the formation of the deletion of this region in SterneL. The sizes of the inverted repeats/IS elements are approx. 1336 bp in size.

pXO1 (Sterne)

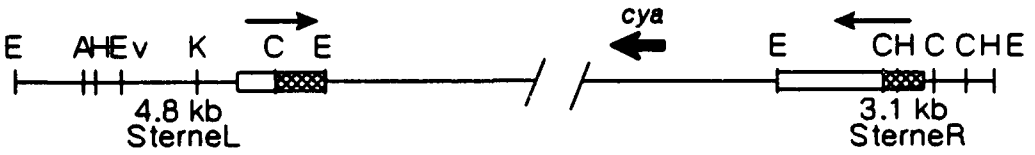

pXO1.1 (Weybridge A UM23)

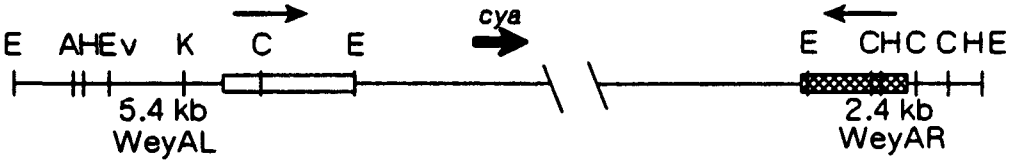

Figure 13. Partial restriction maps of the junction fragments of the toxin-encoding regions of pXO1.1 (Weybridge A UM23) and pXO1 (Sterne). Based on sequence analysis, possible sites of the junctions of the inverted segment are represented by the open and crosshatched boxes. The thin arrows show the locations of the *ca.* 1.3-kb inverted repeats/IS elements. E, *Eco*RI; C, *Cla*I; K, *Kpn*I; H, *Hind*III; A, *Ava*I; and Ev, *Eco*RV.

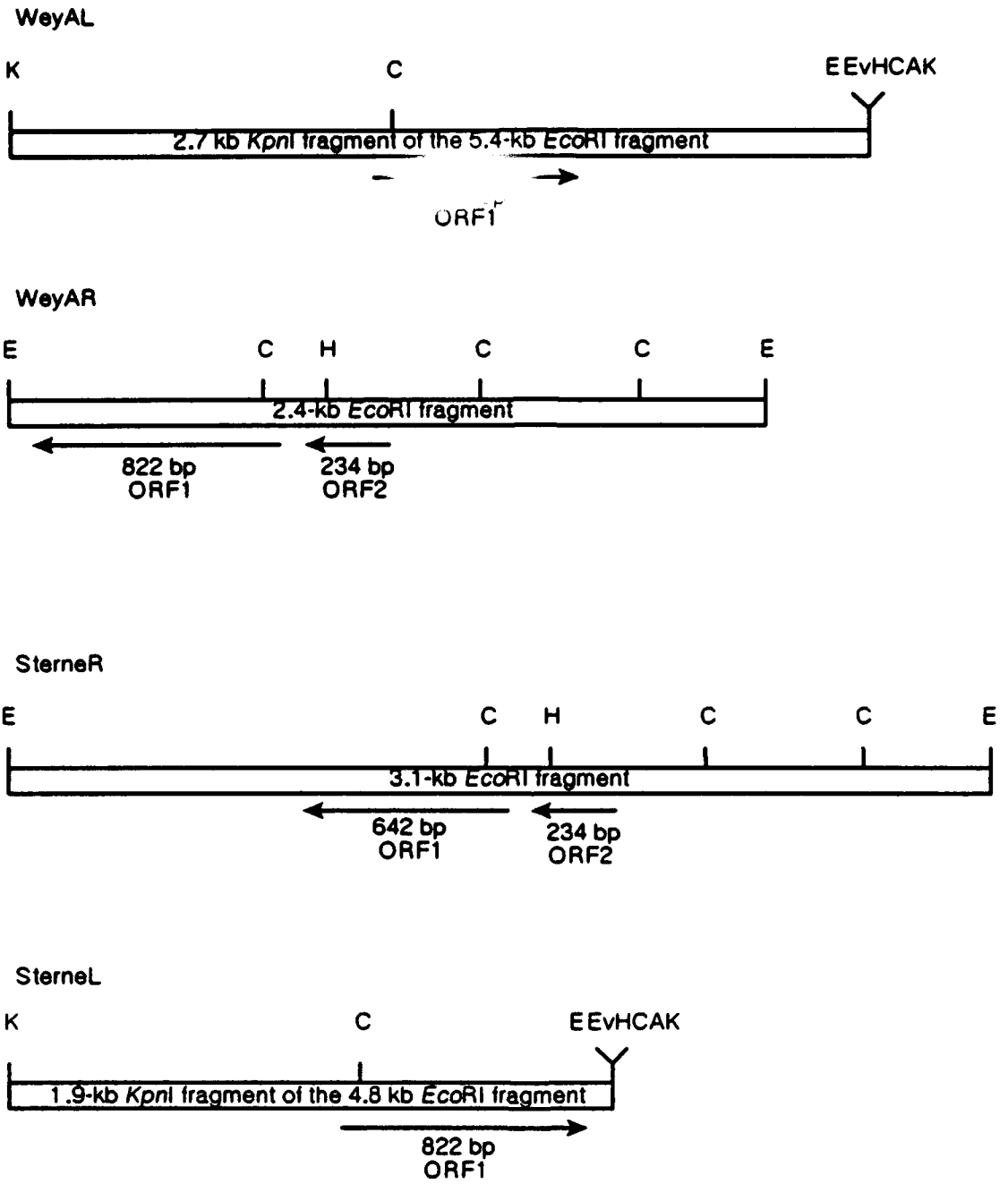

Figure 14. Locations of major ORFs in the cloned junction fragments of the inverted segments of pXO1.1 (Weybridge A UM23) and pXO1 (Sterne). The directions of transcription and the sizes of the ORFs are shown. With the exception of the *Eco*RI site, the restriction sites shown above the Y-shaped line represent the restriction sites found in the MCS of pBluescriptIIKS(+). E, *Eco*RI; S, *Sst*I; C, *Cla*I; H, *Hin*dIII; P, *Pst*I; B, *Bam*HI; A, *Ava*I; Ev, *Eco*RV; K, *Kpn*I.

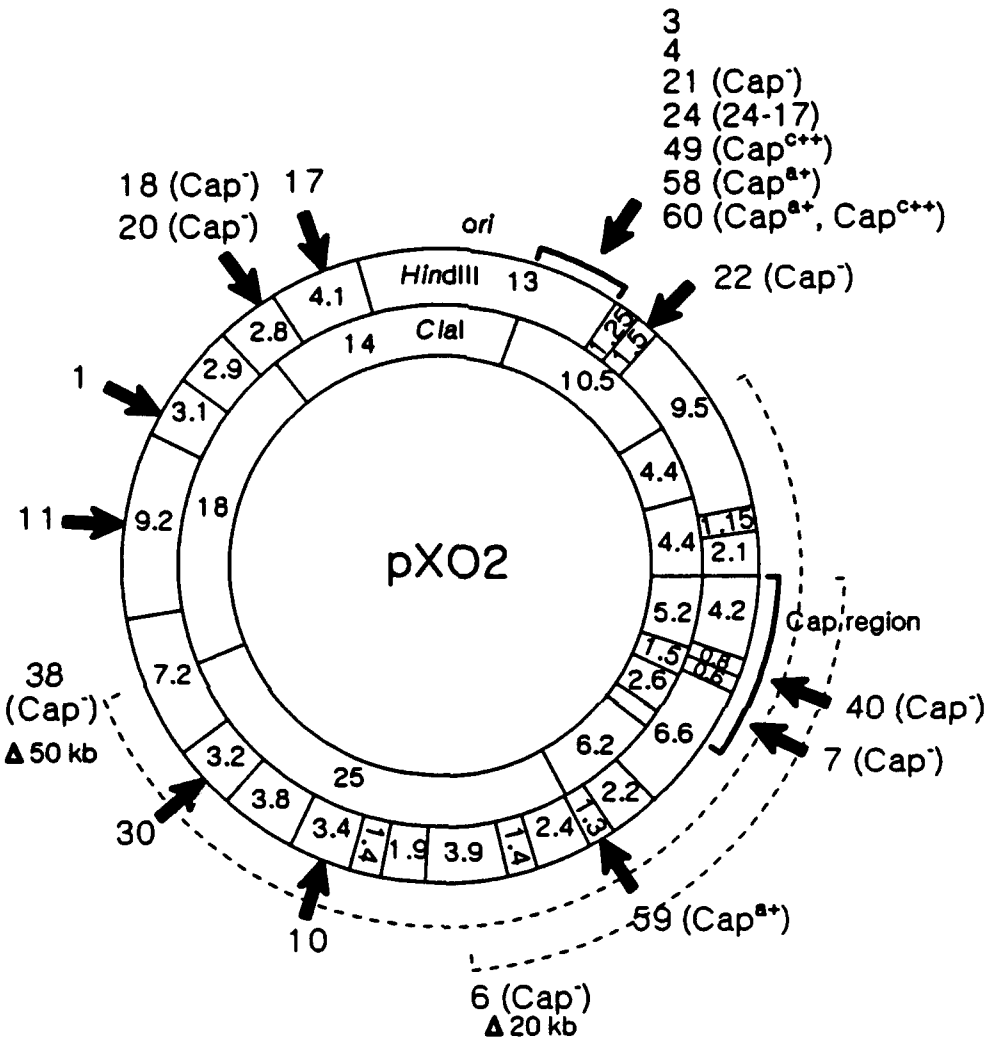

Figure 15. Restriction map of pXO2. The locations of Tn*917* insertions are indicated by the arrows. Insertion mutants that exhibit the parental phenotypes are not labeled with phenotypic designations. Deletions are indicated by dotted lines. Cap⁻, inability to produce capsule; Cap^{a+}, CO_2-independent for capsule production; Cap^{c++}, overproduction of capsular material in CO_2.

REFERENCES

1. **Ausubel, F. M., R. Brent, R. E. Kingston, D. D. Moore, J. B. Seidman, J. A. Smith, and K. Struhl.** 1992. Short protocols in molecular biology, 2nd edition. John Wiley and Sons, New York.

2. **Bragg, T. S., and D. L. Robertson.** 1989. Nucleotide sequence and analysis of the lethal factor gene (*lef*) from *Bacillus anthracis*. Gene **81**:45-54.

3. **Chandler, M., and O. Fayet.** 1993. Translational frameshifting in the control of transposition in bacteria. Mol. Microbiol. **7**:497-503.

4. **Ferrell, R. V., M. B. Heidari, K. S. Wise, and M. A. McIntosh.** 1989. A *Mycoplasma* genetic element resembling prokaryotic insertion sequences. Mol. Microbiol. **3**:957-967.

5. **Green, B. D., L. Battisti, T. M. Koehler, C. B. Thorne, and B. E. Ivins.** 1985. Demonstration of a capsule plasmid in *Bacillus anthracis*. Infect. Immun. **49**:291-297.

6. **Hornung, J. M.** 1994. Characterization of the *Bacillus anthracis* Toxin Plasmid pXO1, Ph.D. Dissertation. University of Massachusetts, Amherst, MA.

7. **Hornung, J. M., A. I. Guaracao-Ayala, and C. B. Thorne.** 1989. Transposon mutagenesis in *Bacillus anthracis*, abstr. H-256, p. 212. Abstr. 89th Annu. Meet. Am. Soc. Microbiol. 1989.

8. **Hornung, J. M., and C. B. Thorne.** 1991. Insertion mutations affecting pXO1-associated toxin production in *Bacillus anthracis*, abstr. D-121, p. 98. Abstr. 91st Annu. Meet. Am. Soc. Microbiol. 1991.

9. **Hornung, J. M., and C. B. Thorne.** 1994. Characterization of an inversion encompassing the toxin-encoding region of the *Bacillus anthracis* toxin plasmid pXO1, abstr. H-257, p. 245. Abstr. 94th Gen. Meet. Am. Soc. Microbiol. 1994.

10. **Leonard, C. G., R. D. Housewright, and C. B. Thorne.** 1958. Effects of some metallic ions on glutamyl polypeptide synthesis by *Bacillus subtilis*. J. Bacteriol. **76**:499-503.

11. **Leppla, S.** 1991. Purification and characterization of adenylyl cyclase from *Bacillus anthracis*. Methods Enzymol. **195**:153-168.

12. **Makino, S., C. Sasakawa, I. Uchida, N. Terakado, and M. Yoshikawa.** 1988. Cloning and CO_2-dependent expression of the genetic region for encapsulation from *Bacillus anthracis*. Mol. Microbiol. **2**:371-376.

13. **Makino, S.-I., I. Uchida, N. Terakado, C. Sasakawa, and M. Yoshikawa.** 1989. Molecular characterization and protein analysis of the *cap* region, which is essential for encapsulation in *Bacillus anthracis*. J. Bacteriol. **171**:722-730.

14. **Matson, S.** 1989. Suggestions and comments from sequencers, p. 18 Editorial comments. Vol. 16. United States Biochemical Corporation, Cleveland, OH.

15. **Robertson, D. L., T. S. Bragg, S. Simpson, R. Kaspar, W. Xie, and M. T. Tippetts.** 1990. Mapping and characterization of the *Bacillus anthracis* plasmids pXO1 and pXO2, p. 55-58. *In* P. C. B. Turnbull (ed.), Proceedings of the International Workshop on Anthrax, Winchester, England. Salisbury Medical Bulletin, No. 68, Special Supplement. Salisbury Medical Society, Salisbury, England.

16. **Robertson, D. L., M. T. Tippetts, and S. H. Leppla.** 1988. Nucleotide sequence of the *Bacillus anthracis* edema factor gene (*cya*): a calmodulin-dependent adenylate cyclase. Gene **73**:363-371.

17. **Ruhfel, R. E.** 1989. Physical and genetic characterization of the *Bacillus thuringiensis* subsp. *kurstaki* HD-1 extrachromosomal temperate phage TP-21, Ph.D. Dissertation. University of Massachusetts, Amherst.

18. **Sambrook, J., E. F. Fritsch, and T. Maniatis.** 1989. Molecular cloning: a laboratory manual. Cold Spring Harbor Laboratory Press, Cold Spring Harbor, NY.

19. **Sanger, J., S. Nicklen, and A. R. Coulson.** 1977. DNA sequencing with chain-terminating inhibitors. Proc. Natl. Acad. Sci. USA **74**:5463-5467.

20. **Thorne, C. B.** 1989. Genetic and physiological studies of *Bacillus anthracis* related to development of an improved vaccine. Annual Report, July 1989. Contract DAMD17-85-C-5212.

21. **Thorne, C. B.** 1990. Genetic and physiological studies of *Bacillus anthracis* related to development of an improved vaccine. Annual and Final Report, July 1990. Contract DAMD17-85-C-5212.

22. **Thorne, C. B.** 1992. Genetic and physiological studies of *Bacillus anthracis* related to development of an improved vaccine. Midterm Report, December 1992. Contract DAMD17-91-C-1100.

23. **Thorne, C. B.** 1993. *Bacillus anthracis*, p. 113-124. *In* A. L. Sonenshein, J. A. Hoch, and R. Losick (eds.), *Bacillus subtilis* and other gram-positive bacteria: biochemistry, physiology, and molecular genetics. American Society for Microbiology, Washington, D.C..

24. **Thorne, C. B., and F. C. Belton.** 1957. An agar diffusion method for titrating *Bacillus anthracis* immunizing antigen and its application to a study of antigen production. J. Gen. Microbiol. **17**:505-516.

25. **Thorne, C. B., C. G. Gomez, and R. D. Housewright.** 1952. Synthesis of glutamic acid and glutamyl polypeptide by *Bacillus anthracis* II. The effect of carbon dioxide on peptide production on solid media. J. Bacteriol. **63**:363-368.

26. **Uchida, I., J. M. Hornung, C. B. Thorne, K. R. Klimpel, and S. H. Leppla.** 1993. Cloning and characterization of a gene whose product is a *trans*-activator of anthrax toxin synthesis. J. Bacteriol. **175**:5329-5338.

27. **Uchida, I., S. Makino, C. Sasakawa, M. Yoshikawa, C. Sugimoto, and N. Terakado.** 1993. Identification of a novel gene, *dep*, associated with depolymerization of the capsular polymer in *Bacillus anthracis*. Mol. Microbiol. **9**:487-496.

28. **Uchida, I., T. Sekizaki, K. Hashimoto, and N. Terakado.** 1985. Association of the encapsulation of *Bacillus anthracis* with a 60-megadalton plasmid. J. Gen. Microbiol. **131**:363-367.

29. **Vietri, N. J., R. Marrero, and S. L. Welkos**. 1994. Identification of a trans-acting factor involved in the regulation of encapsulation by *Bacillus anthracis* abstr. B-115, p. 46. Abstr. 94th Gen. Meet. Am. Soc. Gen. Microbiol. 1994.

30. **Welkos, S. L., J. R. Lowe, F. Eden-McCutchan, M. Vodkin, S. H. Leppla, and J. J. Schmidt.** 1988. Sequence and analysis of the DNA encoding protective antigen of *Bacillus anthracis*. Gene 69:287-300.

APPENDIX

List of Publications

Papers

1. **Thorne, C. B.** 1993. *Bacillus anthracis*, p. 113-124. *In* A. L. Sonenshein, J. A. Hoch, and R. Losick (eds.), *Bacillus subtilis* and other gram-positive bacteria: biochemistry, physiology, and molecular genetics. American Society for Microbiology, Washington, D.C..

2. **Uchida, I., J. M. Hornung, C. B. Thorne, K. R. Klimpel, and S. H. Leppla.** 1993. Cloning and characterization of a gene whose product is a *trans*-activator of anthrax toxin synthesis. J. Bacteriol. 175:5329-5338.

3. **Hornung, J. M., and C. B. Thorne.** Identification and characterization of an inversion encompassing the toxin-encoding region of the *Bacillus anthracis* plasmid pXO1. Manuscript in preparation.

Ph. D. Dissertations

1. **Guaracao-Ayala, A. I.** 1993. Characterization of Insertion Mutants in *Bacillus anthracis* Capsule Plasmid pXO2, Ph.D. Dissertation. University of Massachusetts, Amherst, MA.

2. **Hornung, J. M.** 1994. Characterization of the *Bacillus anthracis* Toxin Plasmid pXO1, Ph.D. Dissertation. University of Massachusetts, Amherst, MA.

Abstracts

1. **Hornung, J. M. and C. B. Thorne.** 1994. Characterization of an inversion encompassing the toxin-encoding region of the *Bacillus anthracis* toxin plasmid pXO1, abstr. H-257, p. 245. Abstr. 94th Gen. Meet. Am. Soc. Microbiol. 1994.

List of Personnel

Principal Investigator: C. B. Thorne, Professor of Microbiology

The following graduate students in pursuit of the Ph. D. degree worked on the project:

Jan M. Hornung (Continued to work on the project as a postdoctoral appointee after she was awarded the Ph. D. degree in May 1994).

Ana Guaracao-Ayala

The following person was employed as a technician for part of the contract period:

James Silva

The following undergraduate students were employed on an hourly basis for various periods of time as laboratory workers:

Jeremy Jorgenson
Bradford Burling
Steven Ellis
Sheryl Egan
Maureen Connor

List of Those Who Received Graduate Degrees While Working on the Contract:

Ana Guaracao-Ayala (September 1993)

Jan M. Homung (May 1994)